AD-A067 055 NAVAL UNDERSEA WARFARE CENTER SAN DIEGO CALIF F/G 9/1
HEATING AND TEMPERATURE DEPENDENT BEHAVIOR SONAR ELEMENT. LABOR--ETC(U)
OCT 68 J A WARD

UNCLASSIFIED NUWC-TN-188 NL

| OF |
AD A
067055

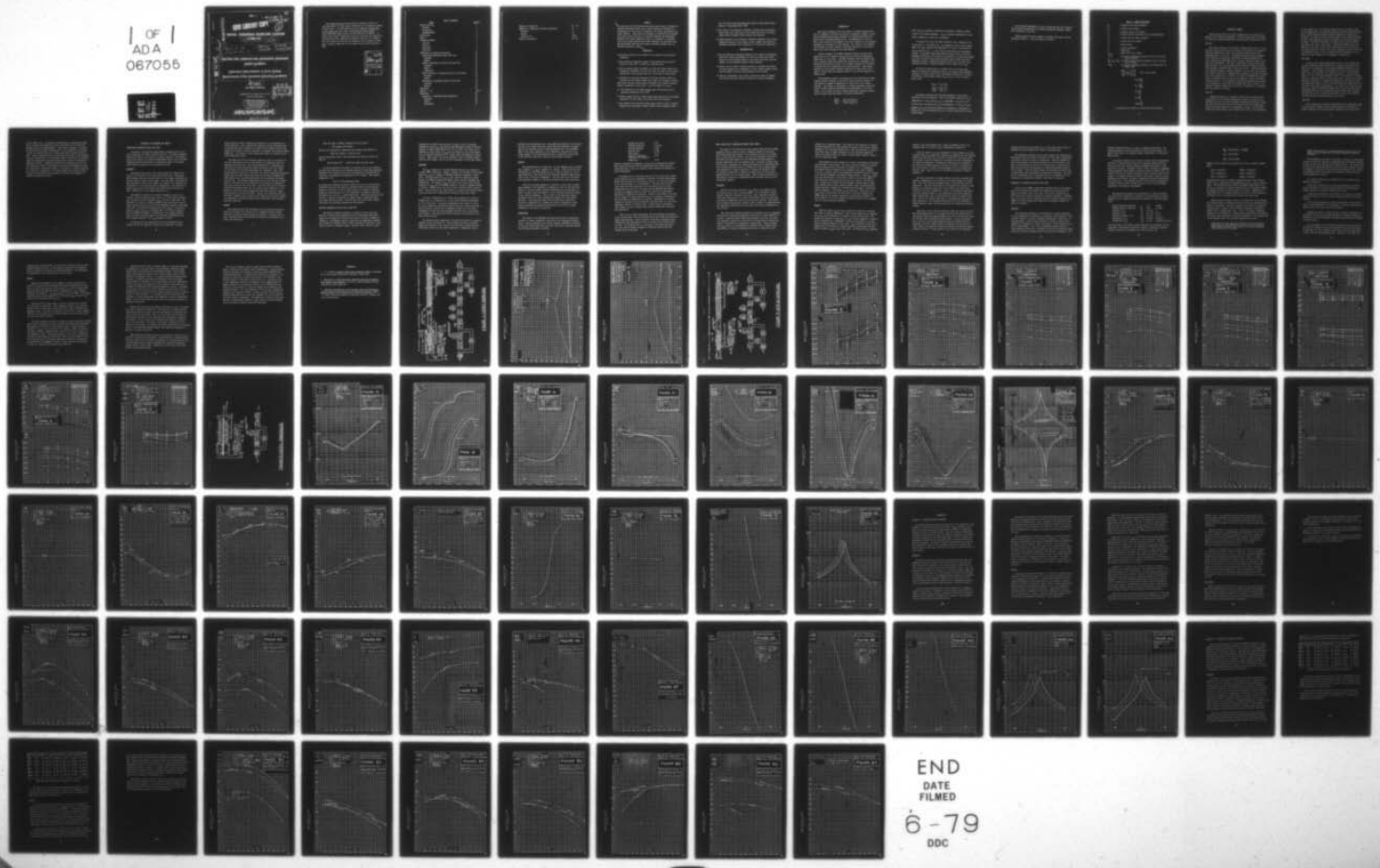

END
DATE
FILMED
6-79
DDC

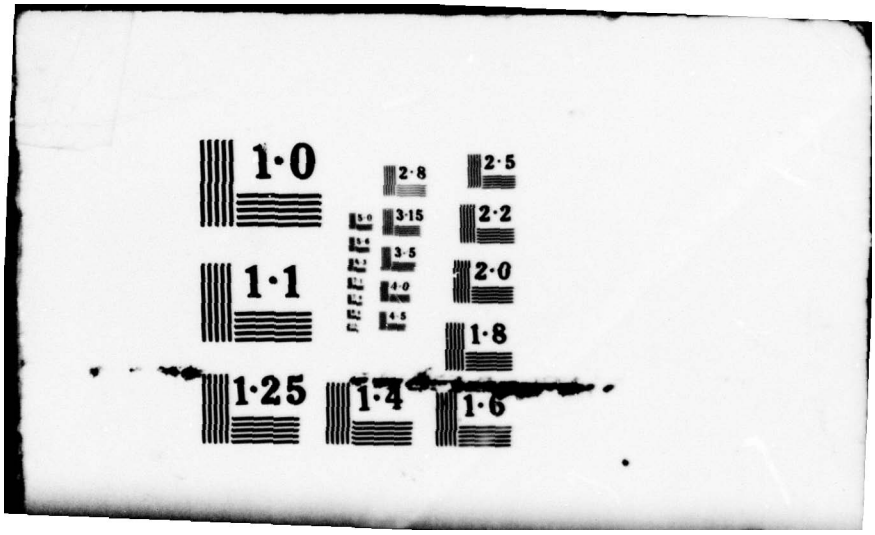
1·0
1·1
1·25
1·4
1·6
1·8
2·0
2·2
2·5
2·8
3·15
3·5
4·0
4·5

LEVEL II

MOST Project 4 B1

(14) NUWC-TN-188

OOVI LIBRARY COPY

(1) B.S.

001927

AD A067055

Good

(9) Technical note
May 66 - Aug 67

(16) S2217, F11121

(17) S2217, SF11121300

(6)

HEATING AND TEMPERATURE DEPENDENT BEHAVIOR SONAR ELEMENT.

Laboratory Determination of Array Cooling Requirements Under Simulated Operating Conditions

(10) by J. A. Ward

San Diego, California

(11) OCTOBER 1968

(12) 94p.

SUBPROJECT NO. S22-17/SF11 121 300

TASK NO. 8537/8049

DDC FILE COPY

TN-188

DDC RECEIVED APR 5 1979 F

DISTRIBUTION STATEMENT A

Approved for public release; Distribution Unlimited

DISTRIBUTION STATEMENT

This document is subject to special export controls and each transmittal to foreign governments or foreign nationals may be made only with prior approval of the Naval Undersea Warfare Center, San Diego, Calif. 92132

001927

403 023

LB

This Technical Note has been prepared to document results of a study subsidiary to a large project and should not be construed as being a formal report. The work reported here was conducted from May 1966 through August 1967 under NUWC Problem J708 (SS 048 001 (08537)) (Conformal/Planar Array Program) and L301 (SF 101 03 18 (8049)). Although a short paper[3] summarizing portions of this work was presented at the Twenty-fifth Navy Symposium on Underwater Acoustics on 7 November 1967, the contents of this note are believed to be of immediate usefulness to others at NUWC and to a few persons and activities outside of NUWC.

ACCESSION for

NTIS White Section

DDC Buff Section

UNANNOUNCED

JUSTIFICATION Letter on file

BY

DISTRIBUTION/AVAILABILITY CODES

Dist.	AVAIL. and/or SPECIAL	
A		

TABLE OF CONTENTS

PROBLEM

In connection with the Advanced Surface Ship Sonar Project to develop an improved surface-ship sonar array, develop laboratory techniques for determination of the effects of temperature on ceramic longitudinal resonator behavior. Using these new techniques in conjunction with methods and results derived from work in Transducer Research and Development, determine the ceramic temperature range to be expected in a proposed sonar array during operation and further determine any artificial cooling requirements resulting from element performance changes over the operating temperature range.

CONCLUSIONS

1) Artificial cooling is not required in the proposed array which was considered.

2) The operational temperature range in the proposed array was determined to be from 28°F to 120°F for a 25% duty cycle.

3) For the element design considered, we found that element behavior is essentially independent of drive level over the range of drive levels encountered in the proposed array (up to 218 watts of input power).

4) Although the procedures presented in the report provide useful information for the element design under study, no trustworthy information can be derived in this manner for elements which exhibit excessive behavior dependence on drive level - over the ranges of interest.

5) The efficiency of the element design under study increases with increasing temperature up to 125°F.

6) Results suggest that the ceramic capacitance decreases with increasing temperature for the ceramic type used (a PZT4 type material).

7) The control of head velocity through input current control; a feature designed into the element studied; remains within acceptable limits

over the entire operating temperature range but shows marked degradation at temperatures above 125°F.

8) The values of the important variables of interest such as electric field, power loss, and strain in the ceramic portion of the element remain within acceptable limits during array operation.

9) Element behavior at any instant is moderately dependent on the recent temperature history of the ceramic in such a manner that there is a repeatable hysteresis loop in behavior as a function of temperature.

RECOMMENDATIONS

1) Use the laboratory procedures presented in the report in determining artificial cooling requirements for other very large sonar arrays during the initial design stages of the project until such time that cheaper or more dependable methods become available.

2) Develop and use similar laboratory methods to determine the effects of stress changes due to submergence on array element behavior during initial stages of proposed deep-submergence sonar systems.

3) Continue investigation into possible theoretical models of temperature effects and other effects on behavior of ceramic transducers.

INTRODUCTION

This report documents recent work done by the NUWC Transducer Division in attempting to predict the effects of temperature changes on transducer performance during array operation for the Advanced Surface Ship Sonar Project (Conformal/Plannar Array). The emphasis here is not so much on the results of the analysis of the CP1.1 element as on the methods developed for performance of this analysis. The results of the analysis are discussed in detail, however, to provide illustration of the usefulness of and proper perspective for these methods.

A brief statement of the NUWC Transducer Division attitude which guides much of our transducer design work will provide the appropriate perspective for this report. The NUWC Transducer Division believes that only a composite model which adequately represents all components of the system and media should be used for the design, analysis, and evaluation of present day sonar transmitting and receiving arrays.[1] This usually requires the best possible computer techniques for application of the model in array design and analysis because of the size and complexity of modern arrays.

The mathematical model we currently use for the ferroelectric longitudinal resonator elements of the array[2] does not directly account for such things as changes in temperature or stress bias in the ceramic cylinder. The ceramic is represented at a single temperature and stress bias by ceramic parameters determined from measurements at low drive levels. We can write the matrix equation describing transducer behavior from our linear model (see Table 1 for symbol definitions):

$$\begin{bmatrix} E_m \\ I_m \end{bmatrix} = \begin{bmatrix} A_{11} & A_{12} \\ A_{21} & A_{22} \end{bmatrix} \begin{bmatrix} F_r \\ V_r \end{bmatrix}$$

where $[A_{ij}]$ are computed as functions of frequency, mechanical configuration, and ceramic parameters. $[A_{ij}]$ are assumed independent of drive level, temperature, stress bias, and history.

In actual fact, $[A_{ij}]$ are indeed functions of E_m, temperature (θ), stress bias (σ), and history (h). Our assumption to the contrary simply means that $[A_{ij}]$ computed from measurements are tied to the particular set of values for E_m, θ, σ, and h which existed during the measurement process. In previous computerized design of large arrays, we have not emphasized prediction of the effects of temperature or stress bias changes but rather we instead concentrated minimizing these changes by means of appropriate design. Minimization generally meant that our model could successfully predict transducer behavior from a single set of $[A_{ij}]$.

In the work reported here, we reasoned that if we could experimentally determine the temperature range to be expected during shipboard operation, we would be able to gain considerable insight into the nature of functional relationships between $[A_{ij}]$ and E_m, θ, and h by experimental means.

$$[A_{ij}] = [f_{ij}\ (E_m)]$$
$$[A_{ij}] = [g_{ij}\ (\theta)\ ]$$
$$[A_{ij}] = [h_{ij}\ (h)\ ]$$

We wished to separate the functional dependence on these three quantities as much as possible. That is; we wished to show that f_{ij} is independent of θ and h and that g_{ij} is independent of E_m and h, etc. We did succeed in showing that f_{ij} is independent of θ and g_{ij} is independent of E_{in} but all three functions are dependent in some degree on history (h). We also showed that f_{ij} is so nearly linear that it can be safely ignored.

The functional dependence of $[A_{ij}]$ on stress bias was not considered in this work but application of the same experimental philosophy should prove rewarding in this area.

Several symbols are used frequently throughout this report and are tabulated in Table 1. (See also Figures #1 and #4).

TABLE 1: SYMBOL DEFINITIONS

E_m	= voltage on the tuned transducer
E_c	= voltage on the ceramic
E	= electric field in the ceramic
F_r	= force exerted by the head on the surrounding medium
I_m	= current into the tuned transducer
I_c	= current into the ceramic
V_r	= head velocity
θ	= ceramic temperature
η	= efficiency
P_{loss}	= power lost in the ceramic
L_t, Q	= electrical inductance and quality factor for velocity control inductor
E_{33}^T, g_{33}, s_{33}^D	= the three complex ceramic parameters used in our model for the ceramic
Z_{dumi}	= electrical terminating impedance of the Dummy Mech. Impedance Load

$$\begin{bmatrix} E_m \\ I_m \end{bmatrix} \triangleq \begin{bmatrix} A_{ij} \end{bmatrix} \begin{bmatrix} F_r \\ V_r \end{bmatrix} \qquad \text{(For a linear model)}$$

$$Z_{ec} \triangleq \frac{A_{12}}{A_{11}}$$

$$Z_{ic} \triangleq \frac{A_{22}}{A_{21}}$$

$$Z_m \triangleq \frac{E_m}{I_m}$$

$$Z_c \triangleq \frac{E_c}{I_c}$$

$$Z_{rad} \triangleq \frac{F_r}{V_r}$$

All variables are complex and in rms units where possible.

PROCEDURAL SUMMARY

The work reported here is loosely collected into four steps as summarized in the following paragraphs. The EC-64 ceramic used in each step is a PZT-4-like material manufactured by Edo-Western Corporation of Utah.

STEP ONE

The C1CM-5 prototype of the first-cut element design (CP1.1) for the Conformal Planar Array Project (C/P Array) was checked over the ranges of radiation impedances and drive levels predicted theoretically from a programmed model of the array. The DUMILOAD (Dummy Mechanical Impedance Load) technique for laboratory simulation of radiation impedance[2] was used in laboratory measurements and the thermal conditions present in the array were approximated. The range of temperature expected during shipboard operation due to self-heating without artificial cooling was determined by means of DUMILOAD work at high power levels. Previous experience with different ceramic in another transducer (for the Lorad array) showed that drastic effects due to temperature were possible in certain situations and further showed that a redesign in the light of DUMILOAD data and theoretical predictions might be the only way possible to obtain acceptable array performance. We concluded that acceptable performance was possible in the temperature region from 28°F through 120°F using, at worst, a redesigned transducer element once the effects of temperature on transducer and array behavior were known.

STEP TWO

Transducer behavior as a function of drive level at various fixed temperatures over the operating temperature range was determined to be sufficiently linear to allow valid model predictions at high drive levels. The model uses low drive level (less than ten milliwatts) ceramic parameters and assumes behavior to be independent of level. We had considerable data showing nearly linear behavior with level at room temperature

for the ceramic used. We could have assumed that this linearity exists at all temperatures in the operating range, but previous work with certain other ceramics showed excessive nonlinear dependence at elevated temperatures. We therefore decided that knowledge of drive level dependence at other fixed temperatures would be necessary for valid application of our model. The ECP1-18 transducer was used in these tests for reasons discussed in the body of this report. DUMILOAD measurements were conducted over the range of drive levels encountered in the C/P array and the results show this ceramic to be nearly independent of drive level over the operational range. Also, the slight functional dependence on level which was observed appears to be independent of temperature.

STEP THREE

In view of the linearity demonstrated in Step 2, we concluded that our model adequately predicts high level transducer performance at any fixed value of temperature θ using ceramic parameters measured at temperature θ. This statement was considered valid only for the ranges of drive level and temperature and considered in Step 2. Low level parameters of a CP1.1 prototype transducer (C1CM-1) were measured at several values of temperature within the operational range. These sets of ceramic parameters, designated as "temperature parameters", were then used with our computerized model to predict transducer performance under array conditions of drive level and temperature. The "worst case" method of analysis using radiation impedances computed from an array model was used in determining the severity of temperature effects during array operation. We found that the CP1.1 element is acceptable for use in the proposed C/P array insofar as heating effects are of concern.

STEP FOUR

While conducting the parameter measurements over a temperature range, we were strongly reminded that the ceramic parameters determined at a single temperature can be significantly dependent on the recent history

of the ceramic (e.g.: the magnitude and direction of temperature changes prior to fixing the temperature and the time duration of the fixed temperature prior to the measurements). This caused a dilemma as to whether we should allow two weeks "stabilization" at each temperature of interest (as was our standard practice) or whether some other procedure should be used. Since we suspected that the operational "histories" in the shipboard array are important here, an operational "range of histories" was proposed, along with preliminary thoughts and observations relative to hysteresis in temperature effects. Temperature parameters were measured again for the CP1.1 prototype (C1CM-1) with emphasis on hysteresis information and these were used with our computerized model in an analysis of transducer behavior as a function of temperature at a single frequency and radiation loading. Further work with temperature parameters for the ECP1-18 transducer is included in Appendices A and B.

DISCUSSION OF PROCEDURES AND RESULTS

OPERATIONAL TEMPERATURE RANGE (STEP ONE)

The results of self-heating measurements at maximum power for the ClCM-5 transducer are shown in Figures #2 and #3. The ClCM-5 transducer, fabricated in 1966 as a prototype of the CP1.1 design for the Conformal Planar Array Project (C/P array) was DUMILOADED (Figure 1) with available components and used to determine the temperature range to be expected during shipboard operation of the proposed C/P array.

Procedure

The maximum output power from a single element was computed from theory to be 218 watts for the cavitation-limited array. The element which produced this power was also found to be the element which lost the greatest amount of power in the ceramic. For this reason, and because of time limitations, study of this element was assumed to be sufficient for determination of the operating range of temperatures. The radiation impedance (Z_{rad}) seen by this element was computed theoretically to be 8856 + j1902 Kg/sec at the midband frequency of f_o.

The DUMILOAD transducer was originally designed to operate in a "loafing" condition (minimum strain, power loss, field) when terminated with a passive electrical impedance (Z_{dumi}) of 1335 + j2876 ohms. This minimizes any changes in ceramic parameters which would result from excessive heating and electric field in the DUMILOAD transducer during high-power work. The mechanical matching device (see Figure 1) was then designed to present the Z_{rad} for maximum power to the ClCM-5 transducer when the DUMILOAD transducer is terminated for the loafing condition. Figure #3 shows the stable temperature indicative of DUMILOAD loafing which insures stability in the Z_{rad} presented to ClCM-5.

To simulate the heat losses which occur in the shipboard array through the case by conduction, convection, and radiation, a can was

placed around the C1CM-5 transducer and assumed to be an approximation of actual conditions. Also, thermocouples mounted at various positions along the ceramic were used to monitor the ceramic surface temperature which was assuemd in the light of previous experience to represent the internal ceramic temperature. The results of these measurements should be interpreted with these assumptions in mind.

The C1CM-5 was driven continuously (100% duty cycle) at 218 watts for the first 100 minutes to heat up the ceramic to a temperature above the suspected operating value. This insured measurement of a temperature no lower than the actual steady-state value for 25% duty cycle (20 seconds on, 60 seconds off) when the measurements were completed. Thus, after several minutes of 25% drive at 218 watts, the surface temperature approached steady-state from above rather than below, and the results represent the worst possible case of self-heating existent in the proposed cavitation-limited array. The different temperatures near the head and tail of C1CM-5 (see Fig. #2) might be due to differences in conduction and radiation in these areas even with the can in place. Since our model and the low-level parameter measurements apply only for uniform ceramic temperature, it is important to note that severe temperature differences along the ceramic could invalidate our entire procedure. However, the differences noted for the C1CM-5 transducer are not severe and we assume that the center temperature represents the highest possible uniform temperature under shipboard operating conditions.

Results

The reasoning behind this development of an operational temperature range can be summed up as follows for the conditions previously stated. The effect of several thousand elements in proximity is ignored since no data is available which would indicate the resulting small change in ambient ocean temperature.

Since the range of ambient temperature in any ocean is

28° through 100°F Ambient

and since the experimental temperature above ambient from Graph #1 is

20F° above ambient at 25% duty cycle

then the temperature found in the operating array should be within the range of

28°F through 120°F Operational Range (25% duty cycle)

To provide additional information of interest, much of the following work has been conducted over an expanded temperature range which adequately represents the operational range and allows additional interpretation of trends up to the maximum safe temperature for the ceramic. This range is designated as the

25°F to 175°F Measurement Range

The operational temperature range for 25% duty cycle is not severe and we ordinarily would not worry about the possible effects on array behavior. Because of the nature of the C/P array, however, we decided to develop a scheme for predicting the effects of temperature on transducer and array performance for use with our computerized model. Experience assures us that, at worst, acceptable performance is possible using a redesigned element once these effects are known. The following three steps present results and discuss the procedures developed for this purpose.

BEHAVIOR DEPENDENCE ON DRIVE LEVEL (STEP TWO)

The ECP1-18 transducer behavior as a function of drive level was measured at several fixed temperatures over the operating region determined for the proposed C/P array and the results are shown in Figures #5 through 12. The DUMILOAD composite (Figure #4) was immediately available and the ECP1-18 transducer used a ceramic configuration identical to that used for the CP1.1 transducer design. Because of this, and due to time

limitations, the ECP1-18 was used here in place of a CP1.1 prototype. Although the single Z_{rad} used during these measurements cannot be directly compared to those values predicted for the C/P array, the results can be expanded for other values of Z_{rad} since the degree of drive level dependence is primarily determined by the ceramic rather than mechanical configuration. These results may also be extended to other transducer designs using the same ceramic, such as the CP1.1 prototypes, for the same reasons.

Procedure

The Z_{dumi} required for "loafing" DUMILOAD operation was computed to be about 1420 + j2940 ohms. Figure #5 displays the variation of the average measured Z_{rad} due to changes in DUMILOAD transducer parameters vs drive level. The random nature of Z_{rad} vs test transducer temperature exists because the DUMILOAD temperature remained nearly constant throughout the measurements. The changes in Z_{rad} with drive level result only from nonlinearity in Z_{dumi} and the DUMILOAD transducer, and may be assumed constant at 170,000 + j22,000 Kg/sec with little error in ECP1-18 behavior measurements. This particular load allows ECP1-18 to operate with favorable field, strain and power loss, minimizing self-heating at high power levels.

A vel.cont. inductance (L_t) of 382 mh was predicted by our model as peaking $|Z_{ic}|$ at a frequency of f_o, using ceramic parameters determined at 73°F in late 1965. An inductor calibrated at this value (Q = 37.45) at f_o was connected in parallel with ECP1-18 for the current-driven case. Both the vel.cont. inductor and the DUMILOAD inductors are very nearly independent of drive level when operating with 600 volts or more across the terminals. Core heating and similar problems were not severe at the power levels used here.

The ceramic surface temperature of the ECP1-18 was held to a constant temperature with circulated air. This procedure was found to minimize temperature gradients in the ceramic after about thirty minutes and provided better control and more even distribution of temperature than is

possible with self-heating alone. The temperature gradients in the ceramic are zero in our model and we must assume that these gradients are negligible in the operating array if these measurements are to be meaningful. Some of the curves, especially at low temperature, show effects of the slight changes in the fixed temperature due to unavoidable self-heating of the ECP1-18 at high drive levels but these effects are small.

Results

The quantities shown in Figures #6 - #12 are dependent only on ECP1-18 and L_t behavior if Z_{rad} is assumed to be constant. These curves show that the behavior at each fixed temperature is at least as linear as it is at room temperature. This means that the functional dependence seen on drive level is not a function of temperature. Note the size of the variations with temperature compared to the small variations with drive level alone.

Since the functional dependence of behavior on drive level is negligible compared to the dependence on temperature, then, for any fixed temperature, low-level ceramic parameter measurements may be used with our model to predict high level behavior of any transducer using EC-64 ceramic at any radiation impedance. This is true for the operational range of temperature and drive levels theoretically predicted for the proposed C/P array. The quantities measured for the ECP1-18 are plotted as a function of temperature for a single drive level in Appendices A and B and are compared with theoretical predictions from low-level ceramic parameters in the spirit of Step Four.

Limitations

The results of the DUMILOAD work reported here must be interpreted relative to certain fundamental limitations of the experimental measurements. Previous experience with various transducer DUMILOAD work assures us that the present high drive level (above 500 watts) techniques provide the following measurement accuracies:

Voltage and Current	± 2%
Frequency Stability	± 1/2 Hz
Velocity Magnitude	± 10%
Velocity Ratio	± 10%
Phase Angles	± 1.0°
Electrical Components (inductors and resistors)	± 5%
Temperature	± 2°F

Recently, following the completion of this work, we acquired an accelerometer calibration system from the manufacturer which should bring our uncertainty down to one or two percent on both absolute and relative velocity measurements.

In previous work, we have seen errors of 50 to 100 per cent in quantities computed from the trigonometric functions of measured phase angles. These errors resulted from the nature of the sin, cos, and tan functions at the critical angles of 0 and 90 degrees. The major errors in efficiency power and other quantities due to one degree errors in angle measurements have forced us to conclude that any DUMILOAD measurements can show only trends in behavior until the technology of audio phase measurement is significantly improved. We have no confidence in the exact values computed for these quantities since, for instance, efficiencies of more than 100% are commonly seen in the data. Measurement of relative changes in efficiency (up with frequency, down with load, etc.) have been dependable, however, in previous work. In this report, the method of least squares is used to display these trends in quantities of interest when appropriate.

Prior to any of these measurements, two accelerometers were mounted at the surfaces where velocity was measured and the flexing resonances were mapped experimentally. Care was taken to avoid these frequencies since longitudinal mode measurements tend to be erroneous when flexing motion is large. The frequency used, f_o, was shown to be removed by several per cent from the nearest frequency of excessive flexing before any further work was initiated.

MODEL PREDICTION OF TEMPERATURE EFFECTS (STEP THREE)

The results of the previous two steps justify using low-level ceramic parameters with our model to predict transducer behavior at the drive levels and temperatures existent in the proposed C/P array if the transducer is made from EC-64 ceramic. The low-level parameters (6-12-66) of the ClCM-1 prototype (Figure 13) were determined from measurements at several temperatures over the operating range. We choose to define these several sets of parameters as "temperature parameters" to distinguish them from "ceramic parameters" which is a single set of three complex quantities determined at a single temperature. Figures #14 through #21 show the extrema of quantities of behavior occuring in the C/P array during midband operation at all steering angles. These extrema are searched out and computed by means of a computerized search procedure which we call a "worst-case" analysis.

Procedure

Because of the wide variation in Z_{rad} seen by each element in the C/P array over the range of steering angles, it is reasonable to assume constant temperature throughout the array. Other temperature distributions could cause changes in velocity distribution to such an extent that the radiation impedances across the array would be affected. The results of the analysis reported here, however, tend to support our assumption that the temperature distribution will not affect the velocity distribution of the C/P array.

The "worst-case" analysis procedure was developed for use in analyzing arrays without considering temperature effects and is readily adapted for use here. Assuming constant temperature thrughout the array, the radiation impedances computed over the array for the appropriate frequency and velocity distribution are independent of temperature. Further assuming that Z_{rad} values to be independent of frequency within a specific band, the behavior at cavitation (maximum drive level) is computed for each

element over a frequency range. The extrema of the quantities of interest are then searched out at each frequency and plotted as the "worst" possible anywhere in the cavitation-limited array. When this procedure is repeated for several sets of ceramic parameters over the operating temperature region, the results define the range of extreme element behavior existent over the temperature range.

The proposed C/P array consists of 12 rows of 229 elements (2748 total) with five-inch circular heads. The center-to-center spacing is 0.2 meters and the limiting cavitation pressure is assumed to be 1.5 atmospheres. The midband radiation impedances were computed at the center frequency of f_o for a constant velocity and temperature distribution and were assumed to be constant throughout the midband frequency region. These Z_{rad} values were then searched and a listing made (at each of 21 steering angles) of those which were extrema by one or more of ten criteria. The criteria were: maximum real, maximum positive imaginary, maximum negative imaginary, maximum positive angle, maximum negative angle, maximum magnitude, minimum magnitude, minimum real, minimum positive imaginary, and minimum negative imaginary. The average Z_{rad} was also used. This table of 231 Z_{rad} values was sufficient for use in this "worst-case" analysis even though reducing the original listing was not absolutely necessary (we don't always do it) and even though the extrema in behavior do not <u>always</u> occur at extreme radiation impedances.

Results

Figure #21 shows $|Z_{ic}|$ and $|Z_{ec}|$ plotted as a function of frequency with lines of constant temperature. Both of these quantities are independent of Z_{rad} and are assumed to be constant over the entire array. The parallel L_t necessary to peak $|Z_{ic}|$ at f_o at 75°F was computed to be 489 mh and the resulting $|Z_{ic}|$ "bandwidth" of nearly 18% centered at f_o is adequate for midband operation of this array. $|Z_{ic}|$ bandwidth is arbitrarily defined here as the region of frequency wherein $|Z_{ic}|$ is greater than ten times the maximum $|Z_{rad}|$ found in the array. The effective $|Z_{ic}|$ bandwidth

narrows if the array operates over a range of temperature due to the frequency shift of the peak in $|Z_{ic}|$ illustrated in Figure #21.

Since the spread in Z_m can be minimized if $|Z_{ec}|$ bottoms out at the frequency where $|Z_{ic}|$ peaks, the transducer was designed with this inherent condition as seen from the 75°F curves in Figure #21. The $|Z_{ec}|$ curves are included to show the separation in frequency of these two extrema due to changes in temperature. Although this separation is not desirable, this particular element design is such that the shifts in frequency are not severe enough to disrupt array performance over the operating temperature range. This is not true of the ECP1-18 transducer treated in Appendix A.

The other quantities of interest change in one form or another with changes in temperature but the results in the midband region are acceptable. The curves outside the midband region are included here only for perspective. The worst deterioration in performance with respect to temperature is probably the power loss in the ceramic (Fig. #18), which increases at the lower temperature. This is not altogether undesirable, since the increased losses at low temperatures and decreased losses at higher temperatures result in self-correction similar to negative feedback. That is, the ceramic heats more at low temperatures and less at high temperatures. The increasing losses above 125°F are conducive to thermal runaway, however, and operation above this temperature should be avoided.

Since most of the curves are within the limits set by the curves for the extreme temperatures, we can assume that the array element will always operate within the regions bounded by the 25°F curve and 125°F curve for 25% duty cycle cavitation-limited operation. We may now conclude that, since all of the bounded behavior within the midband region is acceptable, the CP1.1 element design is acceptable for use in the C/P array, insofar as temperature effects and heating are concerned, without artificial cooling. If some portion of the curves was not acceptable,

redesign would have been necessary for no reason other than the lack of acceptable array performance with respect to heating effects.

The temperature parameters used in this analysis were computed from measurements taken in an arbitrary sequence over the range of temperature at intervals of from two hours to several days. These are adequate for use in this analysis, all things considered, but in the process of this work, we were reminded of the need for further study of the effects of short-term history and the hysteresis in temperature-dependent behavior of the ceramic. The next section reviews the laboratory procedures used in determining ceramic parameters and temperature parameters. The existence of a hysteresis loop in transducer behavior vs temperature is confirmed and our preliminary thinking on this matter is discussed.

HYSTERESIS IN TRANSDUCER BEHAVIOR (STEP FOUR)

The two sets of CICM-1 temperature parameters used for the computation of the quantities in Figures #22 through #29 were measured on 16 August and 19 August 1966 in the light of the recent clarification of short-term history effects discussed in following paragraphs. Frequency, Z_{rad}, and L_t were fixed at reasonable values to provide a display of the effects of ceramic changes with temperature on transducer behavior as shown in the graphs.

Procedure

The established procedure for determination of ceramic parameters (at room temperature) is detailed in a previously cited reference.[2] This procedure requires a two-week 'parameter stabilization' period prior to any measurements. This has been sufficient to allow the time-rate-of-change of the parameters to reflect the 'present' ceramic behavior exclusive of aging changes. Also, this established procedure requires a ceramic sample in the form of a stressed stack with a low metal-to-ceramic ratio and a resonant frequency equal to the operational frequency of the

proposed transducer design to be used for parameter measurements. The resulting parameters are then applicable to the particular ceramic, frequency, and stress in all proposed designs irrespective of the amounts of metal present.

A prototype transducer may be used for ceramic parameter measurements instead of a sample stressed stack and the resultant model predictions agree very well with low-level laboratory DUMILOAD measurements of that particular prototype. Parameters measured using a prototype are effective ceramic parameters which depend on frequency, metal-to-ceramic ratio, etc., and which will not be exactly the same for other prototypes using the same ceramic. As standard procedure throughout this report, effective ceramic parameters are used with our model in comparing experimental measurements with predictions. This standard procedure allows accurate determination of model limitations when the same prototype is used for both DUMILOAD measurements and parameter measurements.

The measurements necessary for determination of ceramic parameters are listed below accompanied by statements of the measurement accuracies possible with our present installation and examples of reasonable magnitudes.

Maximum admittance magnitude	y_m	$\pm$ 1%	45 mMho
Minimum admittance magnitude	y_n	$\pm$ 1%	1.0 μMho
Frequency of y_m	f_m	$\pm$ 0.1 Hz	f_o
Frequency of y_n	f_n	$\pm$ 0.1 Hz	1.2 f_o
Arbitrary frequency << f_m	f_{lo}	$\pm$ 0.1 Hz	0.5 f_o
Capacitance at f_{lo}	C_{lo}	$\pm$ 0.01%	23456.7 pf
Dissipation at f_{lo}	D_{lo}	$\pm$ 0.1%	0.002345 (unitless)

With these data, the following complex parameters are determined from the appropriate transcendental equations by means of computerized iterative methods, expressed as a magnitude and a loss multiplier (M).

$$E_{33}^{T} = E33T(1-E33TM) = 1/BETA_{33}^{T}$$

$$g_{33} = G33\ (1-G33M)$$

$$s_{33}^{D} = S33D\ (1-S33DM)$$

Example values of these six quantities for the CP1.1 prototype in RMKS units:

$E33T = 0.1354(10)^{4}$ $\qquad$ $E33TM = 0.1758(10)^{-2}$

$G33 = 0.2206(10)^{-1}$ $\qquad$ $G33M = 0.1668(10)^{-3}$

$S33D = 0.9548(10)^{-11}$ $\qquad$ $S33DM = 0.1794(10)^{-2}$

The measurements used for parameter determination may include several values of f_{1o}, accompanied by corresponding C_{1o} and D_{1o}, over a frequency range. This provides insurance against inadvertant measurement of C_{1o} and D_{1o} at a frequency of bending resonance where the dissipation behaves in a manner different from that assumed in our model. Measurement of these quantities at a bending resonance can result in correct prediction of behavior only at that particular frequency and nowhere else.

Following several months of study, we concluded that an interdependence between history and temperature effects occurs when temperature parameters are determined. The exact parameters were found to be sensitive in several ways to recent history (duration, magnitude of temperature change, value of temperatures, etc.). The act of heating a transducer tended also to accelerate the "aging" process and parameter measurements were never exactly repeatable at a specific temperature. We reasoned that, in the shipboard array, the following assumptions were valid:

> Assume that the array operating conditions result in temperature fluctuations of random magnitude and direction, within an operational temperature range, with intervals of constant temperature less than two hours in duration.

Assume that the change in ceramic parameters during the first two hours of constant temperature following a temperature change is negligible.

These assumptions were made in an attempt to develop a standard measurement procedure for temperature parameters which would closely simulate the history conditions existent in the shipboard array. The results shown in Figures #22 through #29 demonstrate that the ClCM-1 prototype, cycled in temperature, does settle into a well-defined operating curve. Both of the sequences plotted in the graphs were obtained by means of the procedure summarized as follows:

1) A range of temperature is determined for the transducer from available information

2) The exact temperatures to be used in measurements are chosen and are separated by a constant interval (25F°) and sequentially arranged from start to extreme to extreme and so forth.

3) During the measurements, the interior of the ceramic is allowed forty-five minutes to reach the surface temperature before actual measurement.

4) The surface temperature is never held constant for more than two hours. After measurement at one temperature, the surface temperature is moved directly to the next value in the sequence.

Ignoring the effects of aging and rate of change of temperature we can safely say that the functional dependence of transducer behavior on temperature is closely approximated by this procedure minimum of changes in recent history.

The two sequences used to predict the graphed data were started at 75°F and 25°F (stable for 24 hours) respectively and were moved upward in 25F° steps to 175°F, downward in 25F° steps to 25°F and upward again to 25F° above the starting temperatures. As shown in the graphs, the

initial portion (stable history) of each curve is different from the final (unstable history) portion. If the range of histories in the shipboard array is assumed to be unstable, the resulting behavior of the transducer is represented by the final portions of the two curves.

Results

Figures #22 through #29 show the changes in several quantities as a function of temperature with frequency and radiation imperance held fixed. The L_t of 460 mh was predicted to peak $|Z_{ic}|$ at f_o at 25°F (19 August 1966 data) and Figure #33 shows the effect of temperature on $|Z_{ic}|$ frequency dependence and bandwidth. The Z_{rad} used here is the same 8856 + j1902 Kg/sec used in Step One and was computed to be the maximum $|Z_{rad}|$ present at any position in the proposed C/P array at f_o.

Figure #28 shows a large change in electric field per unit velocity over the range of temperature. This undoubtably depends on Z_{rad} and the field is quite low over the operating temperature range in any event (see Appendix A also). The amount of hysteresis of each curve is small compared with the total deviation and the second (unstable) portion of each of the two curves are nearly identical.

The input impedance (Z_m) shown in Figures #22 and #23 exhibits "detuning" which could be explained by a drop in ceramic capacitance with temperature. The magnitude and direction of the change in $|Z_m|$ is probably as much a function of Z_{rad} as it is a property of the ceramic. Again, the amount of hysteresis is within reasonable limits relative to the total changes over the temperature range. The unstable portions of the curves, although not as close as those shown for the electric field, are close enough to allow us to conclude that the functional dependence of behavior on temperature is dependent only on changes in history. Figure #30 shows the variation of $|Z_m|$ with frequency for comparison with Figure #23.

Figures #26 and #27 show the ceramic losses to be inversely dependent on temperature to the upper limit of the operational temperature range (about 120°F) at which point the relationship reverses. This confirms earlier indications and appears to be a ceramic property which is quite desirable (see Appendix A also). At one point during the parameter measurements, we suspected that moisture condensation within the ceramic cylinder might be responsible for the high losses at the low temperatures. Further work using dry nitrogen as a filler resulted in the same type of increases in dissipation with decreasing temperature, however. The amount of hysteresis in each curve is small, especially in Figure #26, but the unstable portions of the curves do not compare nearly as well as do similar curves for other quantities. In the light of previous experience with efficiency and power measurements, the comparison is not too unreasonable, however, and the results show the power loss to be extremely sensitive to parameters and history.

Figures #24 and #25 show the magnitude and angle of v_r/I_m to be nearly flat with no appreciable hysteresis. This means that the known relationship between velocity and input current is insensitive to temperature and recent history in the ceramic. This, in turn, allows current control of the velocity distribution in the operating array independent of temperature effects. The two curves are so identical that only one is shown in each of the two graphs. The velocity curve shown in Figure #31 is also nearly flat with respect to frequency and compares with Figure #25 in similar manner to the comparison between frequency and temperature dependence of $\angle Z_m$ found in Figures #23 and #30.

Figures #29 and #32 show the value of L_t necessary to peak $|Z_{ic}|$ as a function of temperature and frequency. Both curves show a similar relationship and, taken in view of previous comparisons, we conclude that some sort of relationship between frequency dependence and temperature dependence probably exists in this ceramic. Nothing more can be said at this point, however, without further study.

The $|Z_{ic}|$ vs frequency curves in Figure #33 are plotted assuming a fixed L_t of 460.5 mh at several constant temperatures. As was previously noted in Step Three, the frequency of peak $|Z_{ic}|$ shifts downward with increasing temperature. The hysteresis is not shown in the graph in the interest of clarity but we found the severity of the hysteresis to be directly related to that shown in Figure #29 for L_t. The peak in $|Z_{ic}|$ at room temperature computed from parameters with a <u>stable</u> history is sharply removed from the operating frequency and we concluded that the value of L_t used to peak at f_o should be computed from parameters with adjustable history. The $|Z_{ic}|$ bandwidth for the C/P array, assuming the elements to be identical to C1CM-1, is shown in Figure #33 and the temperature range effectively narrows this bandwidth by as much as 20% over the entire range of measurement. The bandwidth is narrowed by less than 10% over the operational temperature range, however, and this bandwidth covers the midband frequency region quite adequately.

REFERENCES

1. J. S. Hickman, Trends in Modern Sonar Transducer Design, Proceedings of the 22nd National Electronics Conference, October 1966.

2. Notes for U. S. Navy Electronics Laboratory Seminar on Transducer Array Analysis and Evaluation, June 1965, by NUWC Transducer Division, Intra-Division Memo. #D604-160.

3. Laboratory Determination of Sonar Element Heating and Temperature Dependent Behavior Under Simulated Array Operating Conditions (CONF.), J. A. Ward, [25th Navy Symposium on Underwater Acoustics, November 1967 (title unclassified)]

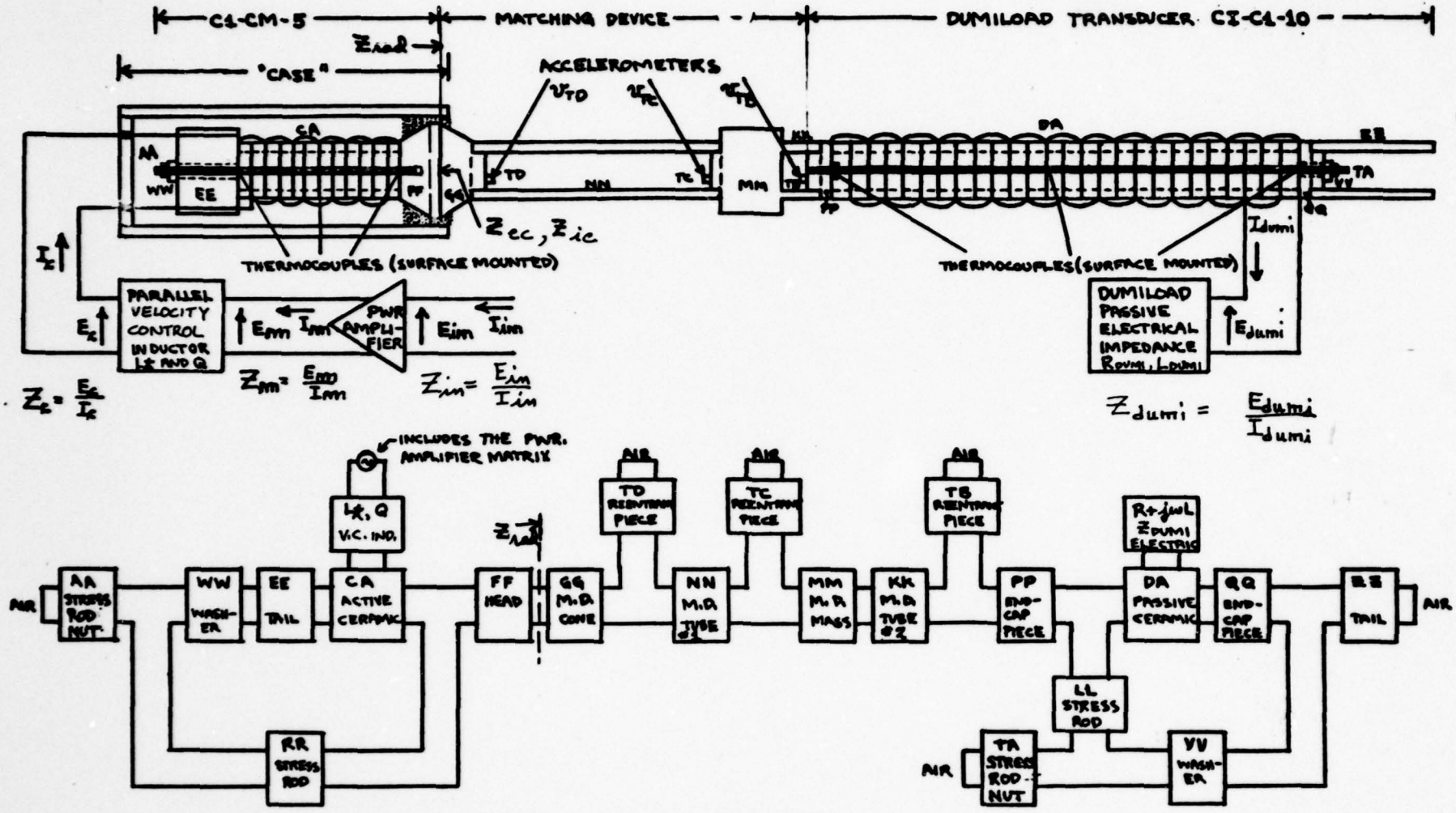

FIGURE 1: C1CM-5 DUMILOAD

K•E 10 X 10 TO ½ INCH 46 1320
7 X 10 INCHES MADE IN U.S.A.
KEUFFEL & ESSER CO.

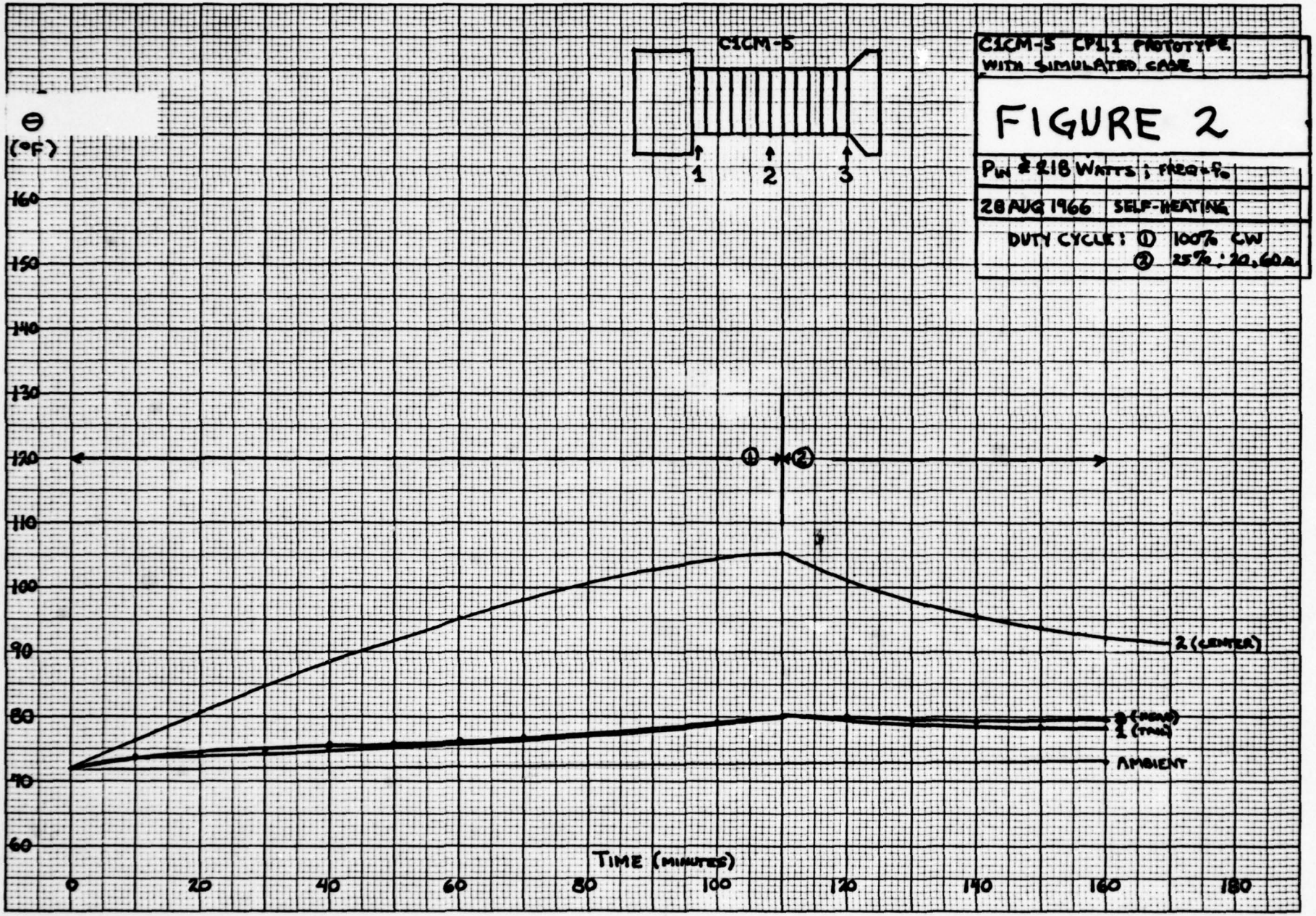

K·E 10 X 10 TO ½ INCH 7 X 10 INCHES 46 1320 MADE IN U.S.A.
KEUFFEL & ESSER CO.

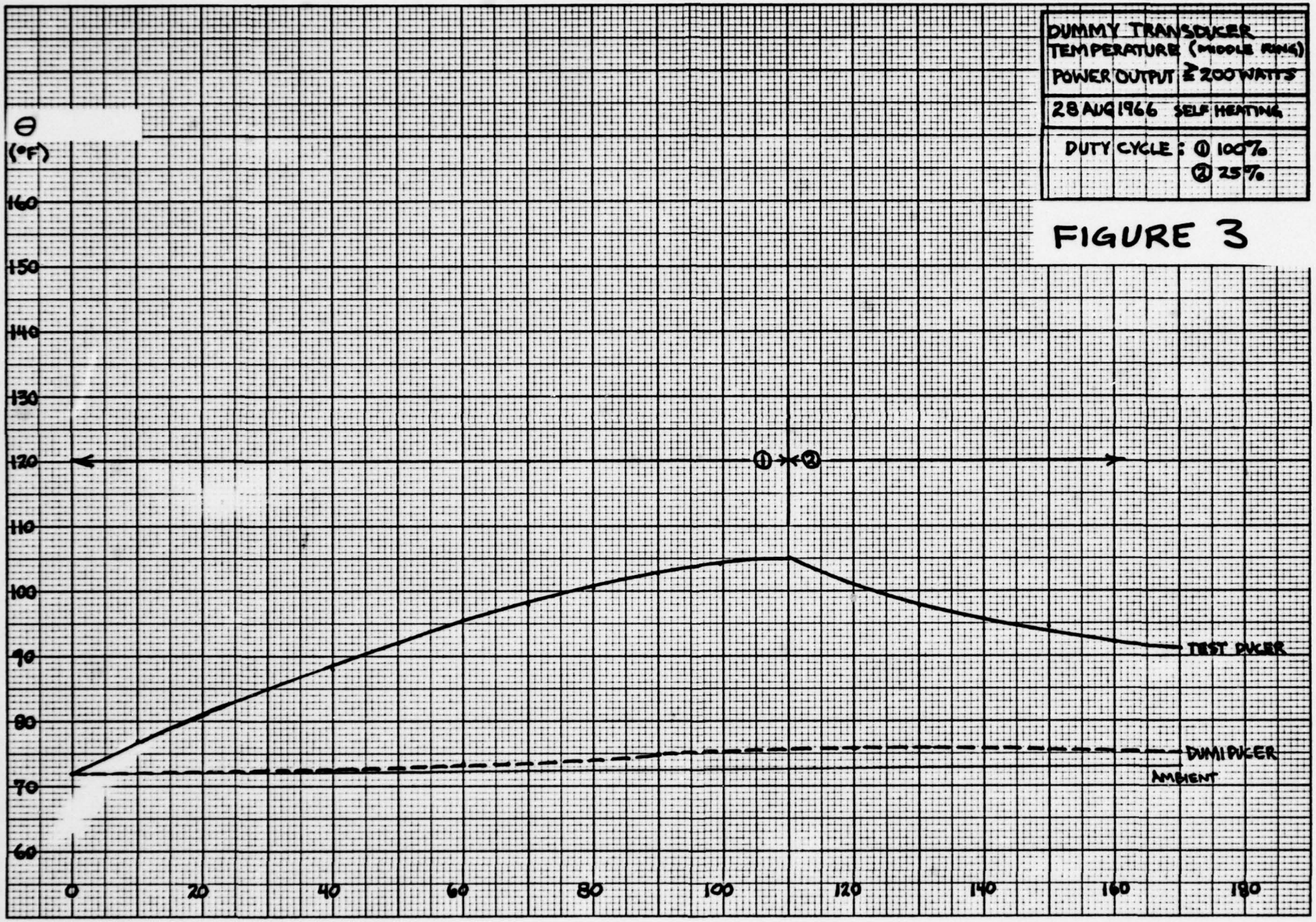

FIGURE 3

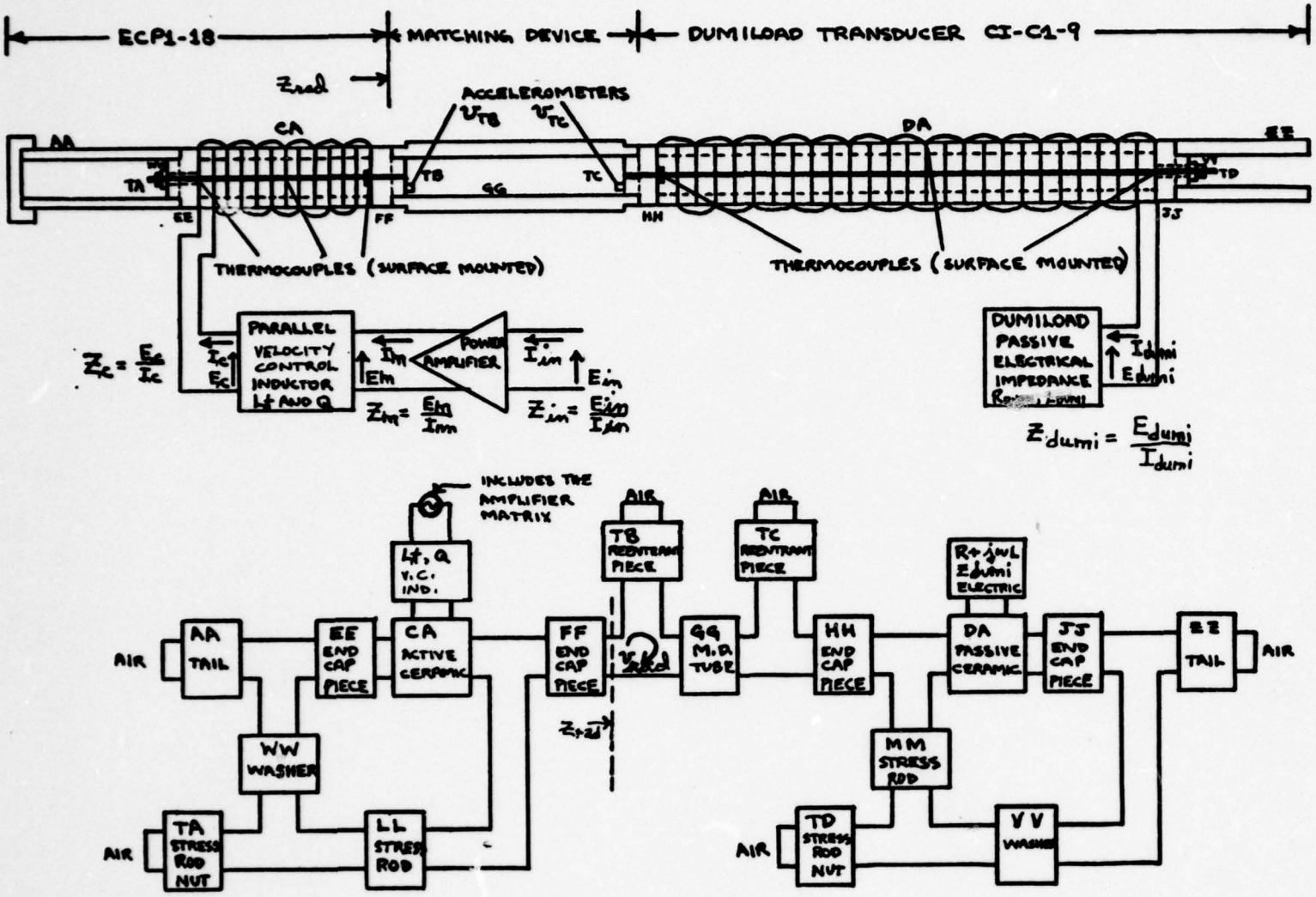

FIGURE 4: ECP1-18 DUMILOAD

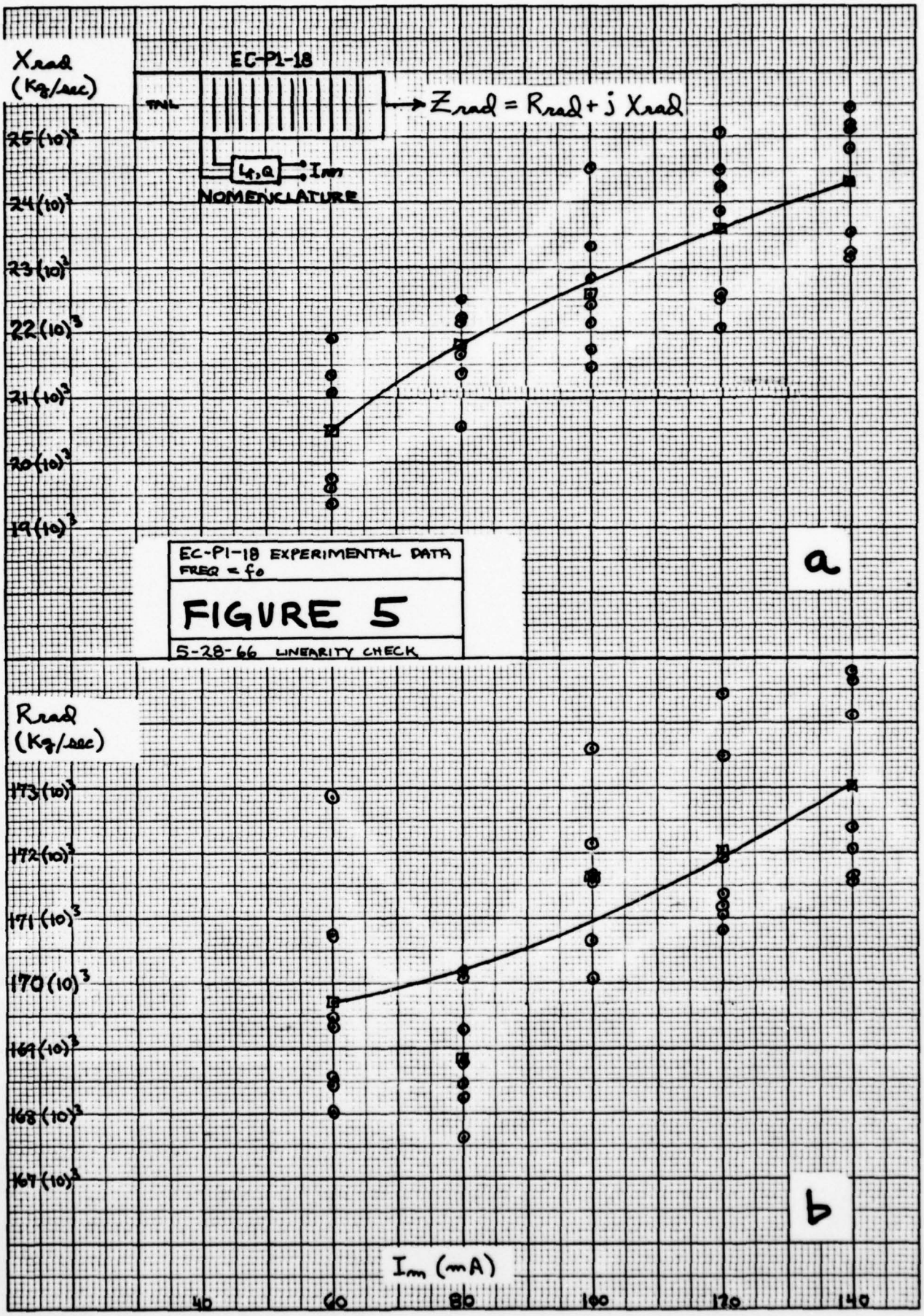

EC-P1-18 EXPERIMENTAL DATA
FREQ = f_0

FIGURE 5

5-28-66 LINEARITY CHECK

K&E 10 X 10 TO ½ INCH 46 1320
7 X 10 INCHES MADE IN U.S.A.
KEUFFEL & ESSER CO.

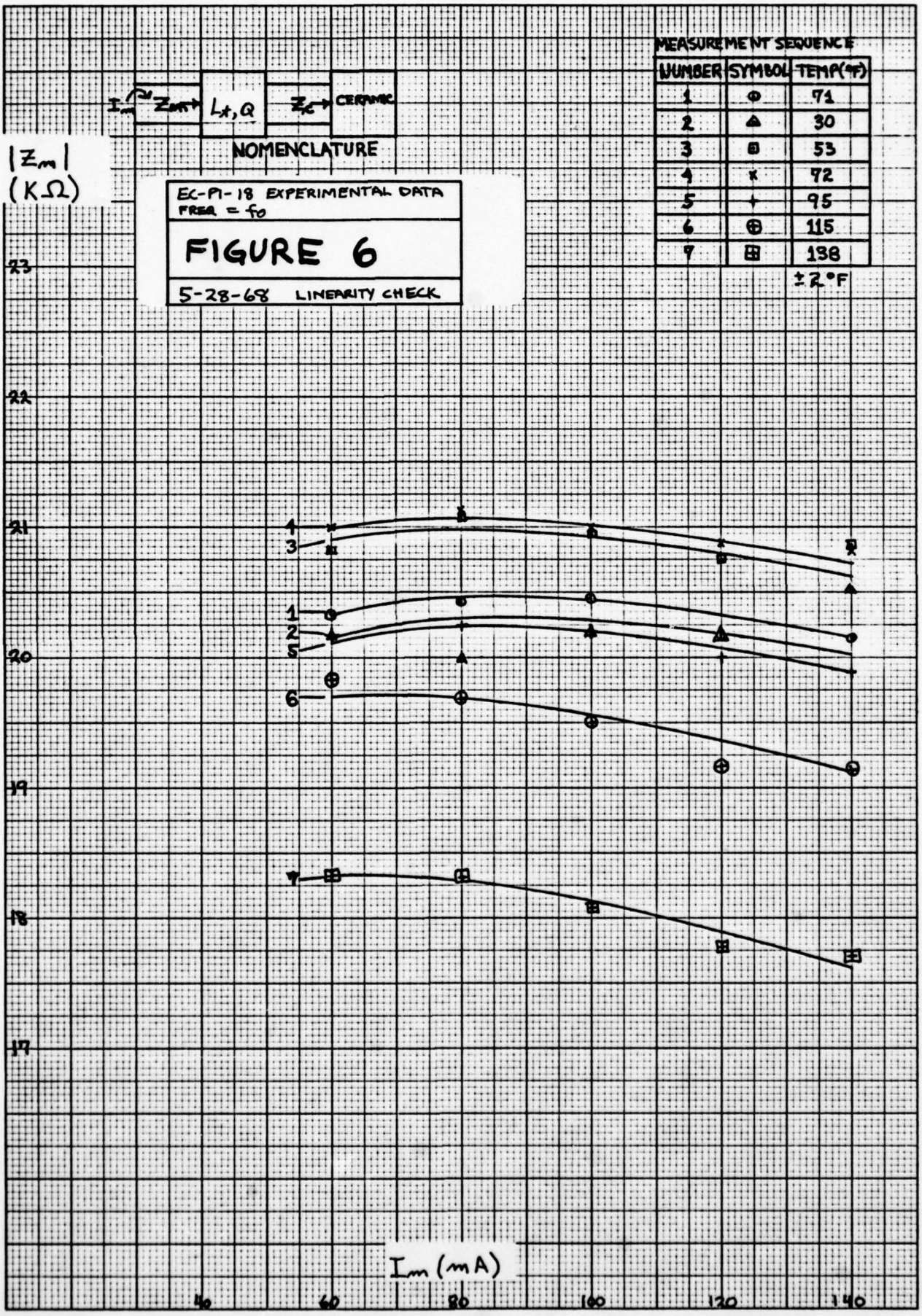

K&E 10 X 10 TO ½ INCH 46 1320
7 X 10 INCHES MADE IN U.S.A.
KEUFFEL & ESSER CO.

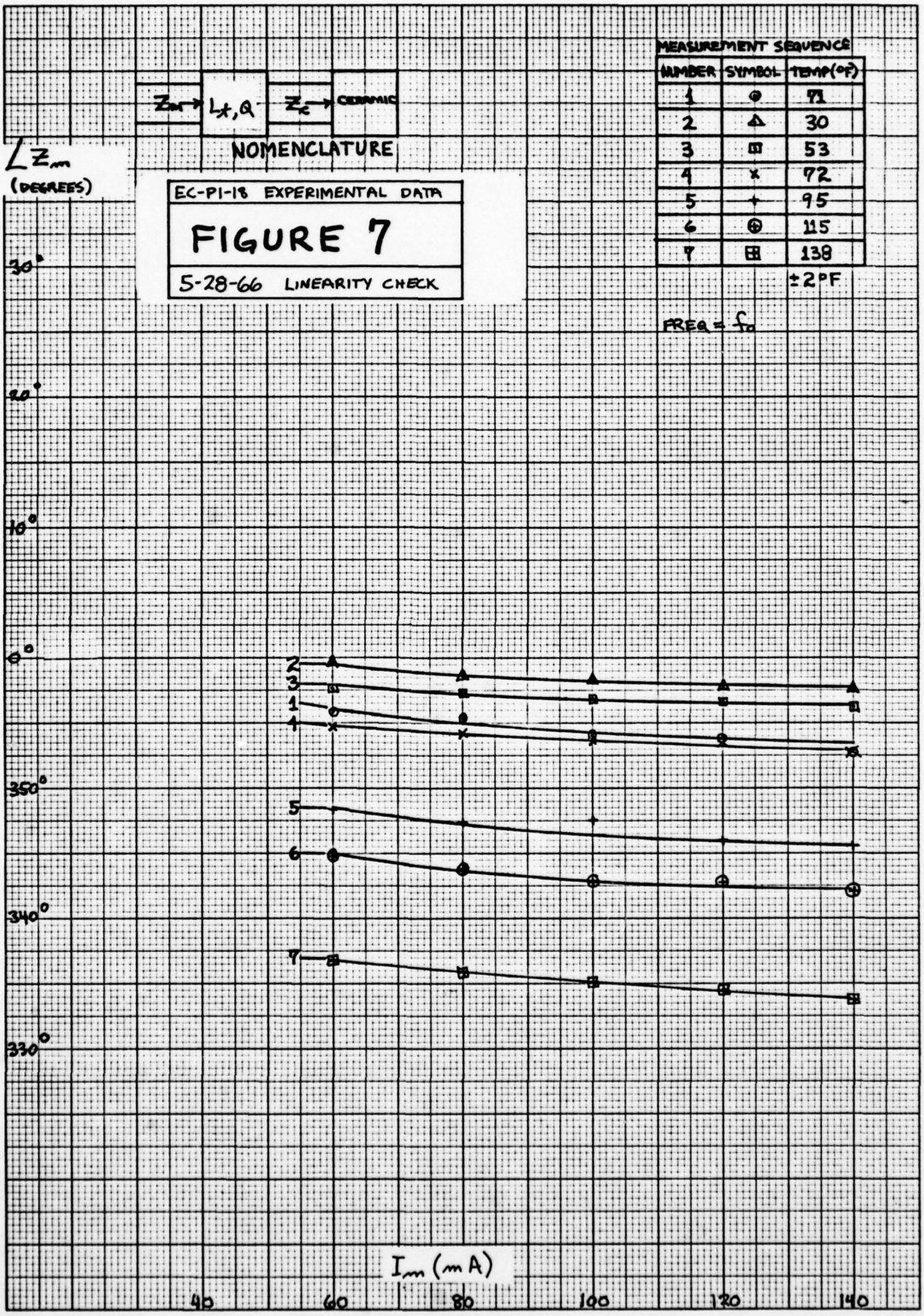

KEUFFEL & ESSER CO. MADE IN U.S.A. 46 1320 10 X 10 TO ½ INCH 7 X 10 INCHES

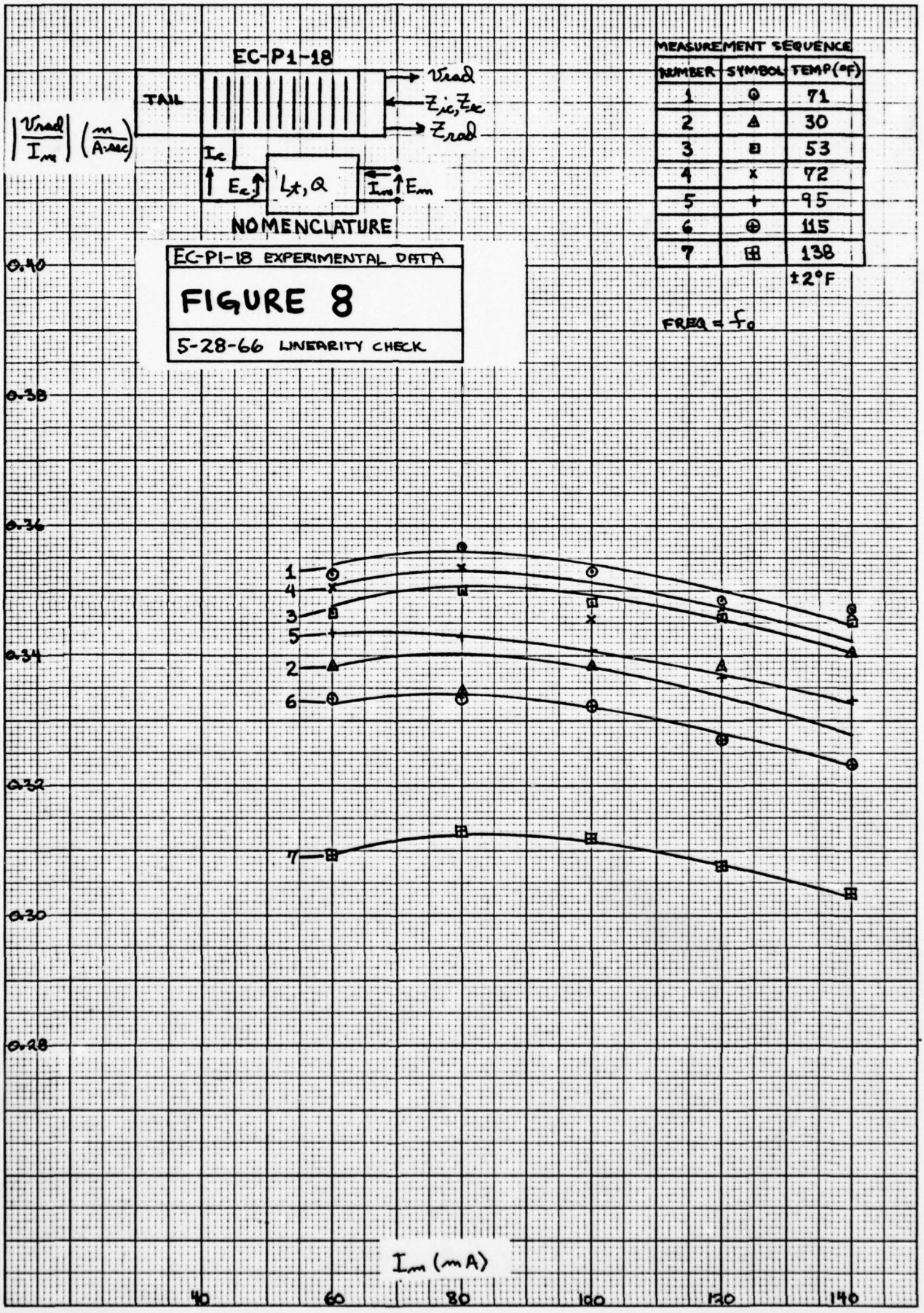

K&E 10 X 10 TO ½ INCH 46 1320
7 X 10 INCHES MADE IN U.S.A.
KEUFFEL & ESSER CO.

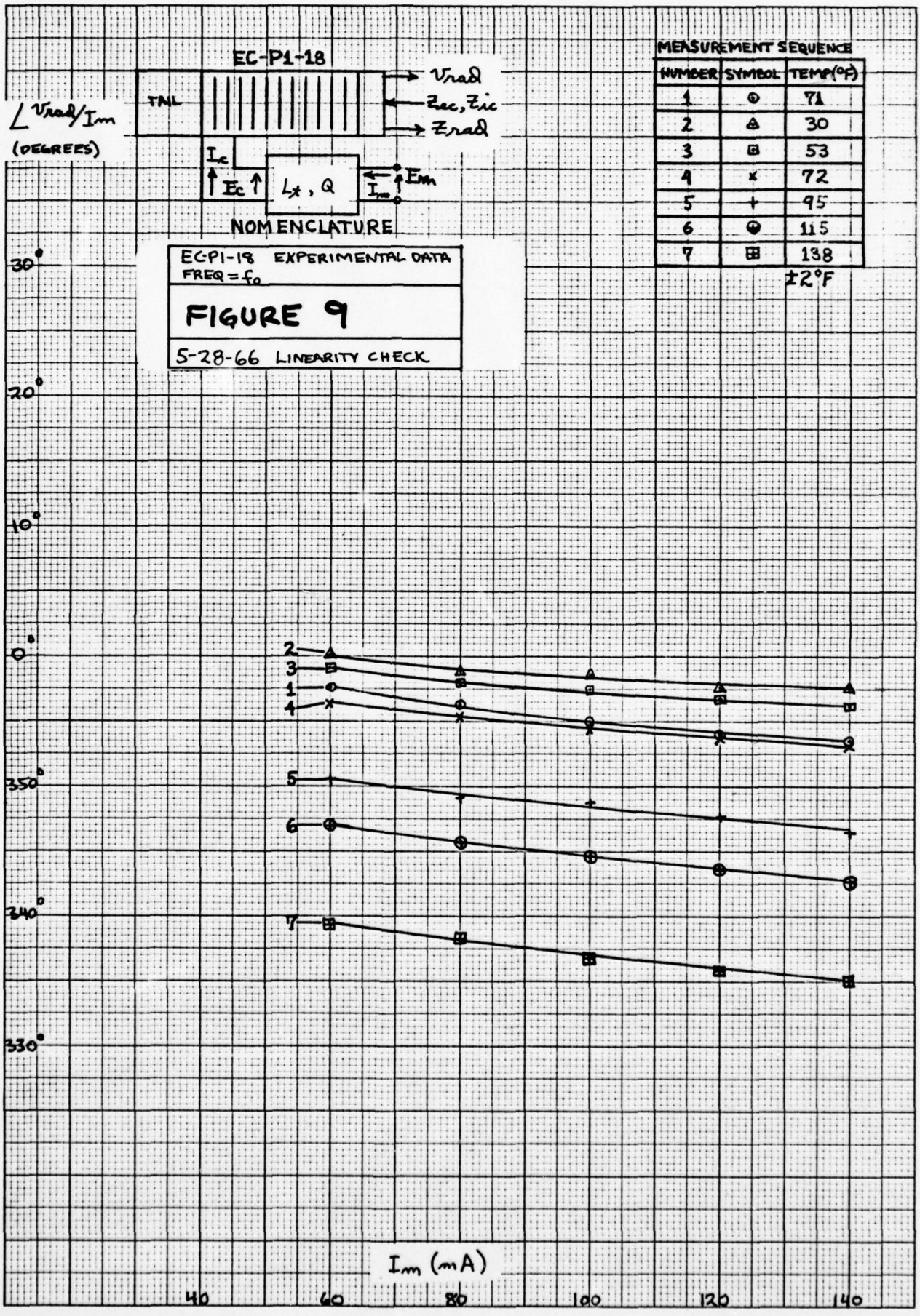

MEASUREMENT SEQUENCE		
NUMBER	SYMBOL	TEMP (°F)
1	⊙	71
2	△	30
3	⊡	53
4	×	72
5	+	95
6	⊕	115
7	⊞	138

±2°F

EC-P1-18 EXPERIMENTAL DATA
FREQ = f_o

FIGURE 9

5-28-66 LINEARITY CHECK

K&E 10 X 10 TO ½ INCH 46 1320
7 X 10 INCHES MADE IN U.S.A.
KEUFFEL & ESSER CO.

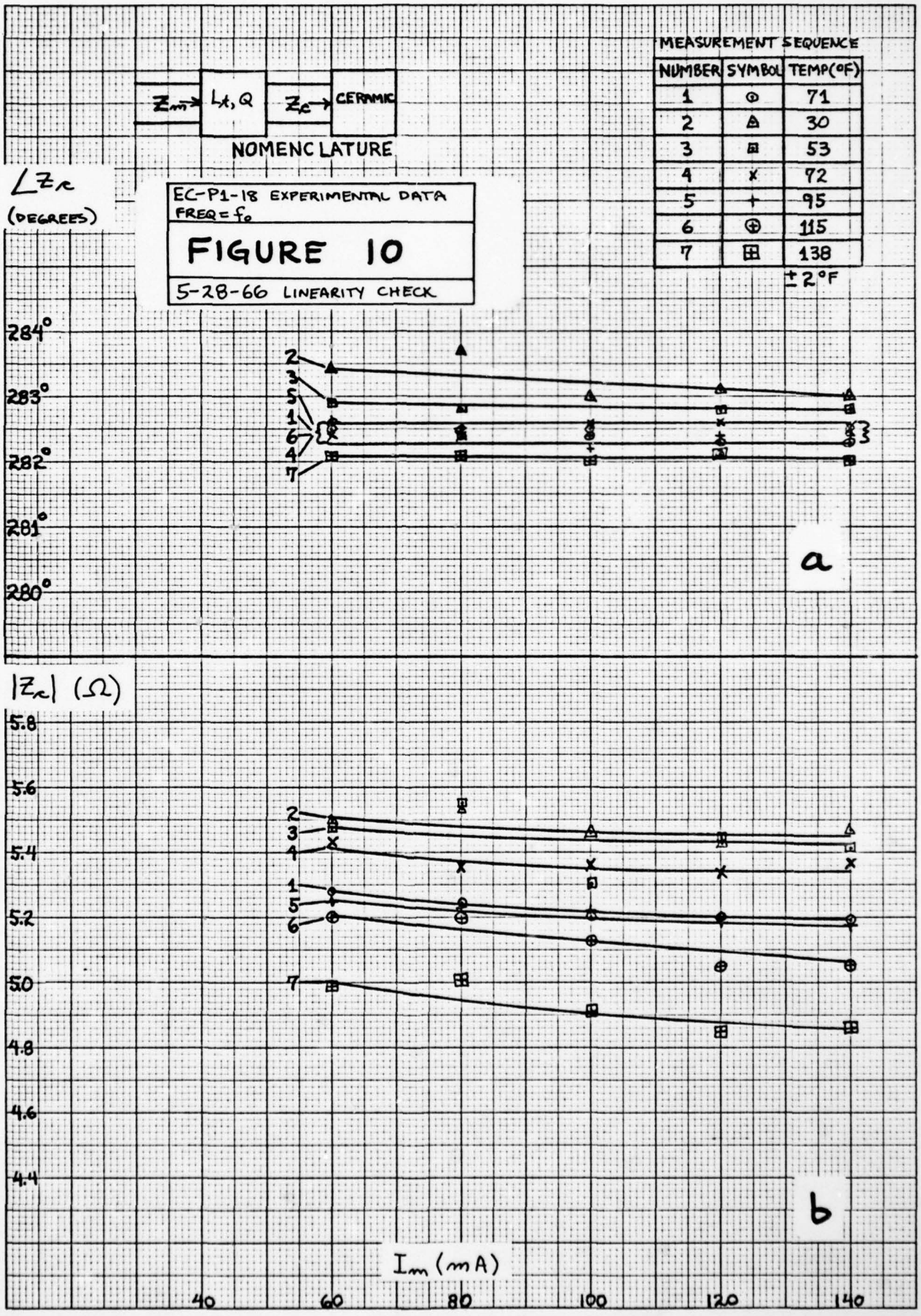

K&E 10 X 10 TO ½ INCH 46 1320
7 X 10 INCHES MADE IN U.S.A.
KEUFFEL & ESSER CO.

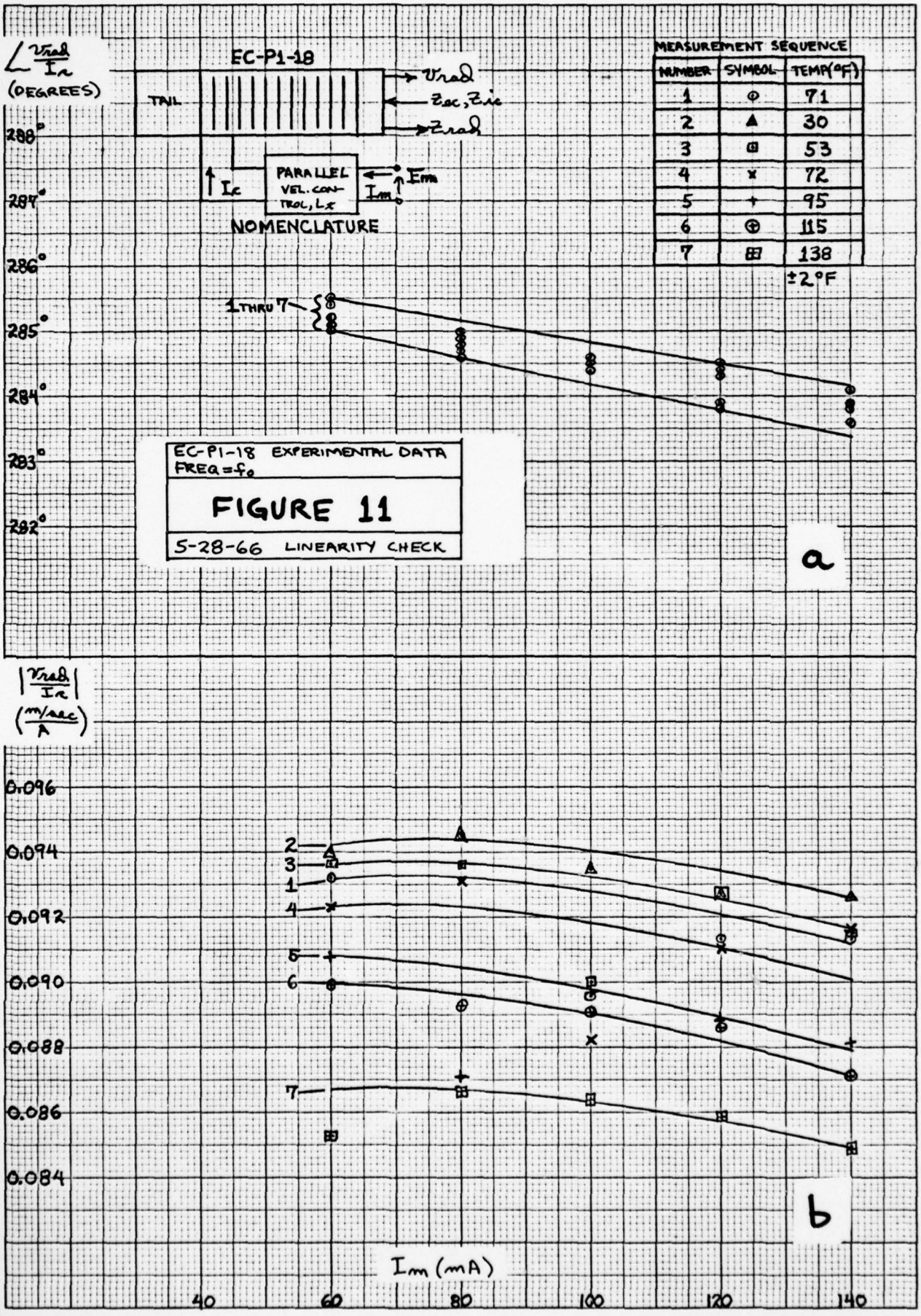

EC-P1-18 EXPERIMENTAL DATA
FREQ = f_o

FIGURE 11

5-28-66 LINEARITY CHECK

KE 10 X 10 TO ½ INCH 46 1320
7 X 10 INCHES MADE IN U.S.A.
KEUFFEL & ESSER CO.

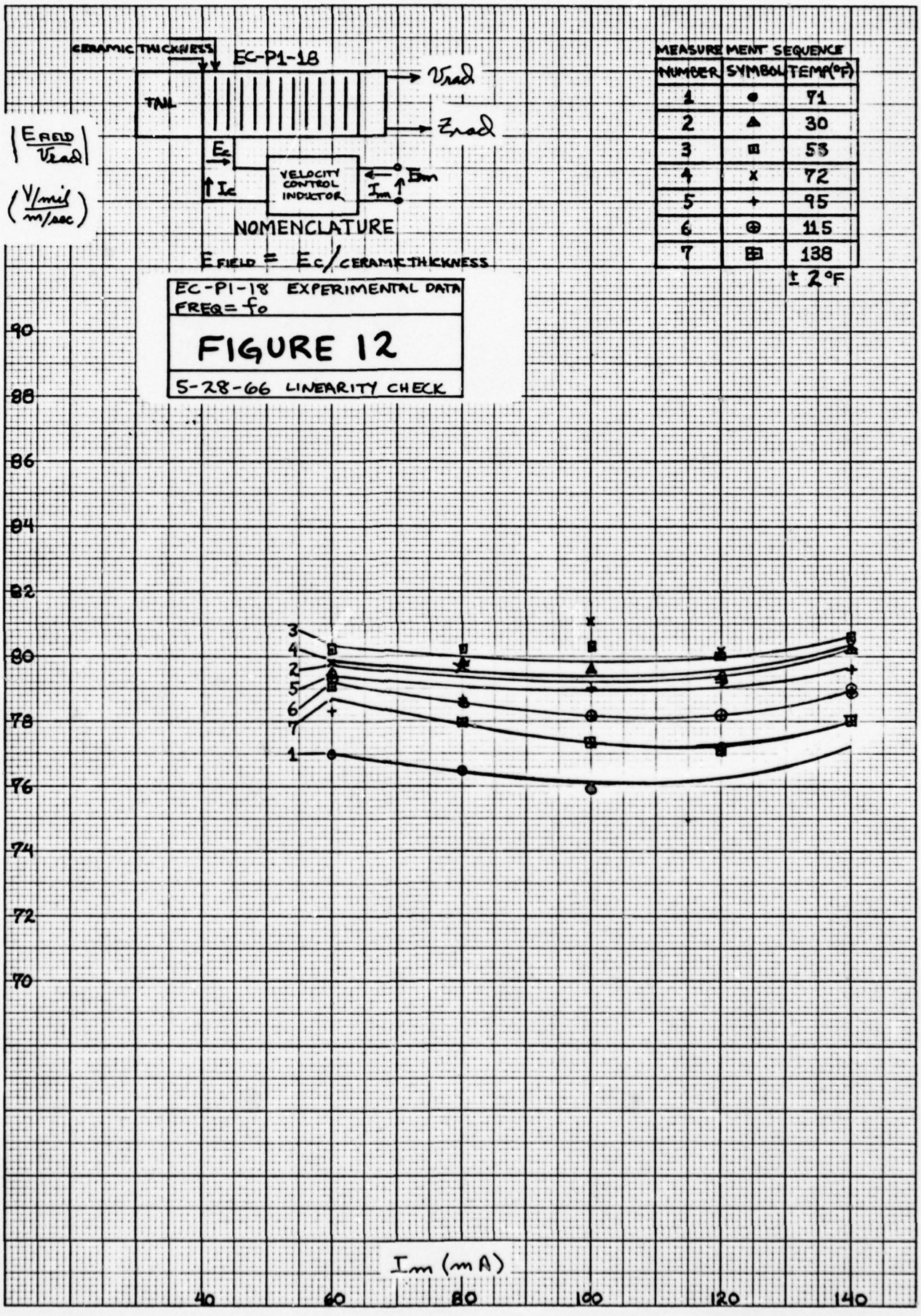

K&E 10 X 10 TO ½ INCH 46 1320
7 X 10 INCHES MADE IN U.S.A.
KEUFFEL & ESSER CO.

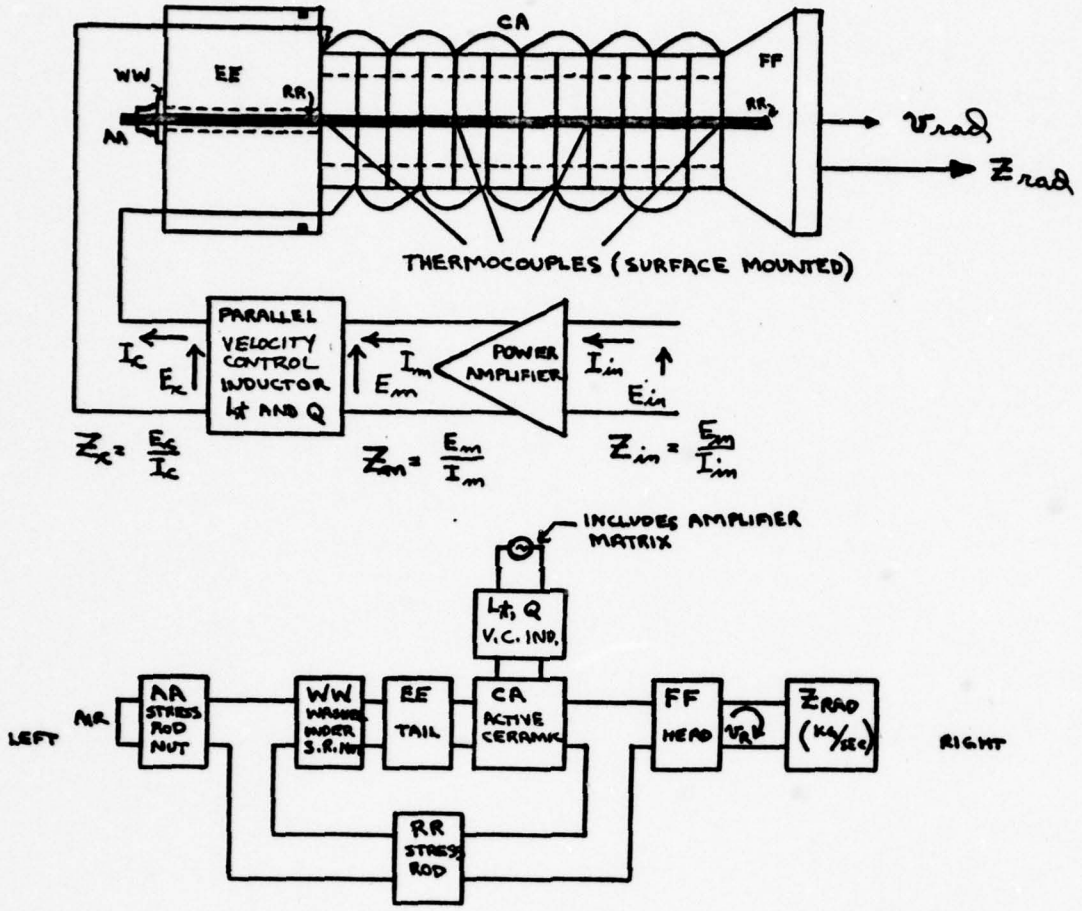

FIGURE 13: C1CM-1 TRANSDUCER

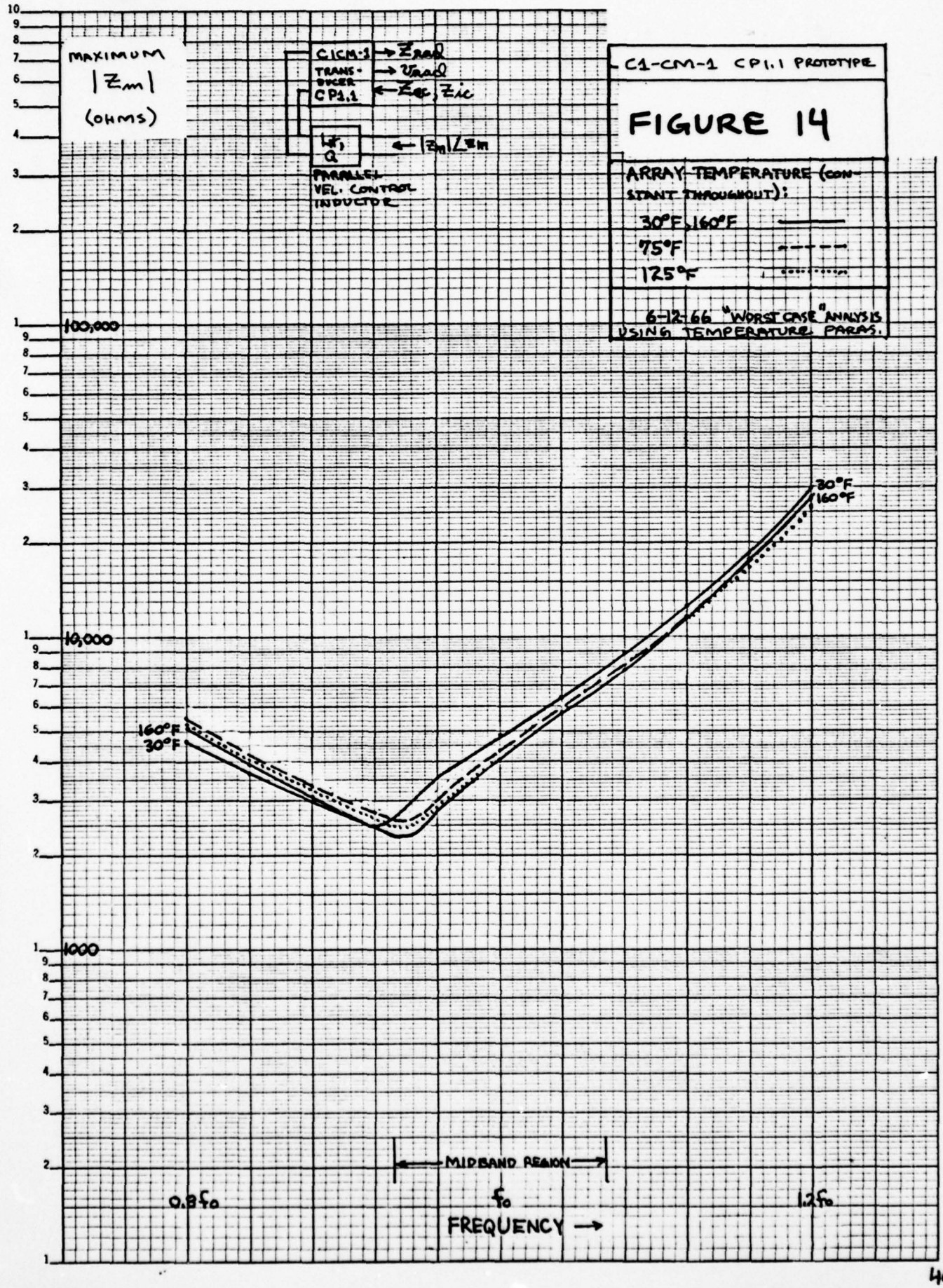

K&E SEMI-LOGARITHMIC 46 6012
4 CYCLES X 70 DIVISIONS MADE IN U.S.A.
KEUFFEL & ESSER CO.

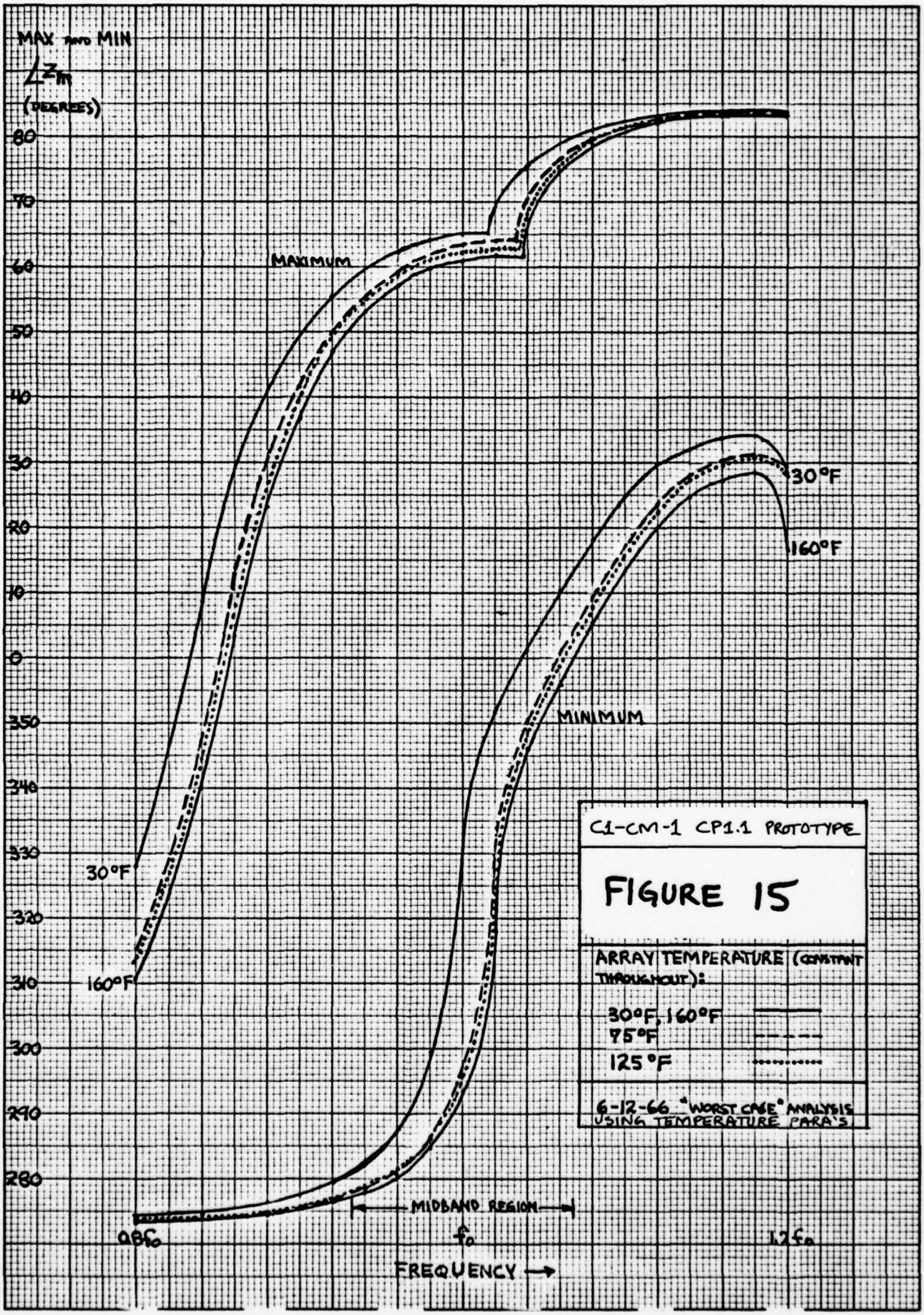

K&E 10 X 10 TO ½ INCH 46 1322
7 X 10 INCHES MADE IN U.S.A.
KEUFFEL & ESSER CO.

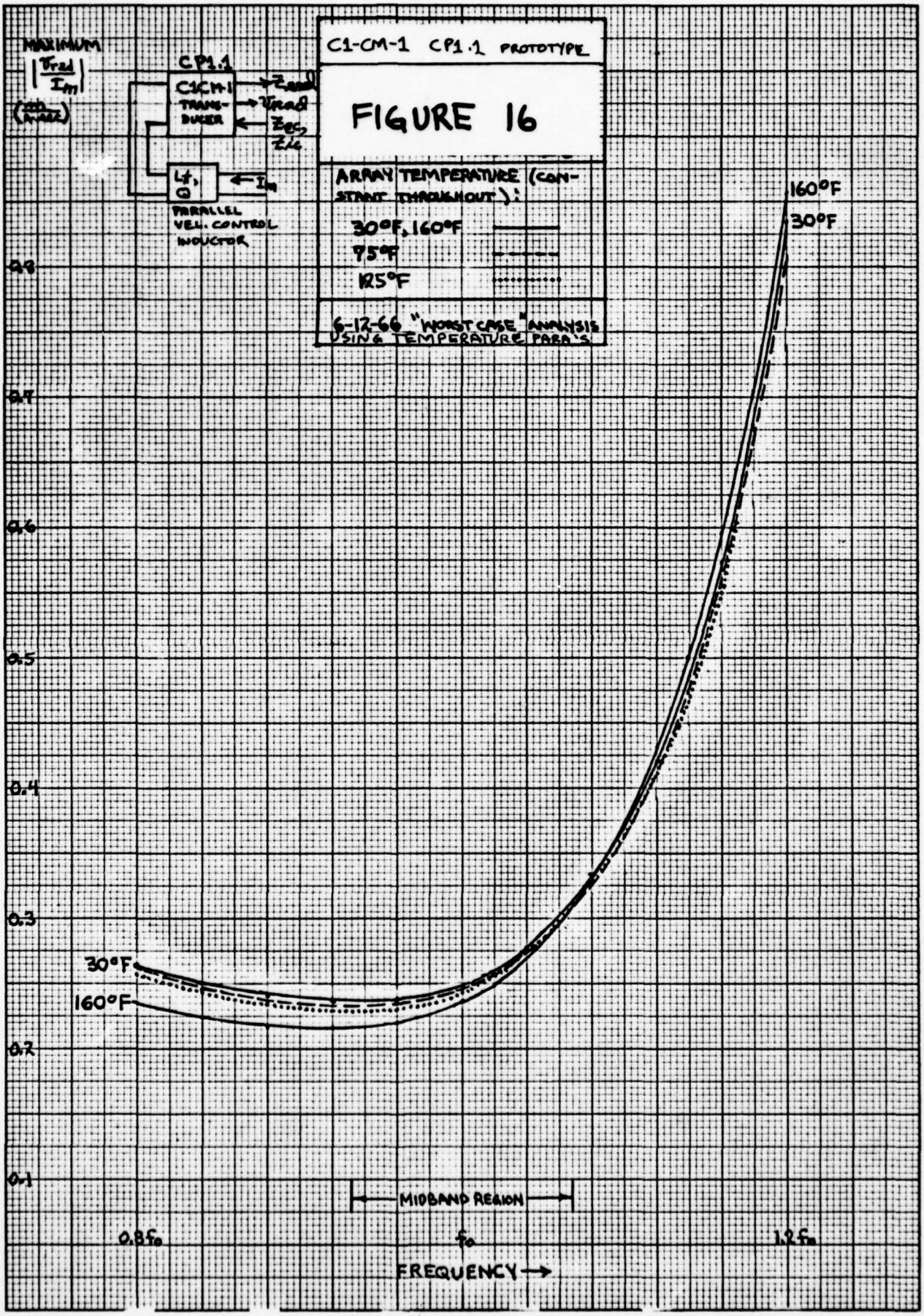

K&E 10 X 10 TO ½ INCH 46 1322
7 X 10 INCHES MADE IN U.S.A.
KEUFFEL & ESSER CO.

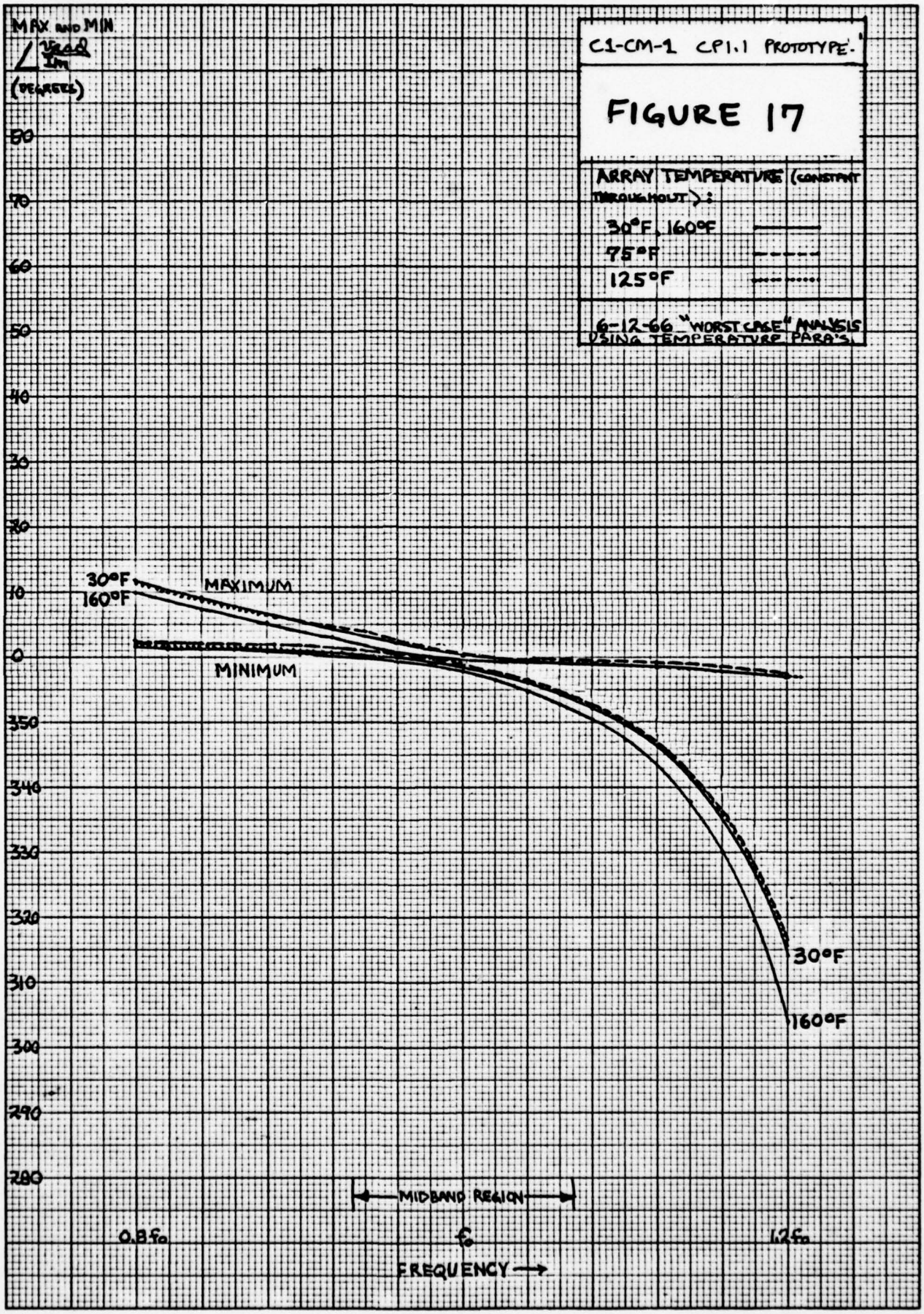

KEUFFEL & ESSER CO. MADE IN U.S.A. 10 X 10 TO ½ INCH 46 1322 7 X 10 INCHES

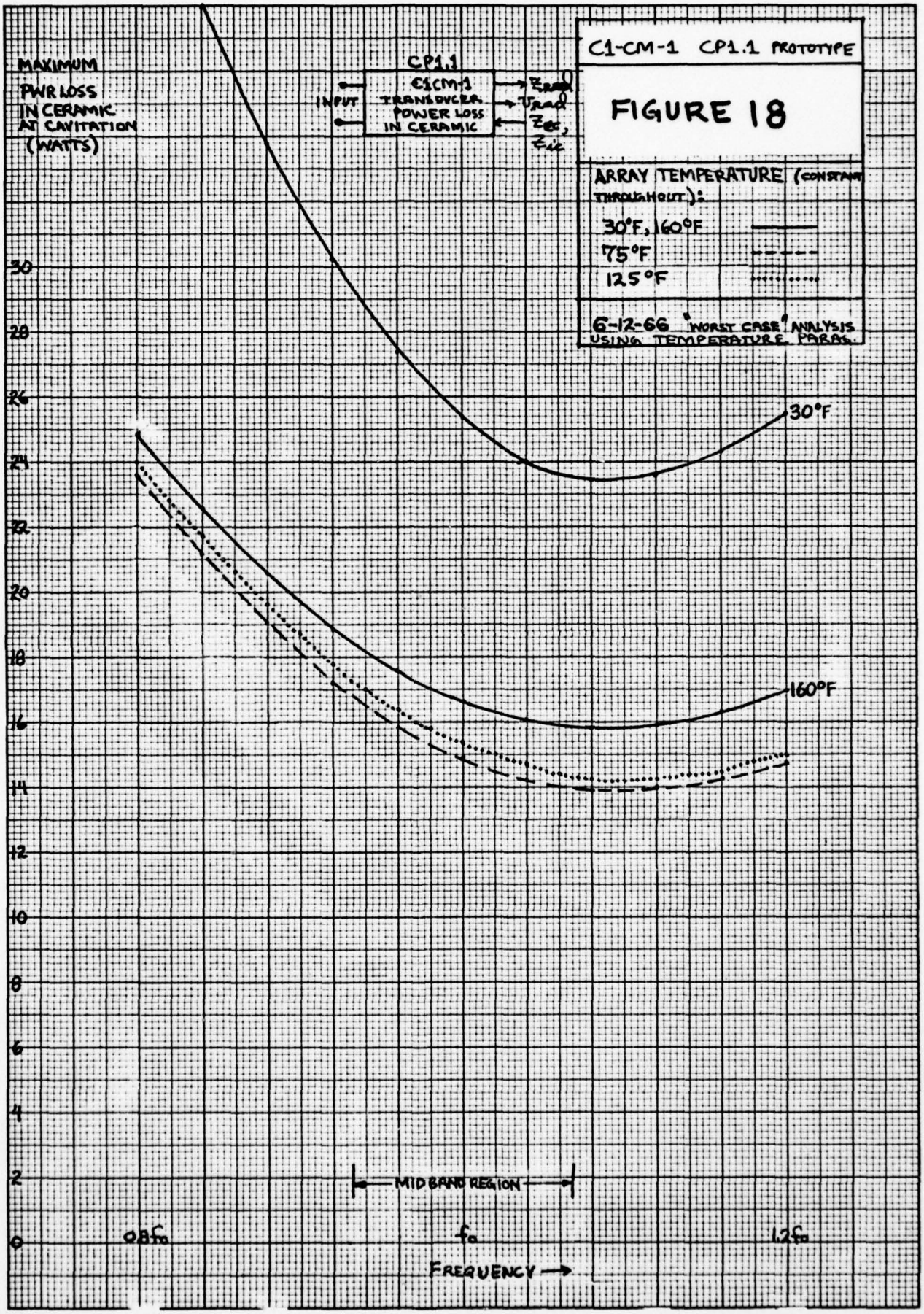

K&E 10 X 10 TO ½ INCH 46 1322
7 X 10 INCHES
MADE IN U.S.A.
KEUFFEL & ESSER CO.

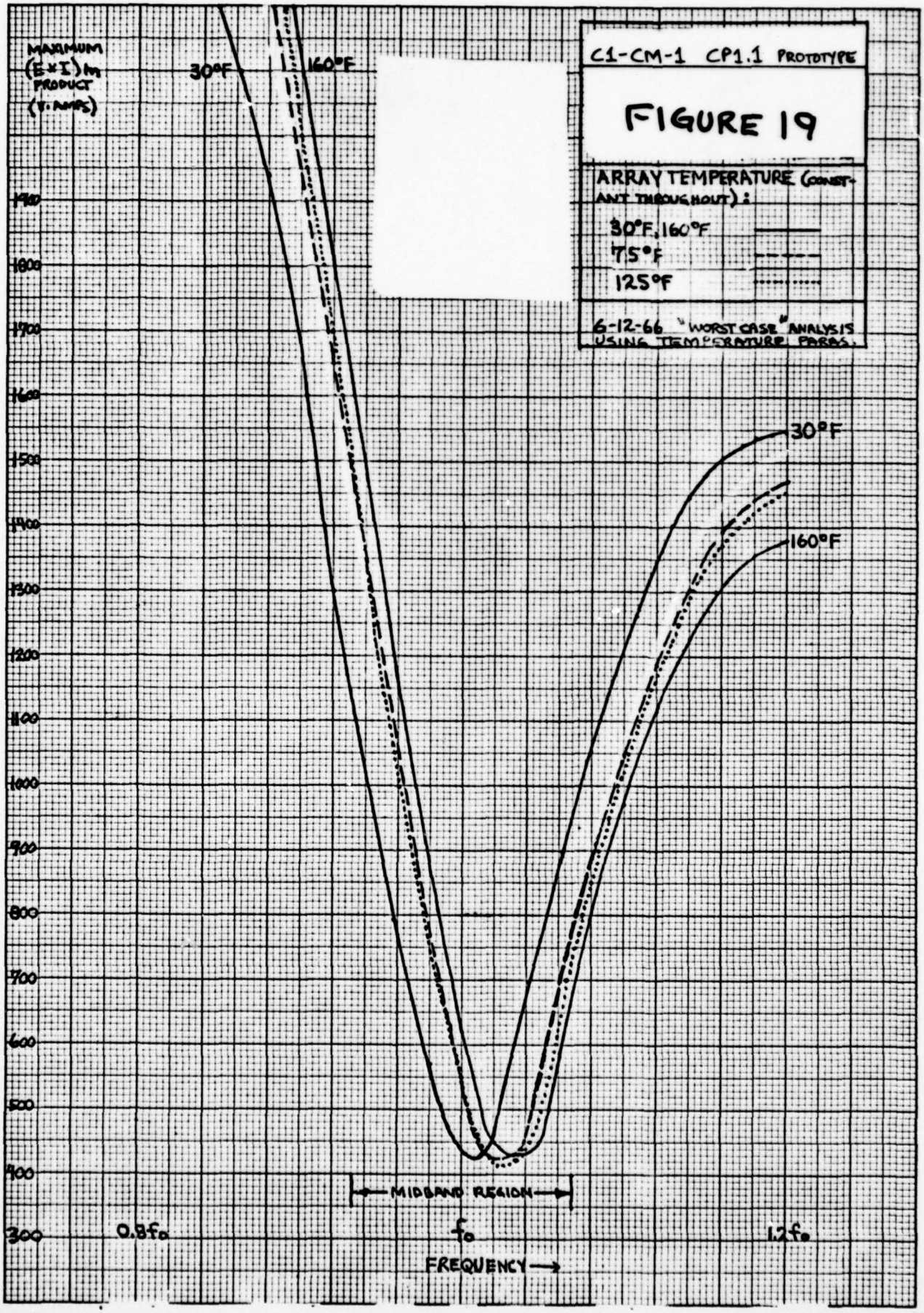

K&E 10 X 10 TO ½ INCH 46 1322
7 X 10 INCHES MADE IN U.S.A.
KEUFFEL & ESSER CO.

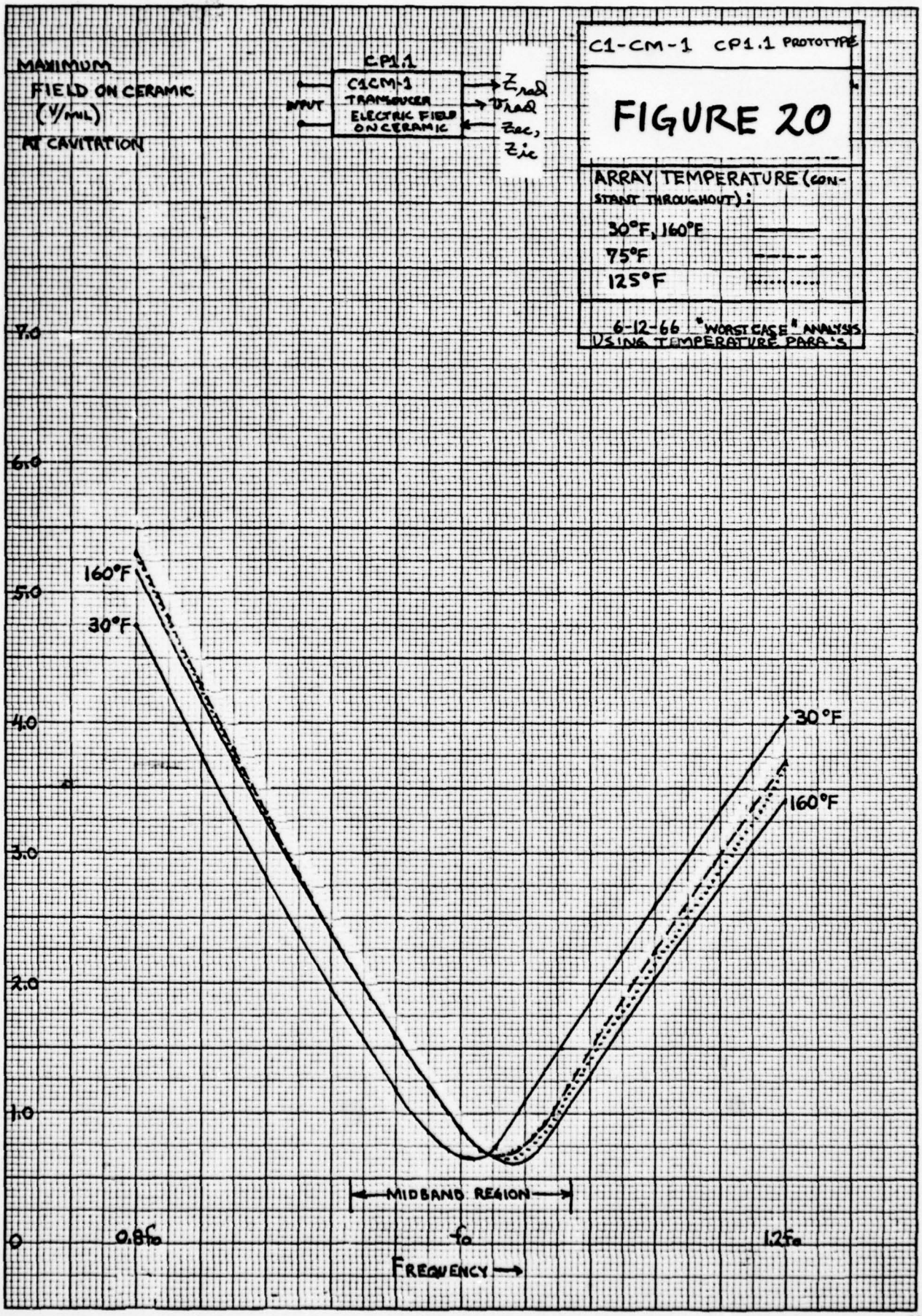

K&E 10 X 10 TO ½ INCH 46 1322
7 X 10 INCHES MADE IN U.S.A.
KEUFFEL & ESSER CO.

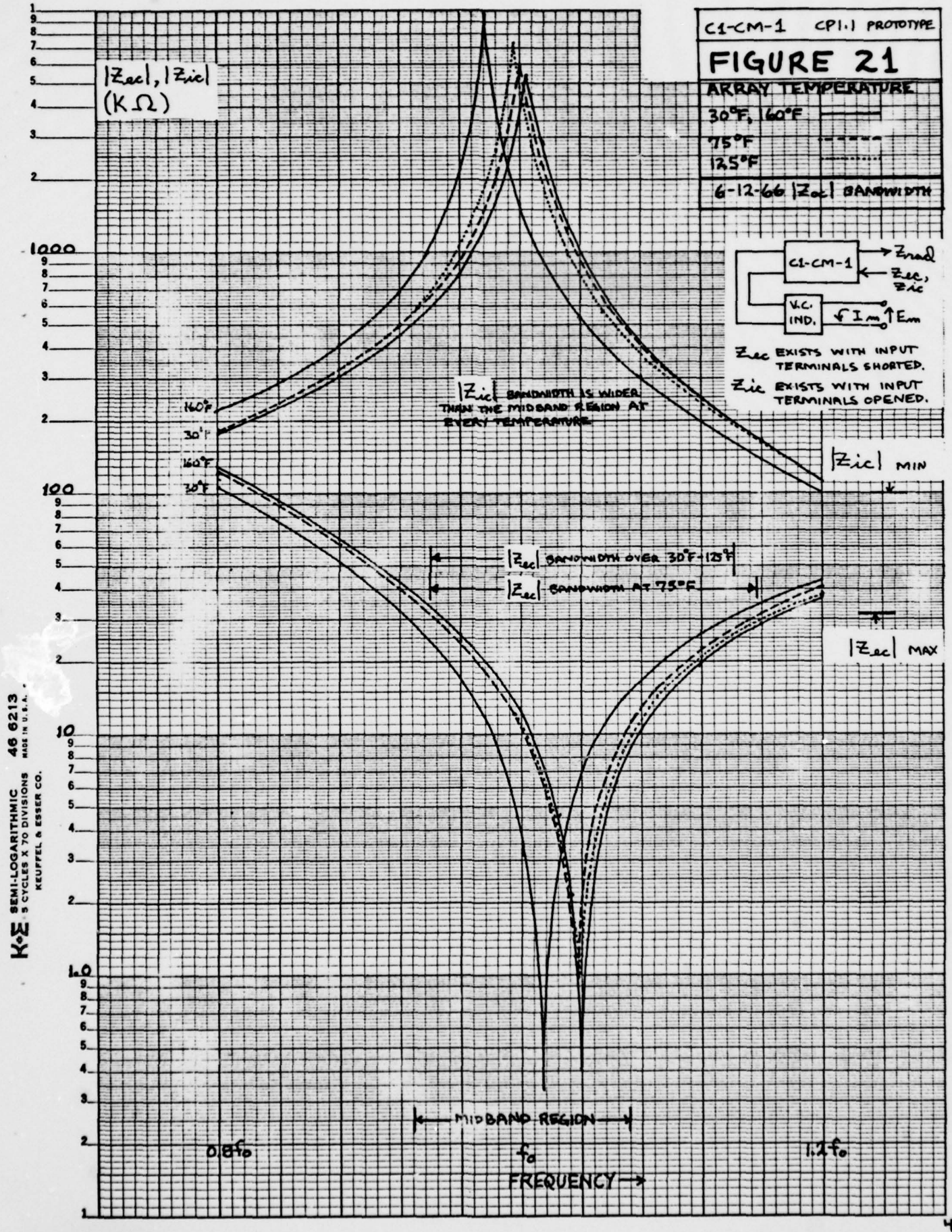
C1-CM-1 CP1.1 PROTOTYPE
FIGURE 21
ARRAY TEMPERATURE
30°F, 160°F
75°F
125°F
6-12-66 |Zec| BANDWIDTH
|Zec|, |Zic| (KΩ)
C1-CM-1
Zrad
Zec, Zic
V.C. IND.
Im
Em
Zec EXISTS WITH INPUT TERMINALS SHORTED.
Zic EXISTS WITH INPUT TERMINALS OPENED.
|Zic| BANDWIDTH IS WIDER THAN THE MIDBAND REGION AT EVERY TEMPERATURE.
160°F
30°F
160°F
30°F
|Zic| MIN
|Zec| BANDWIDTH OVER 30°F-125°F
|Zec| BANDWIDTH AT 75°F
|Zec| MAX
MIDBAND REGION
0.8fo
fo
1.2fo
FREQUENCY
1000
100
10
1.0
K&E SEMI-LOGARITHMIC 46 6213
5 CYCLES X 70 DIVISIONS MADE IN U.S.A.
KEUFFEL & ESSER CO.

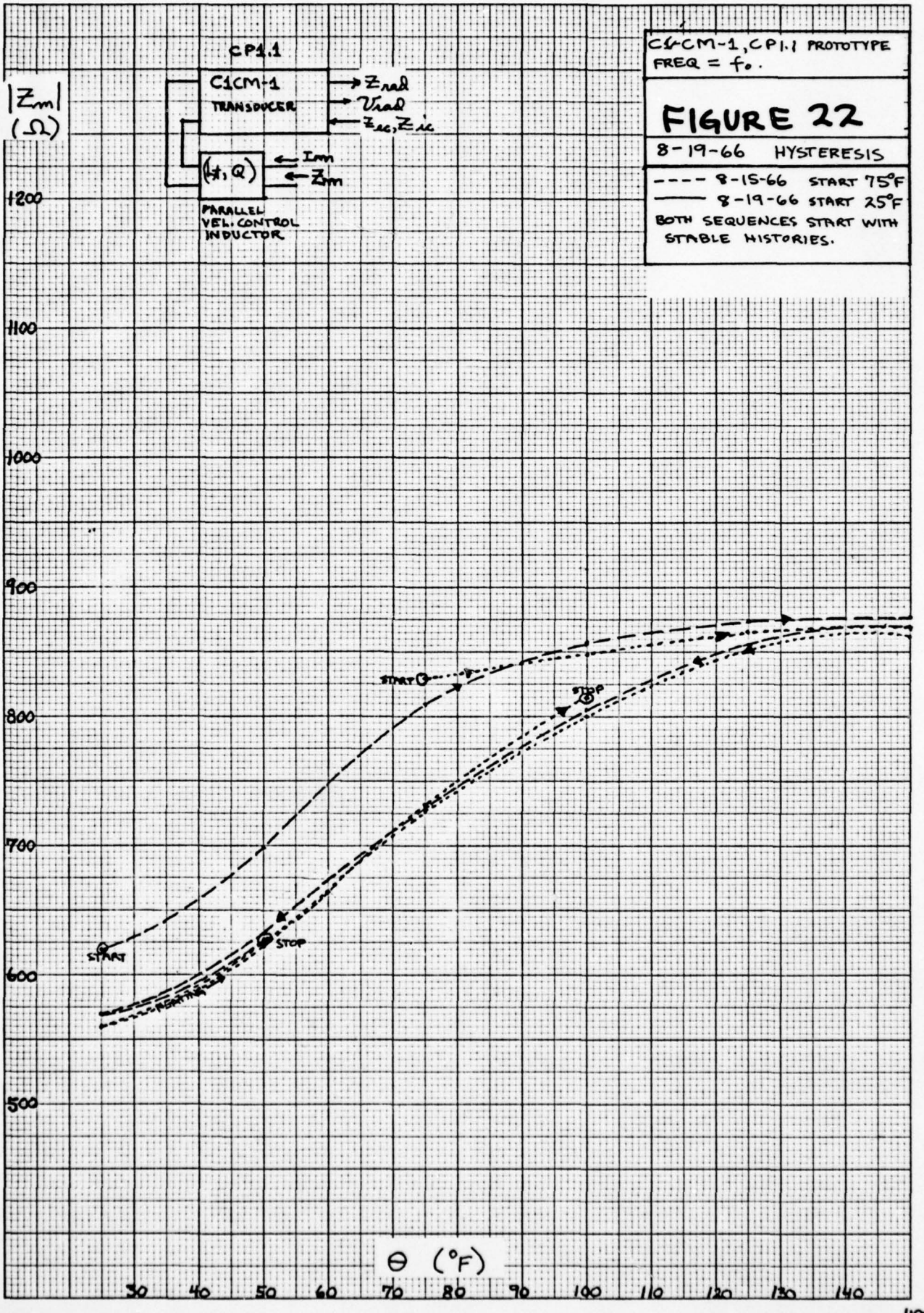

C1-CM-1, CP1.1 PROTOTYPE
FREQ = f_o.

FIGURE 22

8-19-66 HYSTERESIS

---- 8-15-66 START 75°F
——— 8-19-66 START 25°F
BOTH SEQUENCES START WITH STABLE HISTORIES.

K&E 10 X 10 TO ½ INCH 46 1320
7 X 10 INCHES MADE IN U.S.A.
KEUFFEL & ESSER CO.

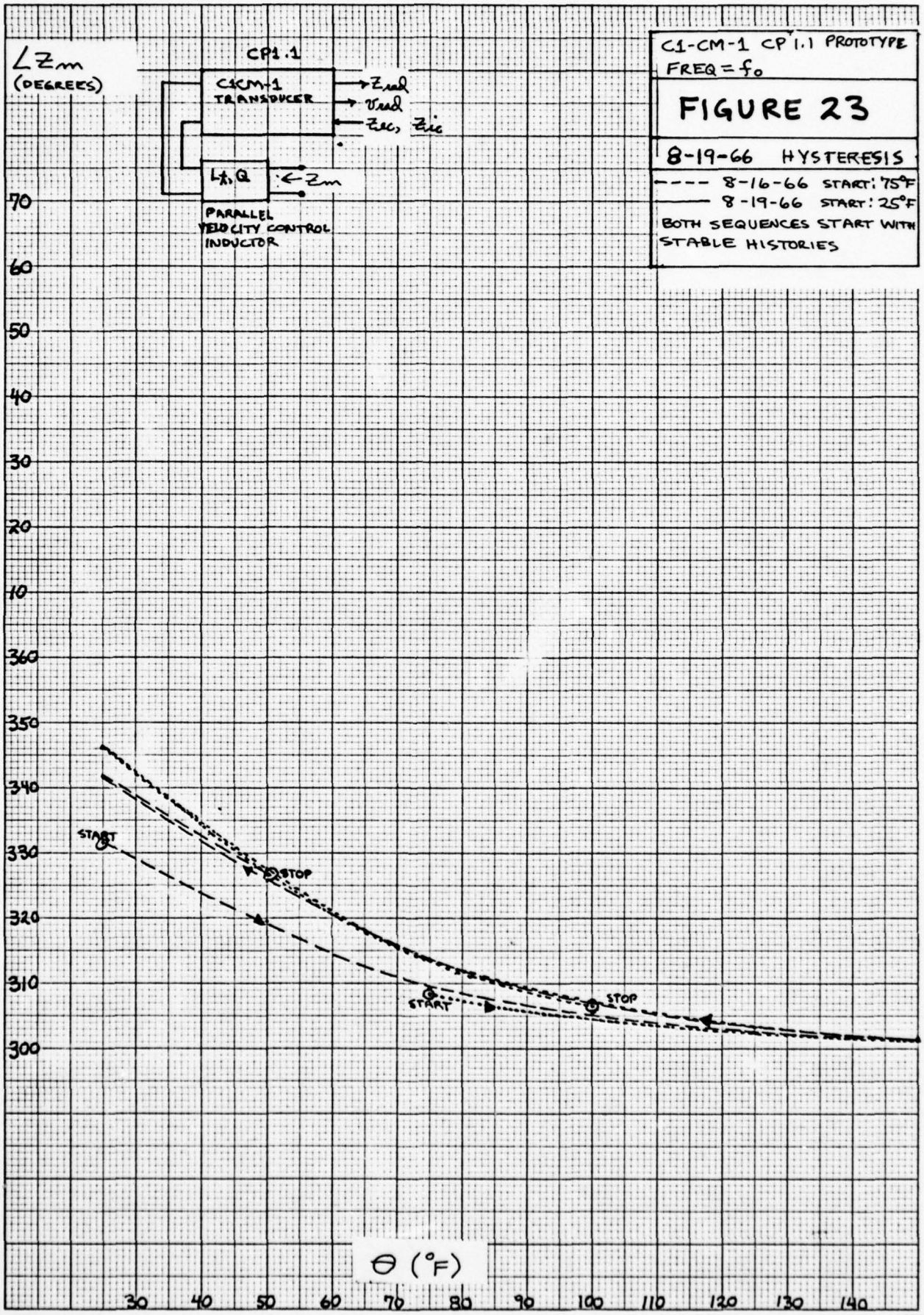

K&E 10 X 10 TO ½ INCH 46 1320
7 X 10 INCHES
KEUFFEL & ESSER CO.
MADE IN U.S.A.

C1-CM-1, CP1.1 PROTOTYPE
FREQ = f_o

FIGURE 24

8-19-66 HYSTERESIS

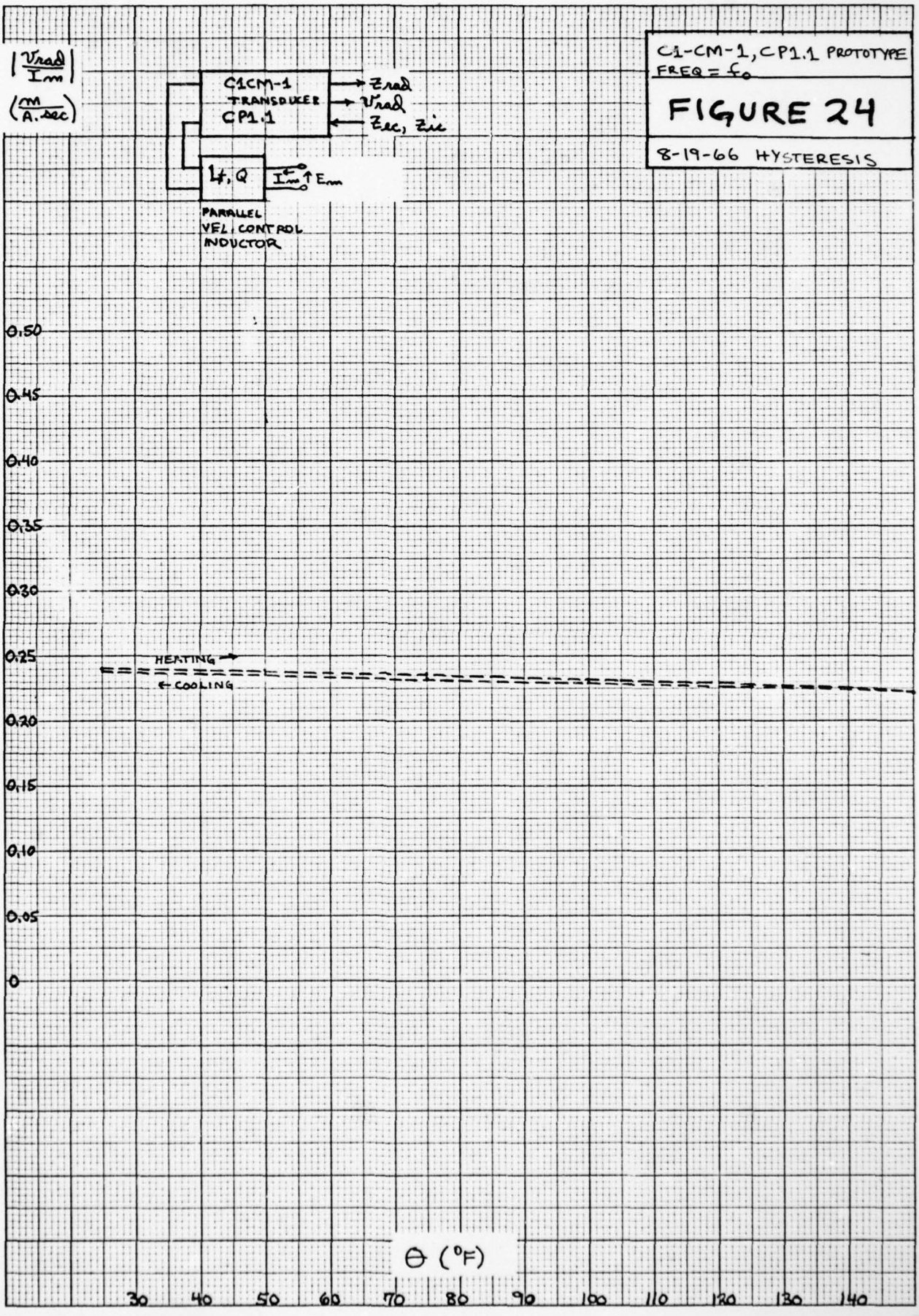

K&E 10 X 10 TO ½ INCH 46 1320
7 X 10 INCHES
MADE IN U.S.A.
KEUFFEL & ESSER CO.

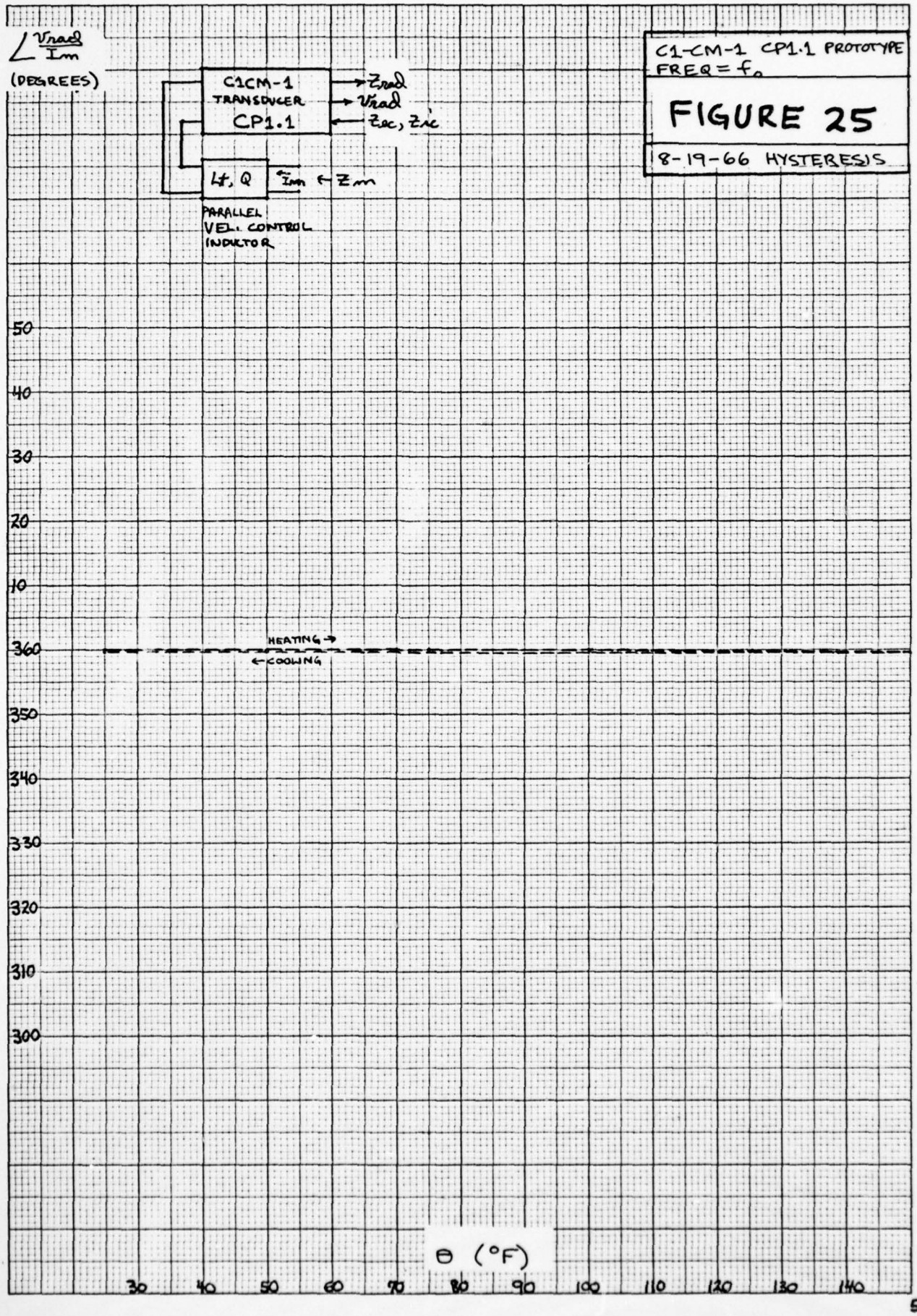

KE 10 X 10 TO ½ INCH 46 1320
7 X 10 INCHES
KEUFFEL & ESSER CO.
MADE IN U.S.A.

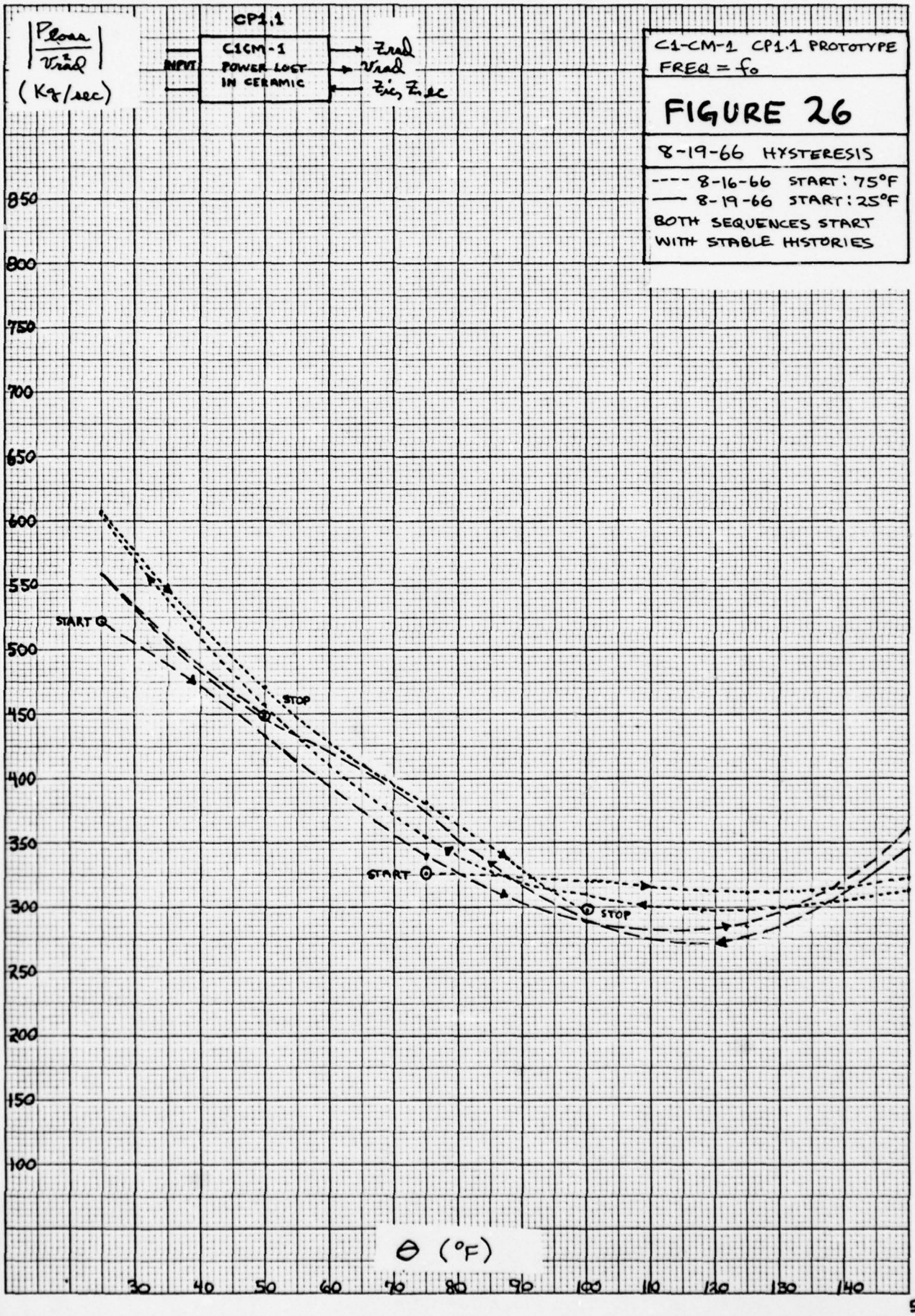

K&E 10 X 10 TO ½ INCH 46 1320
7 X 10 INCHES MADE IN U.S.A.
KEUFFEL & ESSER CO.

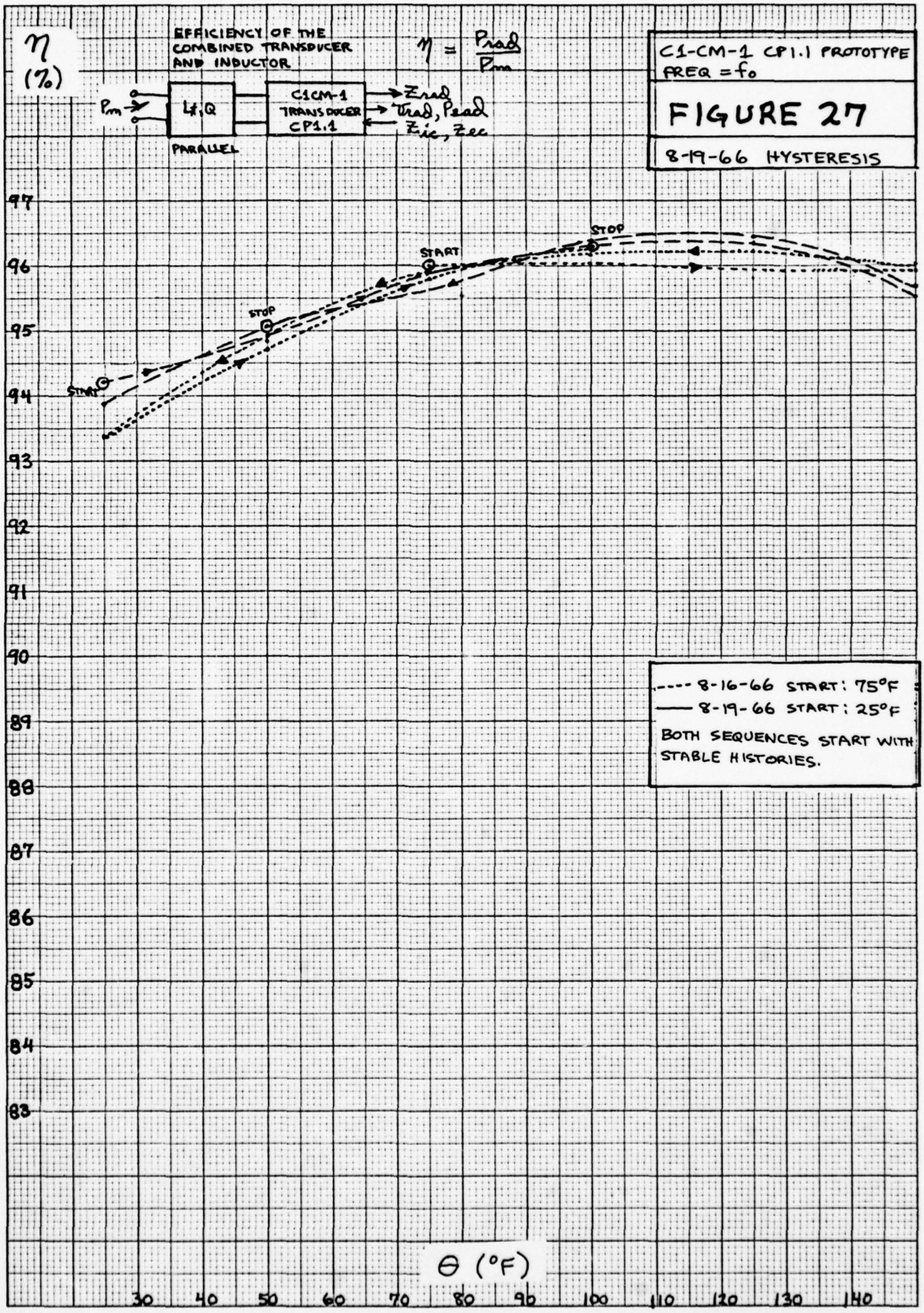

K&E 10 X 10 TO ½ INCH 46 1320
7 X 10 INCHES MADE IN U.S.A.
KEUFFEL & ESSER CO.

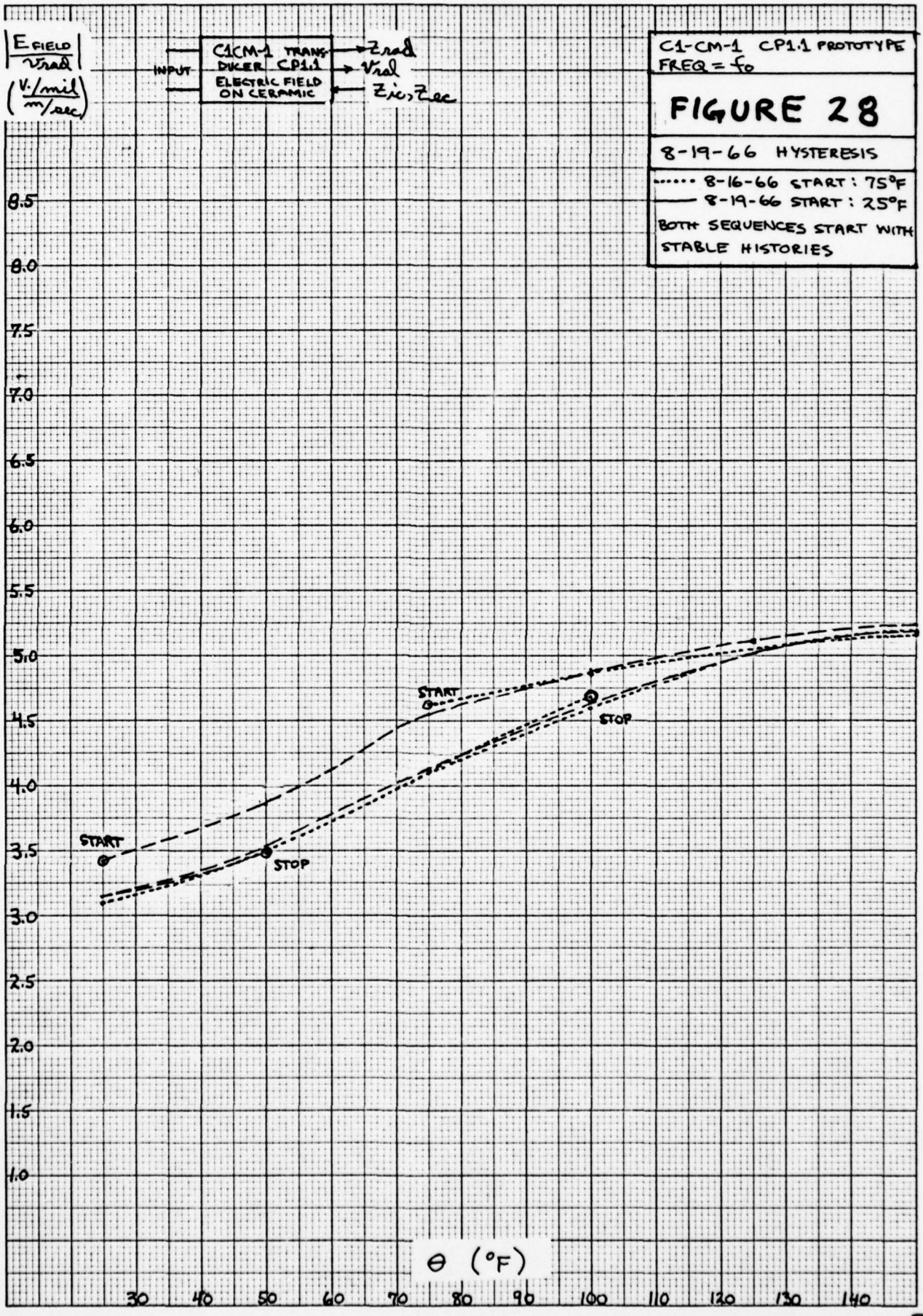

K&E 10 X 10 TO ½ INCH 46 1320
7 X 10 INCHES MADE IN U.S.A.
KEUFFEL & ESSER CO.

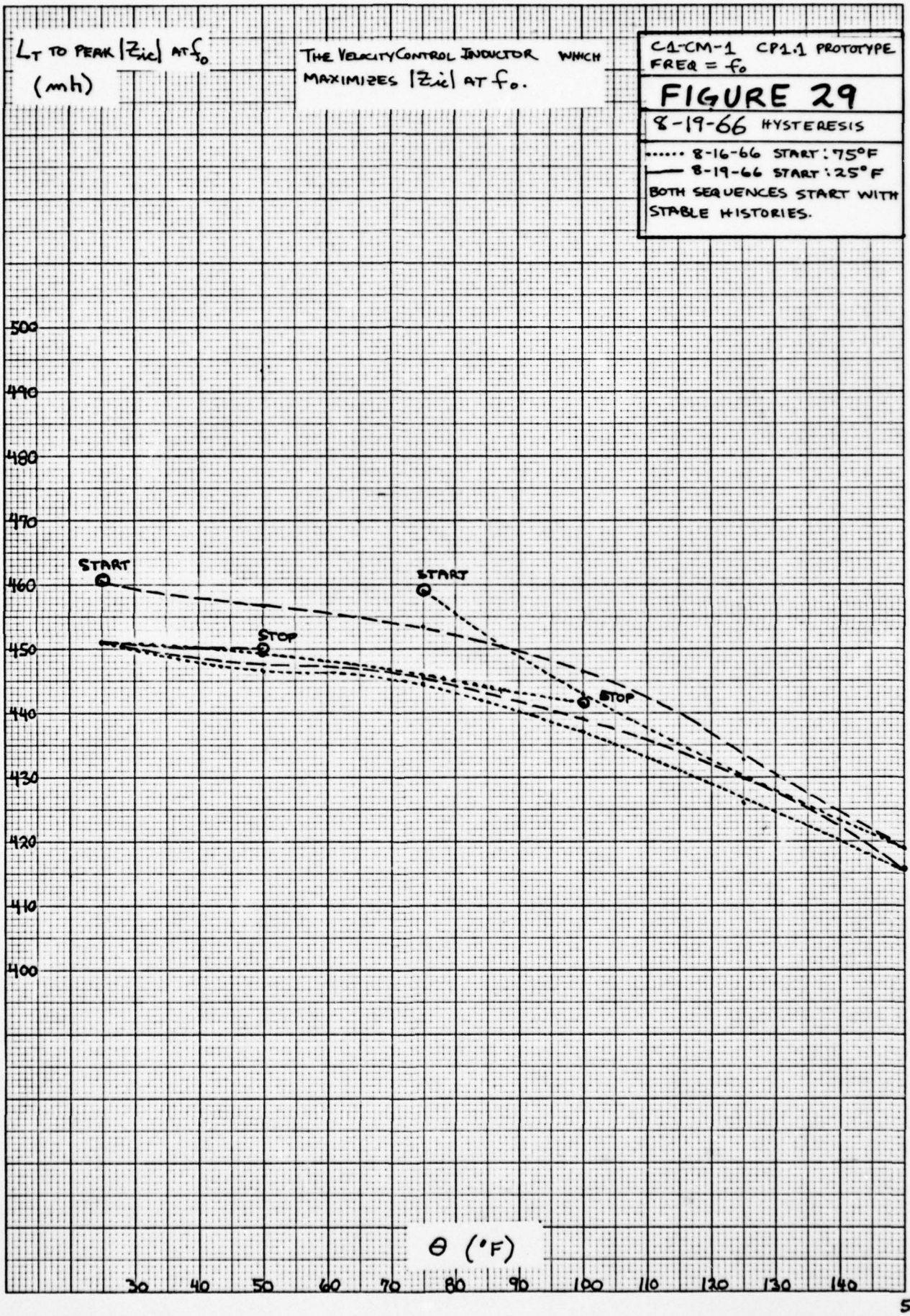

K&E 10 X 10 TO ½ INCH 46 1320
7 X 10 INCHES
KEUFFEL & ESSER CO.
MADE IN U.S.A.

C1-CM-1 CP1.1 PROTOTYPE
TEMPERATURE = 73° F (STABLE)

FIGURE 30

6-12-66 FREQ. SWEEP

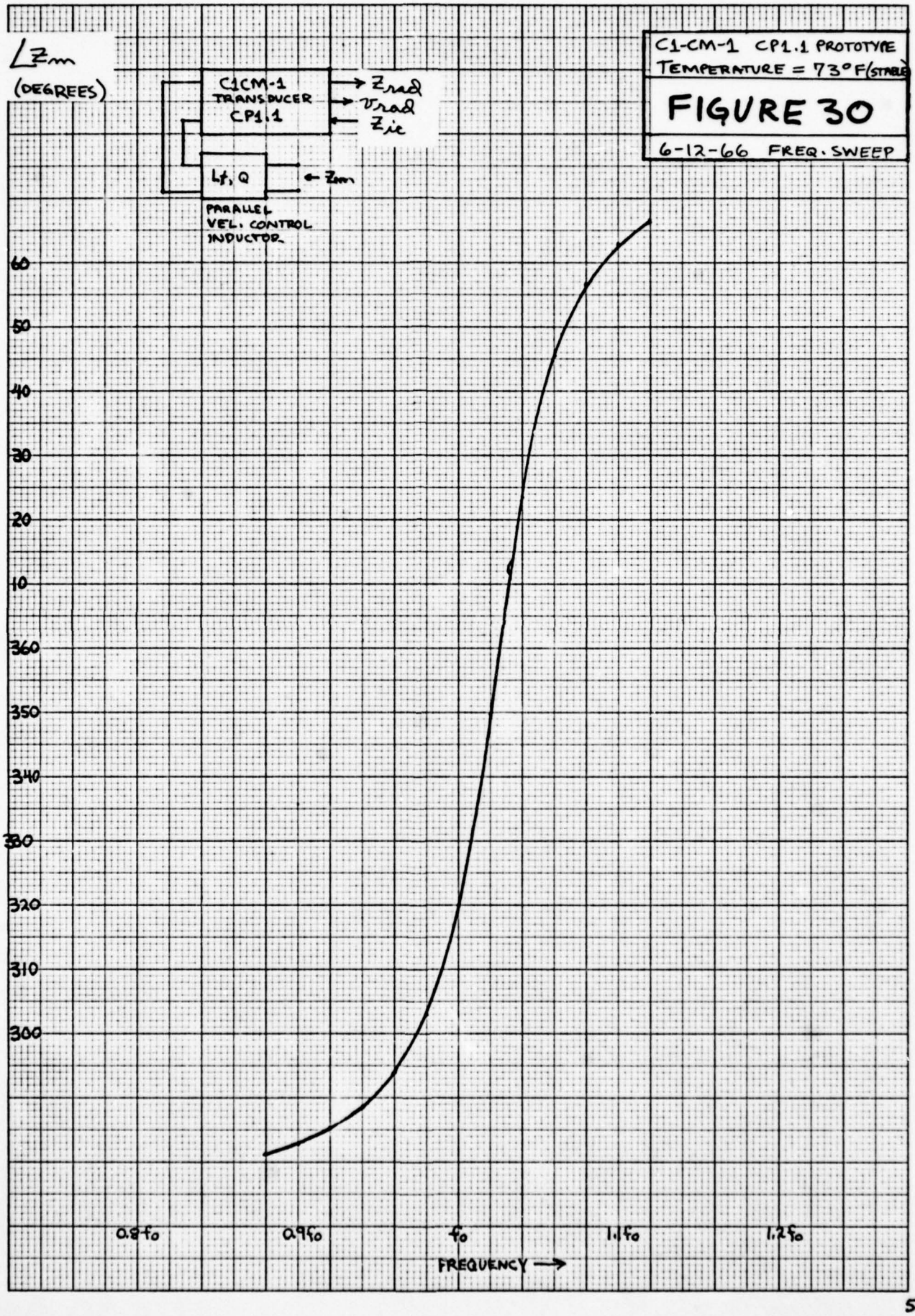

K&E 10 X 10 TO ½ INCH 46 1320
7 X 10 INCHES
KEUFFEL & ESSER CO.
MADE IN U.S.A.

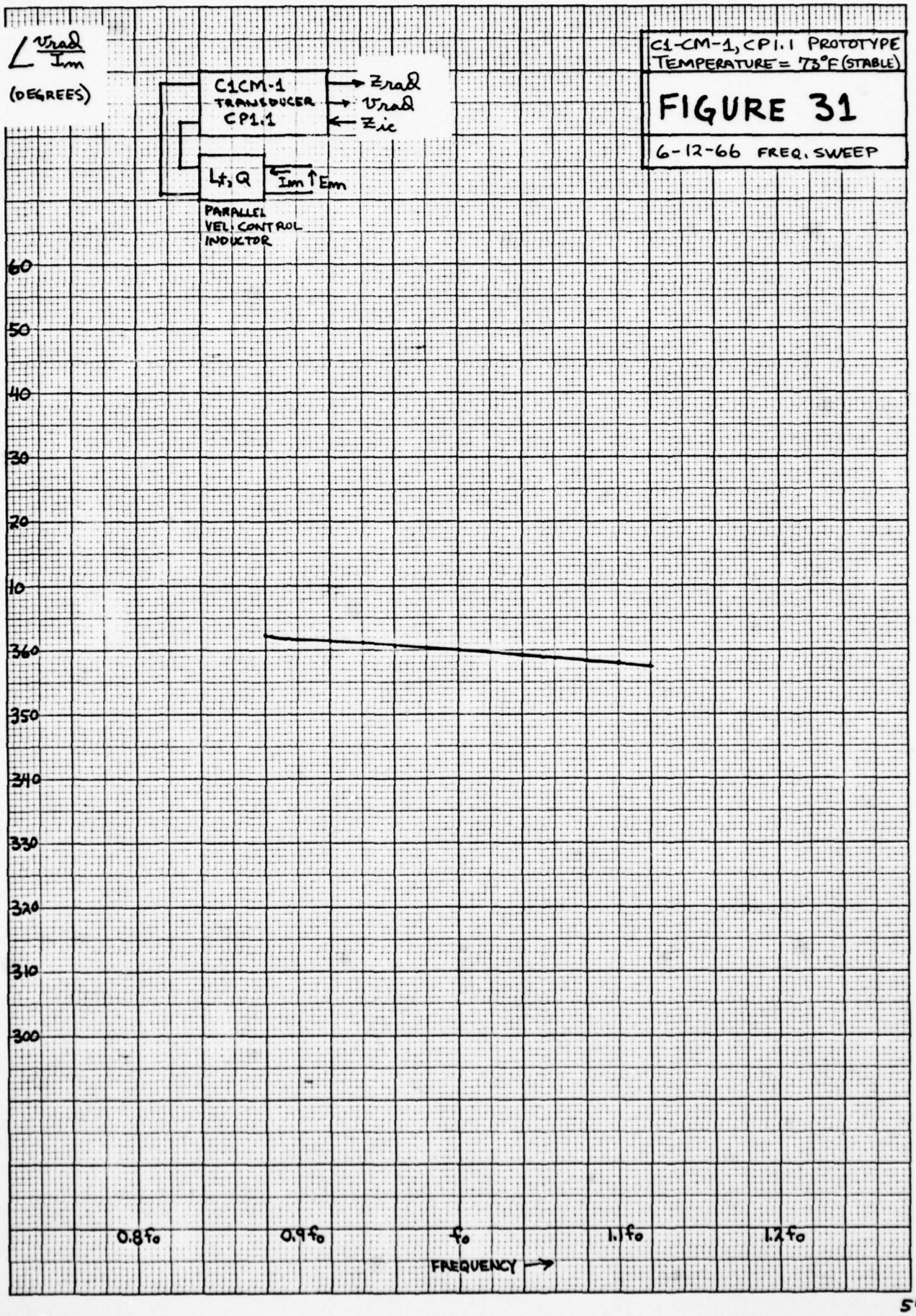

KEUFFEL & ESSER CO. MADE IN U.S.A. 46 1320 10 X 10 TO ½ INCH 7 X 10 INCHES

THE VELOCITY CONTROL INDUCTANCE WHICH MAXIMIZES $|Z_{ic}|$ AT 73°F (STABLE)

C1CM-1 CP1.1 PROTOTYPE
TEMPERATURE = 73°F (STABLE)

FIGURE 32

6-12-66 FREQ. SWEEP

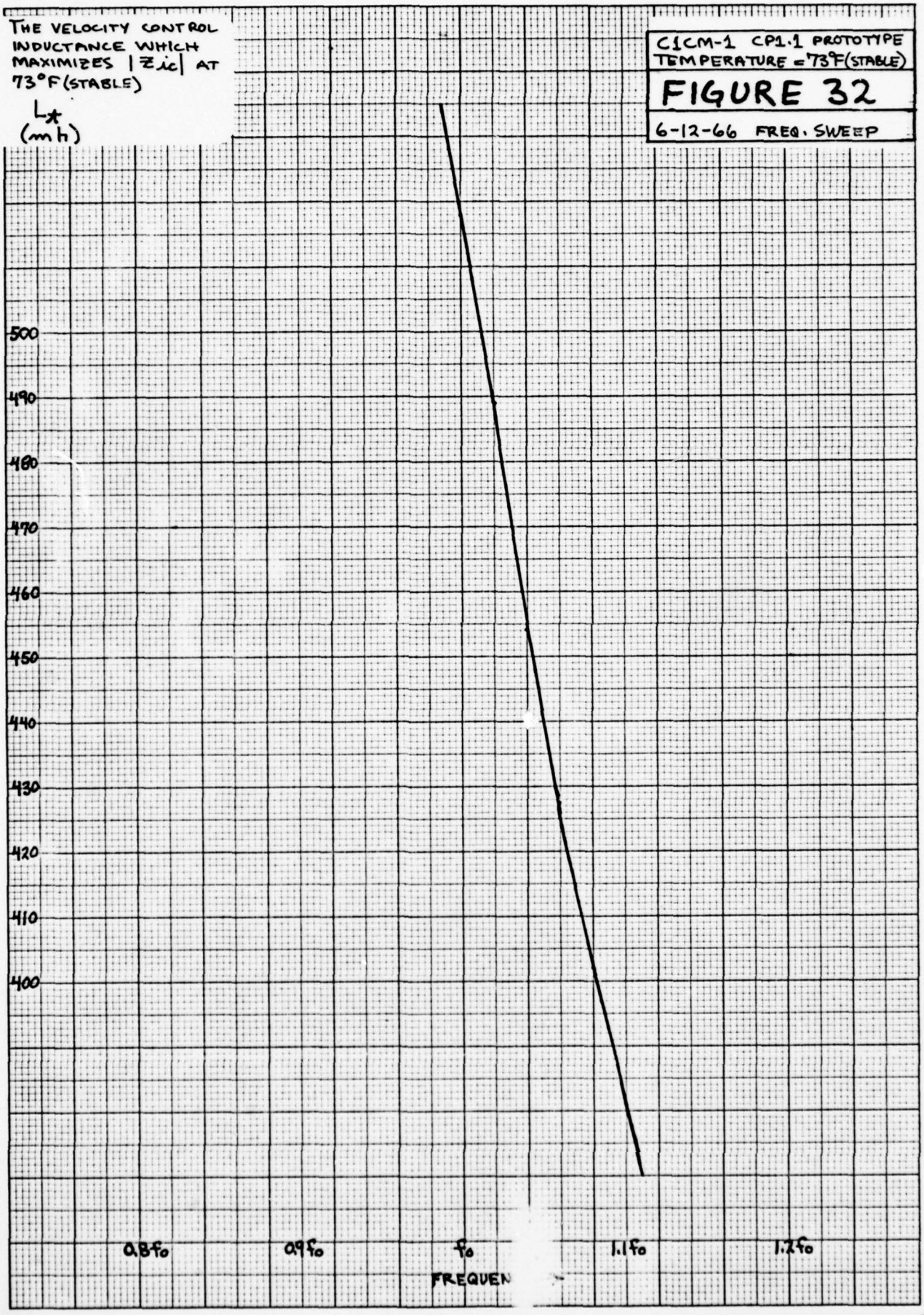

K+E 10 X 10 TO ½ INCH 46 1320
7 X 10 INCHES MADE IN U.S.A.
KEUFFEL & ESSER CO.

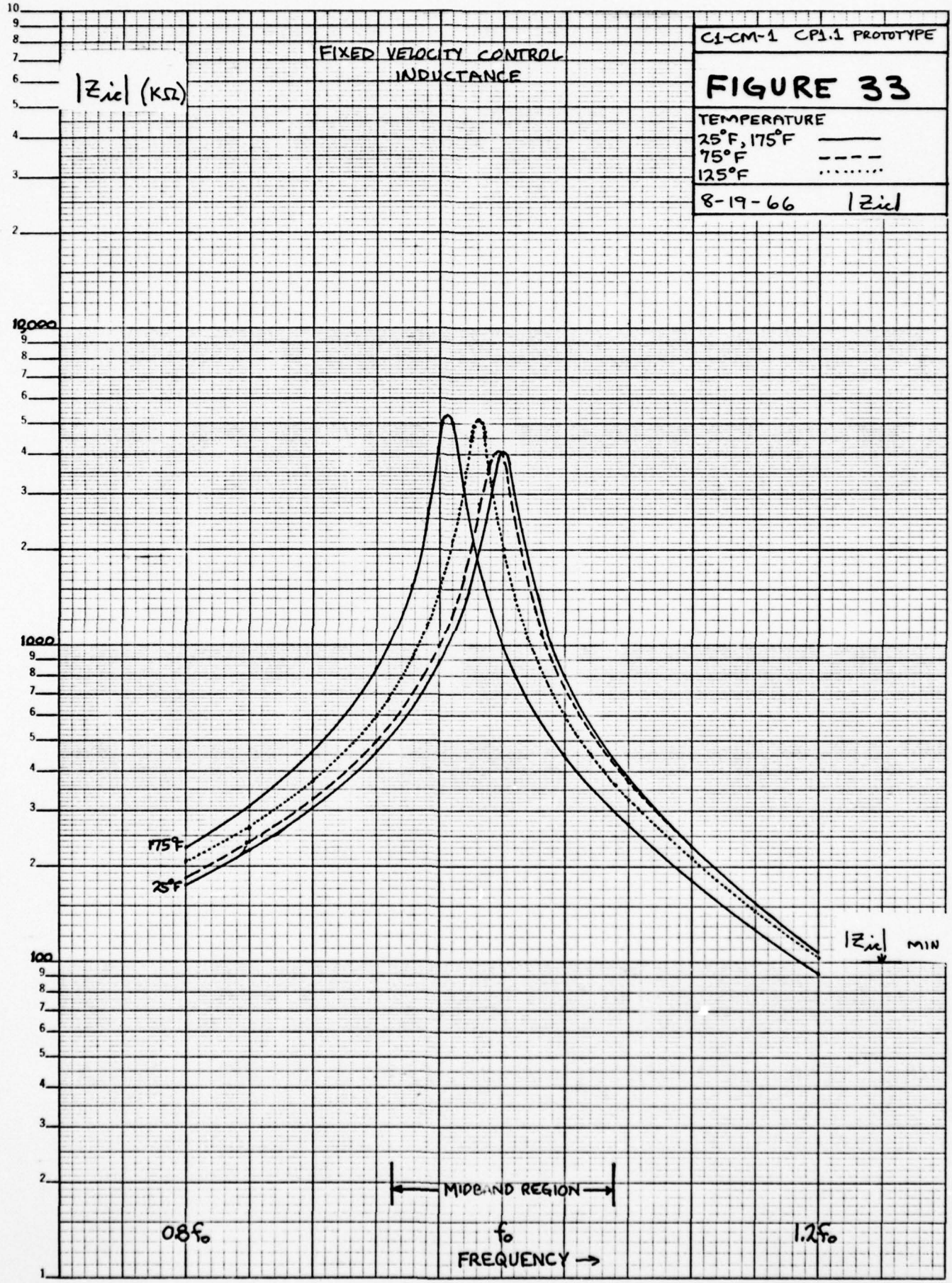

K&E SEMI-LOGARITHMIC 46 6010
4 CYCLES X 70 DIVISIONS MADE IN U.S.A.
KEUFFEL & ESSER CO.

APPENDICES

APPENDIX A: EXPERIMENT-THEORY COMPARISON

The ECP1-18 transducer behavior from Step Two can be displayed to show behavior vs temperature with fixed drive level, Z_{rad}, frequency, and L_t. These are the only experimental measurements of behavior vs temperature available at the time of this writing. Since more complete experimental verification than provided by the work reported in Appendix B was desired to provide confidence in our model predictions, we chose to compare this experimental information with predictions based on measured ECP1-18 temperature parameters. The degree of favorable comparison seen in Figures #A-1 through #A-7 reflects on the probable validity of the C1CM-1 predictions found in Steps Three and Four since identical ceramic was used in each instance.

Procedure

The ECP1-18 temperature parameters were determined a year after the DUMILOAD measurements because of the time limitations during the early work with the CP1.1 transducer. The ceramic aging over this period of time resulted in behavior changes of an indeterminate nature. Also, the parameter measurements were conducted at a frequency somewhat higher than f_o because of the removal of the tail section of the ECP1-18 beforehand. As mentioned in Step Four, the <u>effective</u> ceramic parameters are dependent to some degree on the frequency of operation and metal-ceramic ratio since the temperature parameters measured here are <u>effective</u> parameters, the predicted behavior based on these parameters is affected slightly.

In view of these considerations, we will assume that the <u>trends</u> in behavior with respect to temperature were not significantly affected by aging or frequency and a favorable comparison of predicted and measured trends would be sufficient validation of our methods. This assumption must be considered when interpreting results.

The sequence and duration of the fixed temperatures used in the determination of temperature parameters were held to approximately the values used during the DUMILOAD work. Also, fortunately, the sequence was properly arranged within the meaning of the hysteresis studies of Step Four. The second leg of the sequence (25°F to 150°F) was used in the comparison with the DUMILOAD work to emphasize similarity in the conditions of the two tests.

After determination of temperature parameters, our model was used to predict transducer behavior as a function of temperature. The Z_{rad} of 170,000 + j22,000 Kg/sec used during the DUMILOAD work was also used with the model as was the vel.cont. inductor Q of 37.45. Since the experimental data indicates a $|Z_{ic}|$ peak at about 25°F instead of 73°F temperature used earlier, the L_t with our model was chosen to be 423 mh to peak at 25°F for more meaningful comparison. The different L_t used here (382 mh predicted from earlier stable parameters) shows the sensitive dependence of the quantity on aging and history in the ceramic. The trends noted in the graphs are independent of small changes in L_t and $|Z_{ic}|$ although the exact values of the variables of interest do depend on these quantities.

Results

The measured and predicted behavior as a function of temperature are compared in Figures #A-1 through #A-7 for the ECP1-18 transducer subject to the limitations outlined above. Figures #A-8 through #A-10 show the frequency dependence of three quantities and, when compared to Figures #A-2, #A-4, and #A-7 respectively, tend to confirm a possible equivalence between frequency and temperature dependence of the type mentioned a previous section of this report (Step Four). Figures #A-11 and #A-12 show the effects of temperature on the $|Z_{ic}|$ relationship with frequency for L_t = 382 mh and L_t = 423 mh. As may be noted, small changes in L_t do not affect the temperature-dependence of $|Z_{ic}|$ appreciably.

Figure #A-6 shows the electric field per unit velocity, theory and experiment. The experimentally measured data is plotted by the method of least squares, and the trend in behavior with temperature is accurately predicted by model computations. The value of $|E/v_r|$ is higher than that found in C1CM-1 for Step Four but the Z_{rad} used here is much different than that used in Step Four, the conclusions relevant to this graph are simply that ECP1-18 has a high field at this Z_{rad} and that this field is relatively insensitive to temperature.

Figure #A-1, #A-2 show Z_m to be detuning with increasing temperature in a manner which could be explained by a drop in ceramic capacitance slightly greater than occurred with the C1CM-1 transducer. The value and the direction of change of $|Z_m|$ are functions of $|Z_{rad}|$ and transducer design as well as temperature. The experimental measurements show nearly the same trends in behavior here as predicted by our model using measured temperature parameters even though these trends are different from those computed for C1CM-1 in Step Four. The frequency dependence of $\angle Z_m$ in Figure #A-8 is consistent with the temperature dependence noted in Figure #A-2, which again reminds us of a possible correlation between temperature and frequency dependence for this ceramic.

Figures #A-3, #A-4 show v_r/I_m to be very sensitive to changes in temperature for the conditions studied. This indicates poor current control of velocity and can be attributed to the high $|Z_{rad}|$ compared to the $|Z_{ic}|$ peak as well as poor design. Figure #A-9 confirms this analysis by showing the sensitivity of $\angle v_r/I_m$ to frequency changes for the ECP1-18 transducer. The C1CM-1 transducer showed nearly flat velocity response to both frequency and temperature under different radiation conditions for the same ceramic. The experiment and theory trends for ECP1-18 are in excellent agreement however, and the poor suitability of ECP1-18 for array use does not detract from the meaning of these comparisons.

Figure #A-5 shows the experiment and theory comparison of efficiency. Efficiency is the most difficult to measure of all quantities of interest and even the use of the least squares rule doesn't always smooth the

measured curve. The predicted efficiency shows the same rising trend with increasing temperature but the slope is more shallow than is that of the measured data. The rising efficiency confirms in part the conclusions discussed earlier for the EC-64 ceramic relative to power loss vs temperature.

Figure #A-7 shows the L_t necessary to peak $|Z_{ic}|$ at f_o as a function of ceramic temperature. No measurements were made and this curve, predicted from measured temperature parameters, is included to demonstrate the critical temperature dependence of this quantity. The frequency dependence of L_t to peak $|Z_{ic}|$ at 73°F (based on old parameters) is shown in Figure #A-10 and is equally critical. The Q of the inductor is assumed to be constant at 37.45.

The $|Z_{ic}|$ vs frequency curves in Figures #A-11 and #A-12 are plotted for constant L_t and several constant temperatures. The $|Z_{ic}|$ bandwidth is seen to be non-existent at the Z_{rad} value used during the measurements (195,000 Kg/sec) which explains the variation in velocity at constant current over the temperature and frequency range. The shift in the frequency of peak $|Z_{ic}|$ is 4% of f_o over the operational temperature range of the C/P array and 8% of f_o over the measurement range. These shifts compare with 0.8% and 4% of f_o respectively for the C1CM-1 transducer (Figure #33) and this demonstrates the fact that the design of a transducer can be an important contribution towards minimizing the effects of temperature changes even when the type and configuration of the ceramic is fixed.

Conclusions

These conclusions are valid at this point only for transducer fabricated from Edo-Western EC-64 ceramic. Further work with other ceramics using procedures outlined in this report is necessary for proper verification of these conclusions relative to other ceramics. The conclusions relative to ECP1-18 performance by itself are not listed here since they were included only for the purposes of illustration.

1) On the basis of theory-experiment comparisons using the ECP1-18 transducer, the use of temperature parameters with our model allows accurate prediction of the trends in behavior of a transducer as a function of temperature.

2) The comparisons provide further justification for assuming the existence of some type of relationship between frequency-dependence and temperature dependence of transducer behavior.

3) The effects of temperature changes on behavior can be minimized for a particular ceramic by design methods. The iterative design technique may be a valuable aid for such optimization.

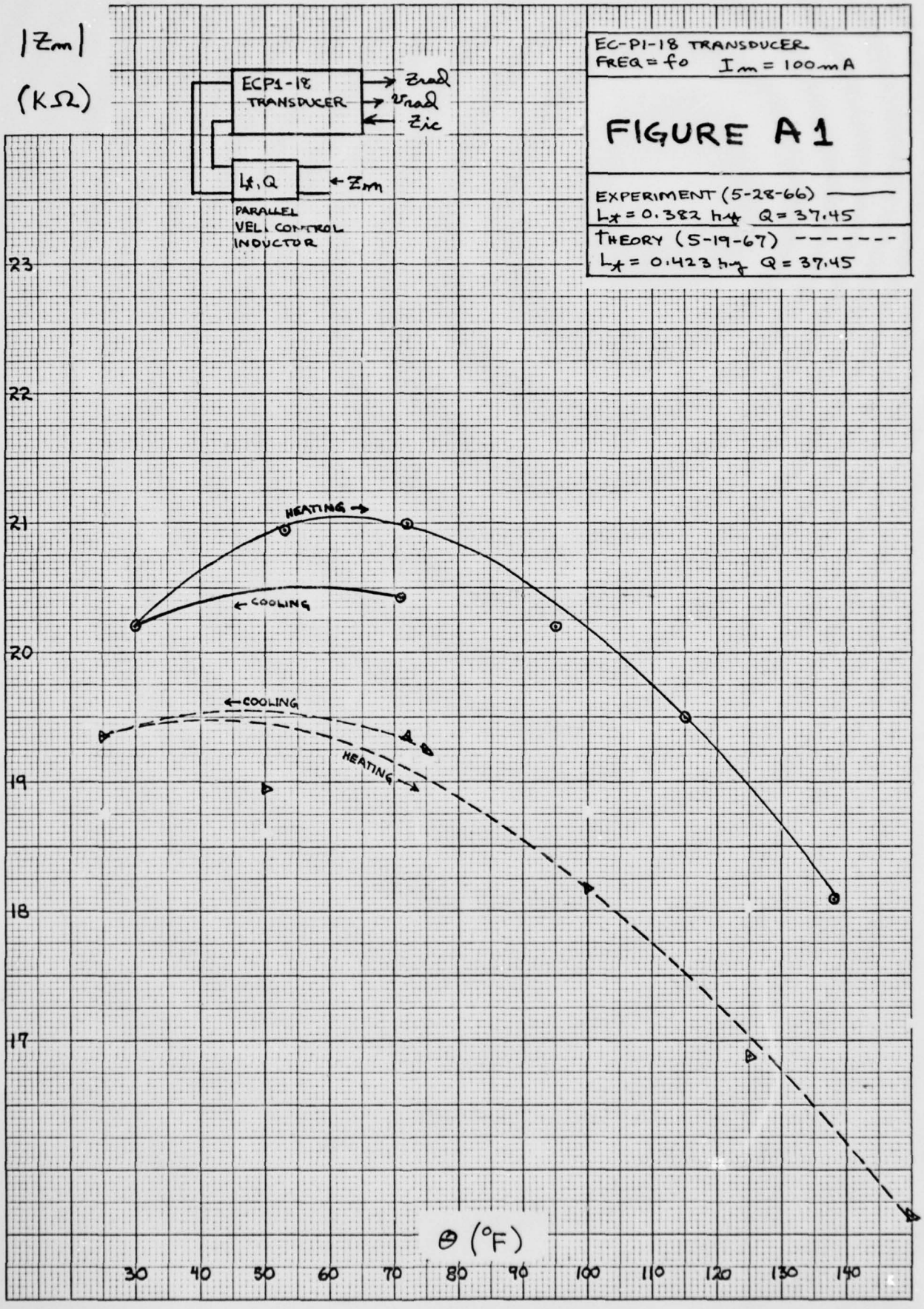

KE 10 X 10 TO ½ INCH 46 1320
7 X 10 INCHES
KEUFFEL & ESSER CO.
MADE IN U.S.A.

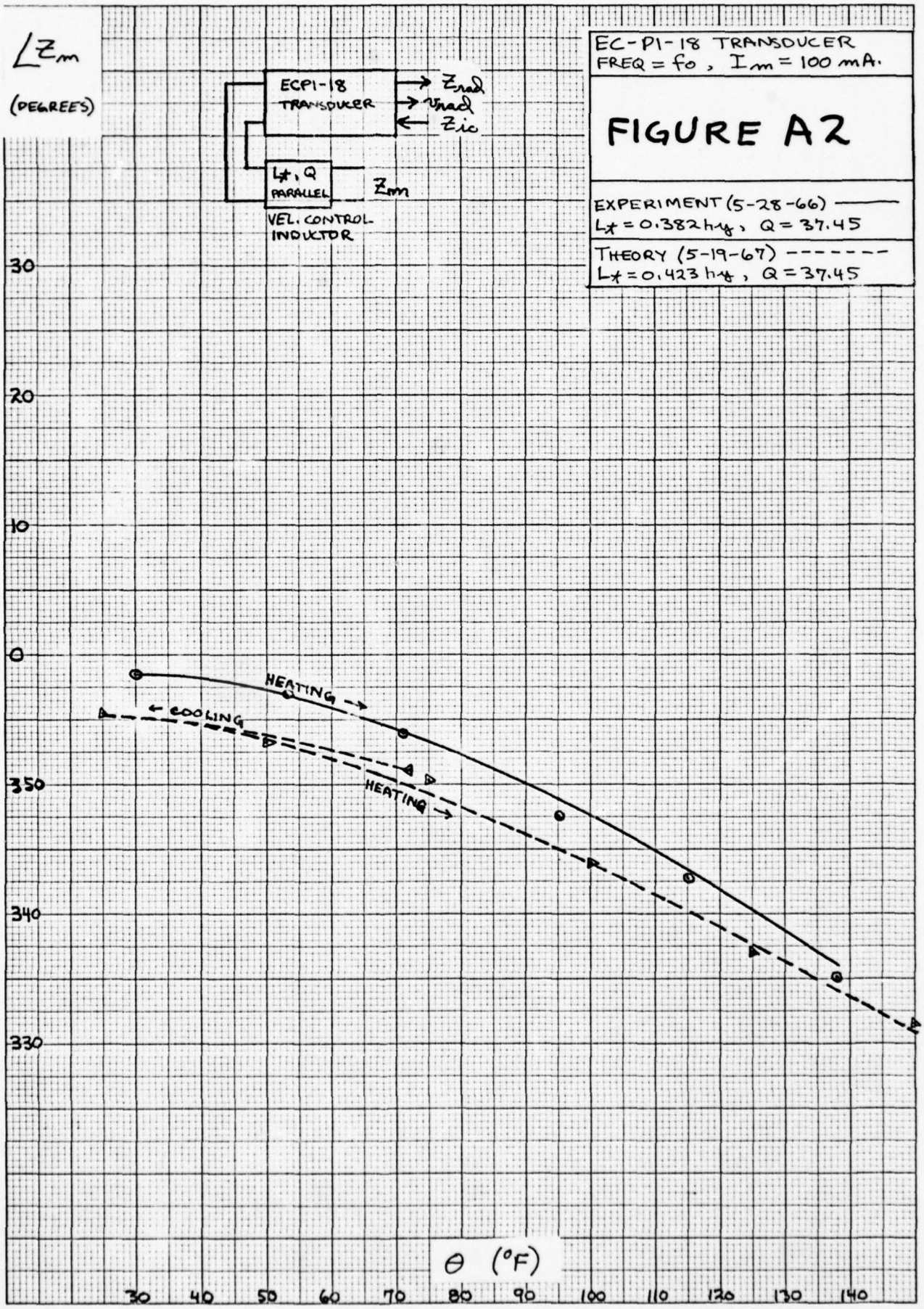

K&E 10 X 10 TO ½ INCH 46 1320
7 X 10 INCHES MADE IN U.S.A.
KEUFFEL & ESSER CO.

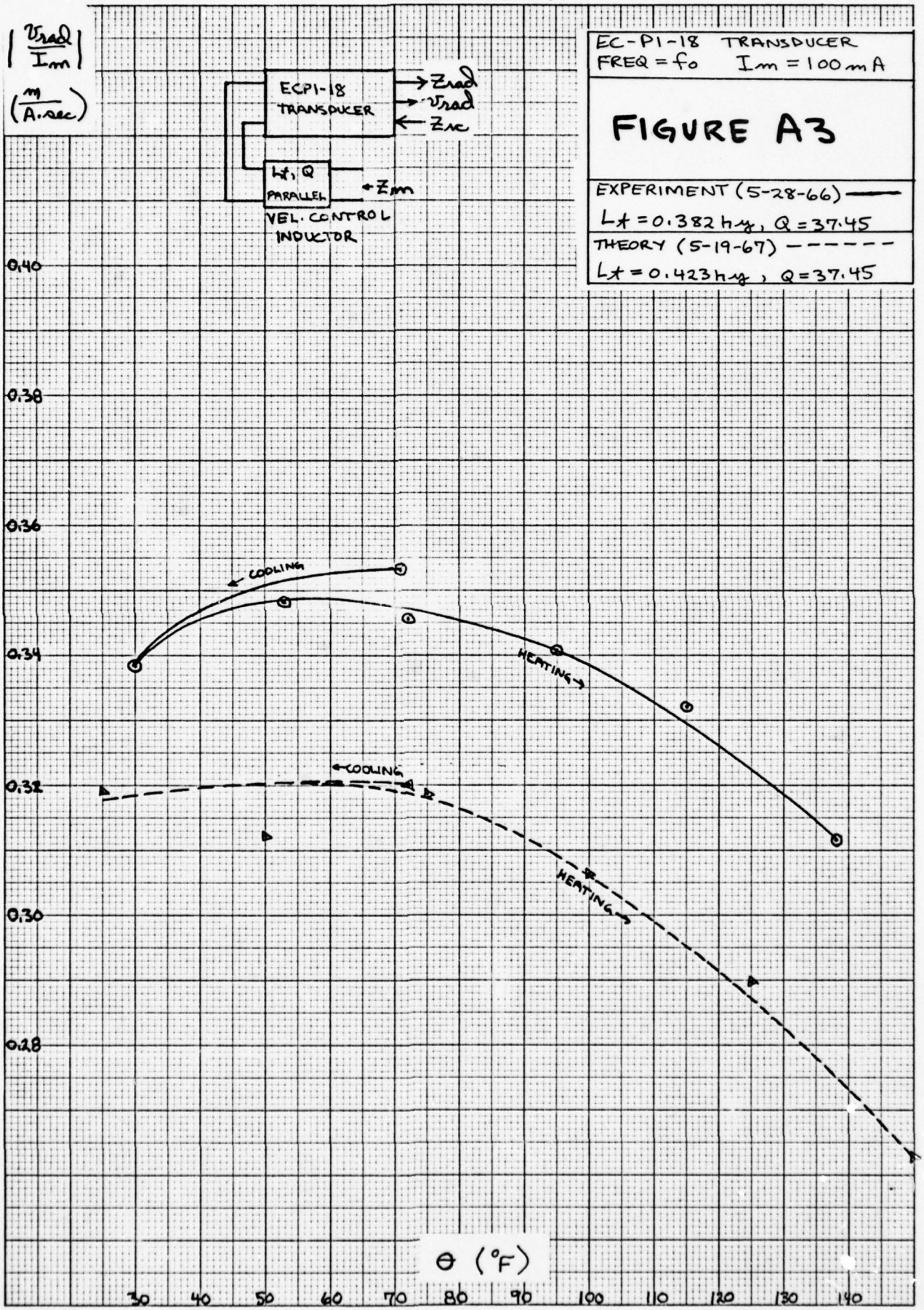

K&E 10 X 10 TO ½ INCH 46 1320
7 X 10 INCHES MADE IN U.S.A.
KEUFFEL & ESSER CO.

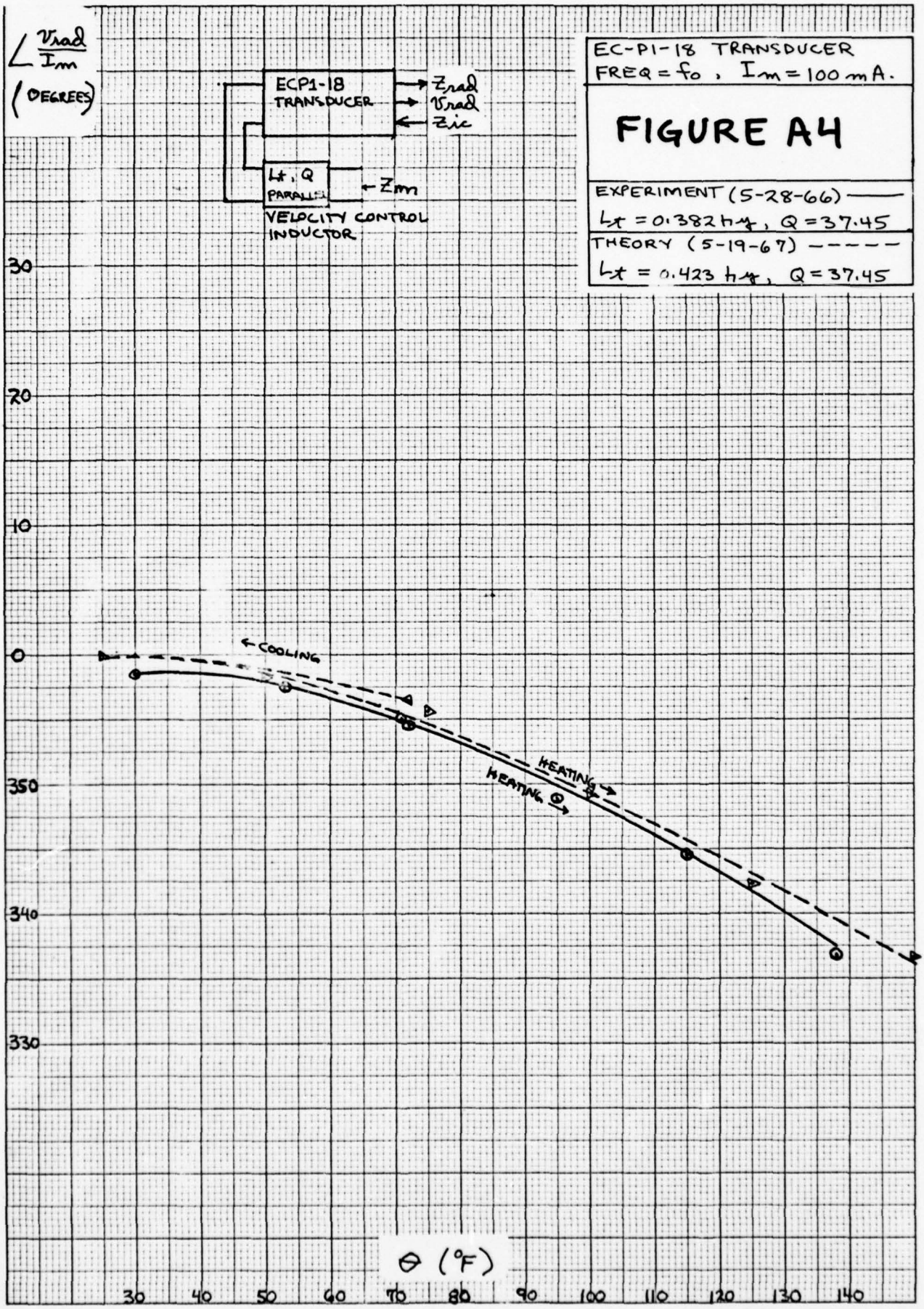

K&E 10 X 10 TO ½ INCH 46 1320
7 X 10 INCHES MADE IN U.S.A.
KEUFFEL & ESSER CO.

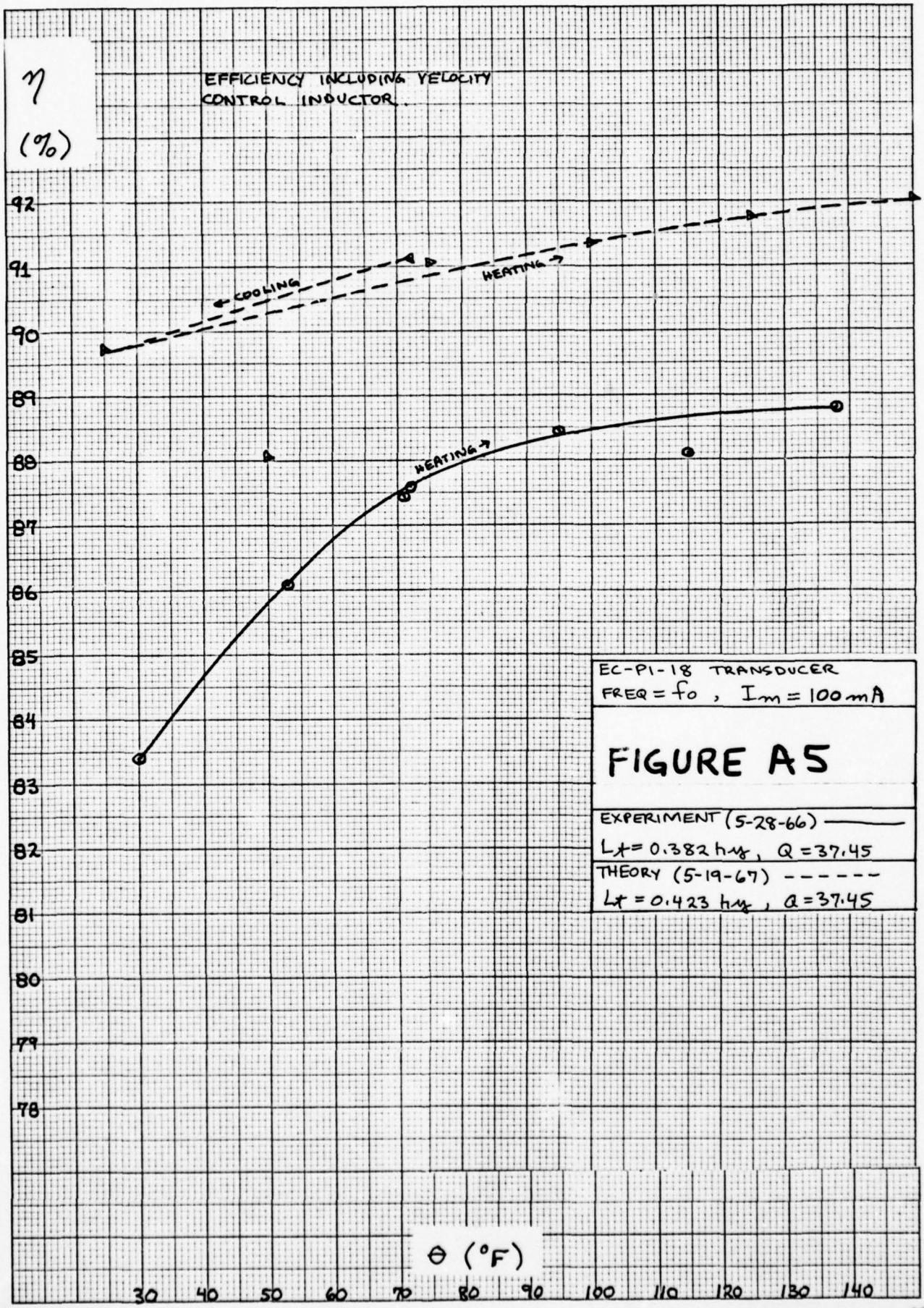

K&E 10 X 10 TO ½ INCH 46 1320
7 X 10 INCHES
MADE IN U.S.A.
KEUFFEL & ESSER CO.

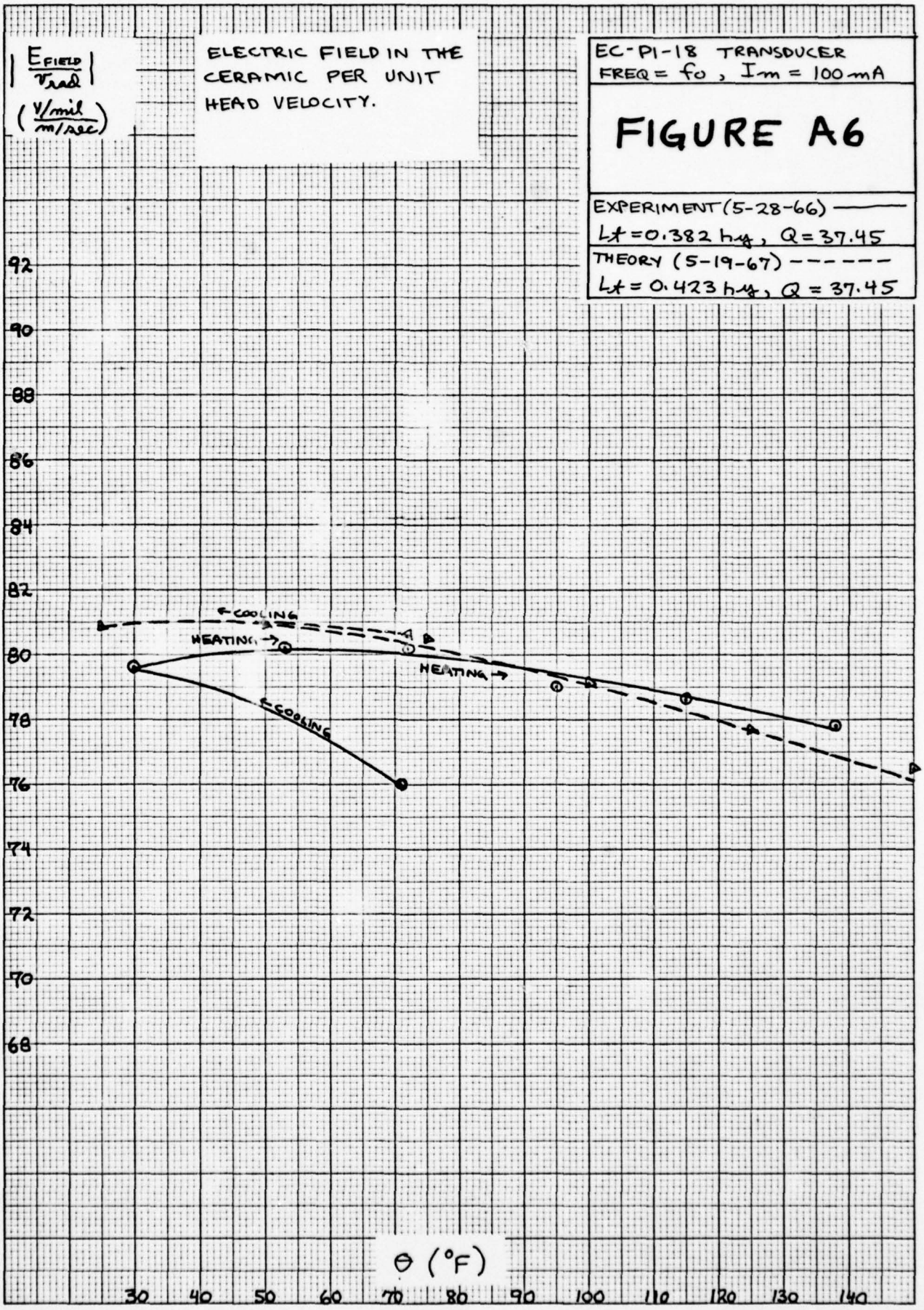

K&E 10 X 10 TO ½ INCH 46 1320
7 X 10 INCHES MADE IN U.S.A.
KEUFFEL & ESSER CO.

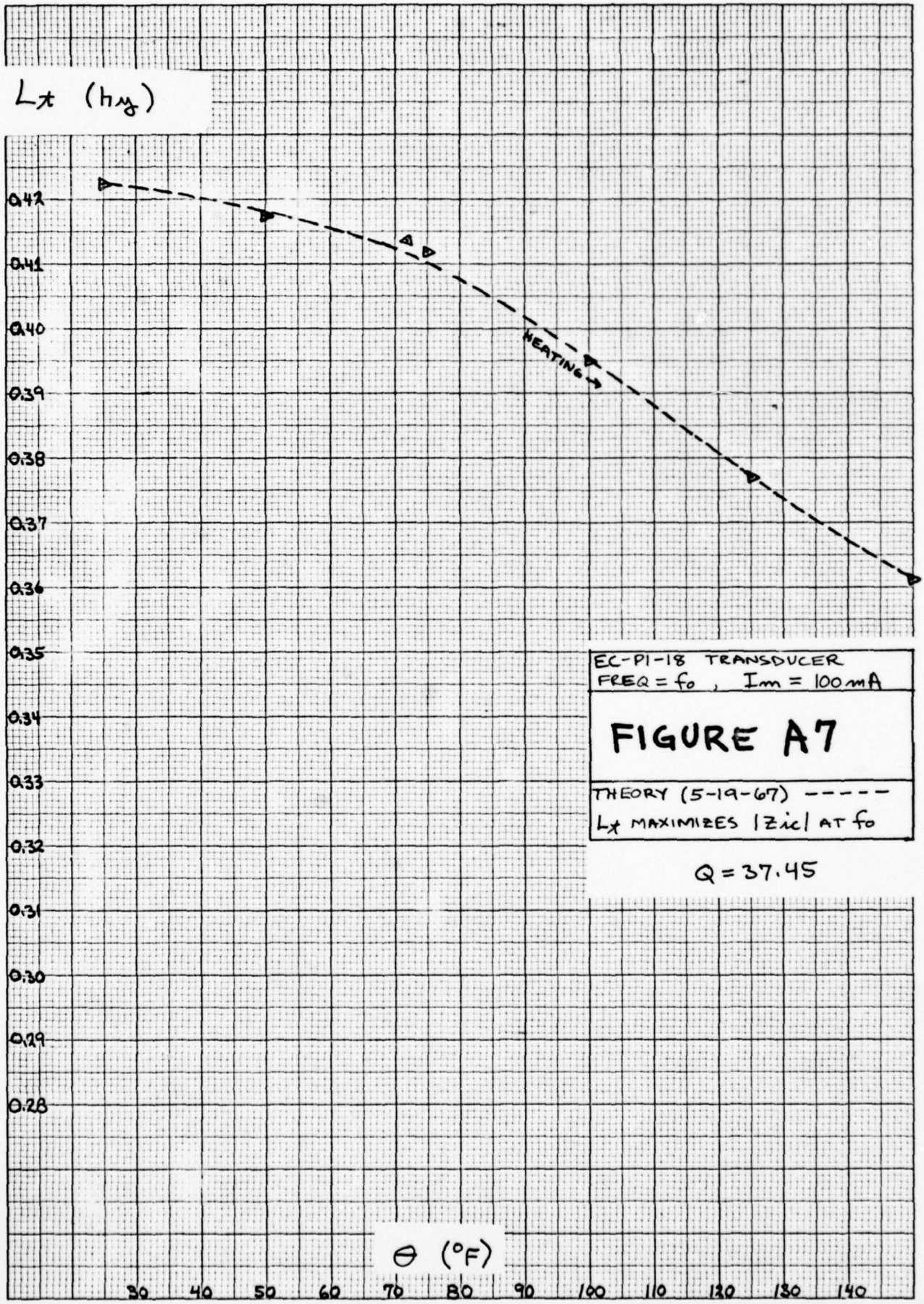

EC-P1-18 TRANSDUCER
FREQ = f_o , I_m = 100 mA

FIGURE A7

THEORY (5-19-67) - - - - -
L_x MAXIMIZES $|Z_{ic}|$ AT f_o

Q = 37.45

K&E 10 X 10 TO ½ INCH 46 1320
7 X 10 INCHES MADE IN U.S.A.
KEUFFEL & ESSER CO.

EC-P1-18 TRANSDUCER
θ = 73°F (STABLE HISTORY)

FIGURE A8

THEORY (5-28-66) ——————

FREQUENCY SWEEP, L_s = 0.382hy

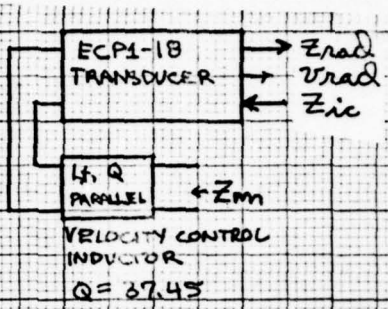

K&E 10 X 10 TO ½ INCH 46 1320
7 X 10 INCHES MADE IN U.S.A.
KEUFFEL & ESSER CO.

EC-P1-18 TRANSDUCER
θ = 73°F (STABLE HISTORY)

FIGURE A9

THEORY (5-28-66) ———
FREQ. SWEEP, L_t=0.382 h

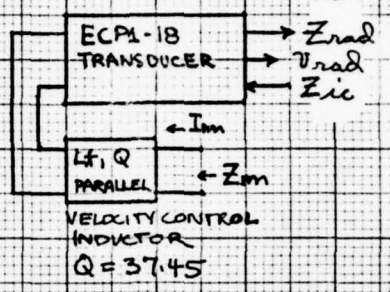

$\angle \frac{V_{rad}}{I_m}$ (DEGREES)

30
20
10
0
350
340
330

0.8f_o f_o 1.2f_o

FREQUENCY

KE 10 X 10 TO ½ INCH 46 1320
7 X 10 INCHES MADE IN U.S.A.
KEUFFEL & ESSER CO.

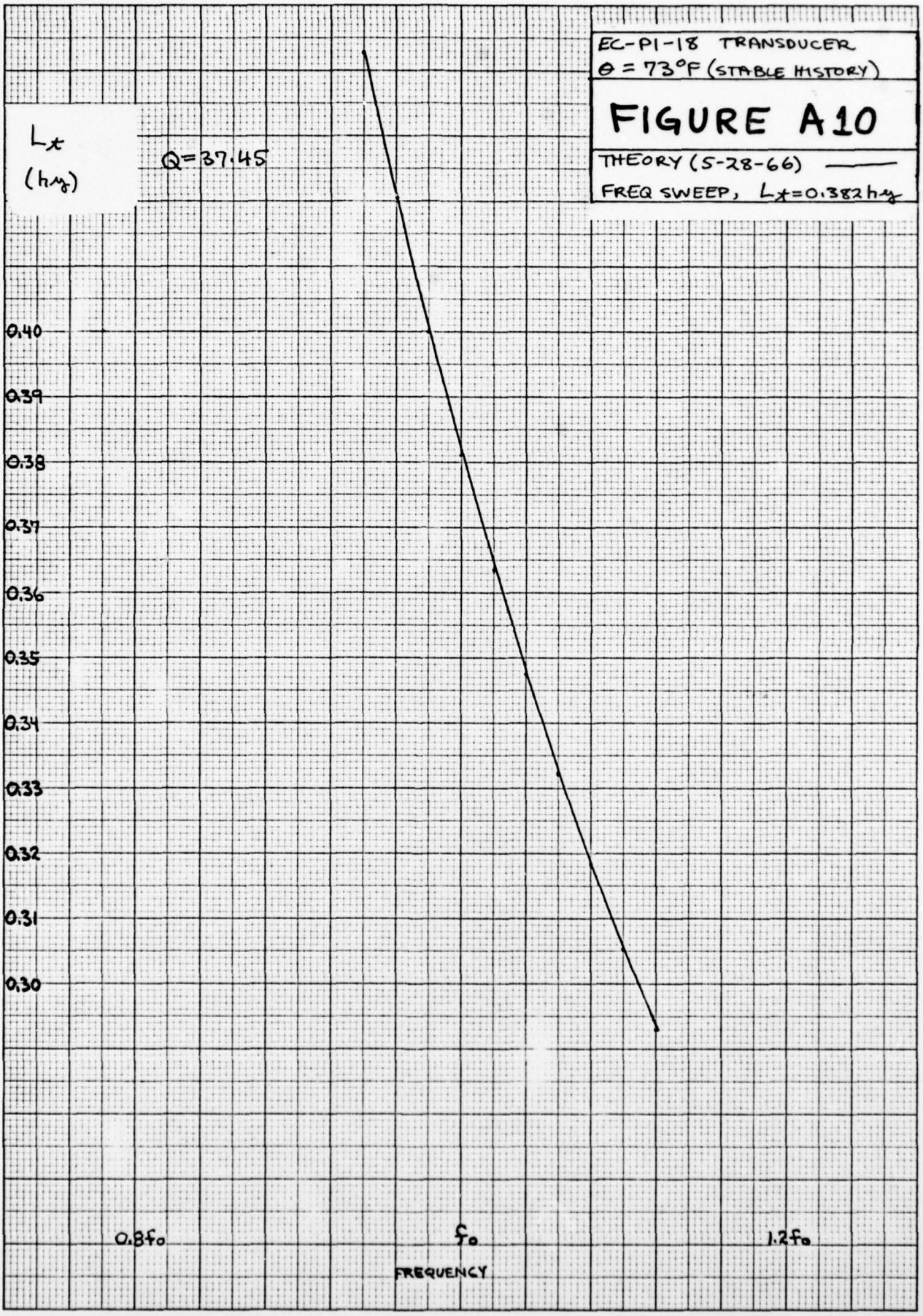

KE 10 X 10 TO ½ INCH 46 1320
7 X 10 INCHES
KEUFFEL & ESSER CO.
MADE IN U.S.A.

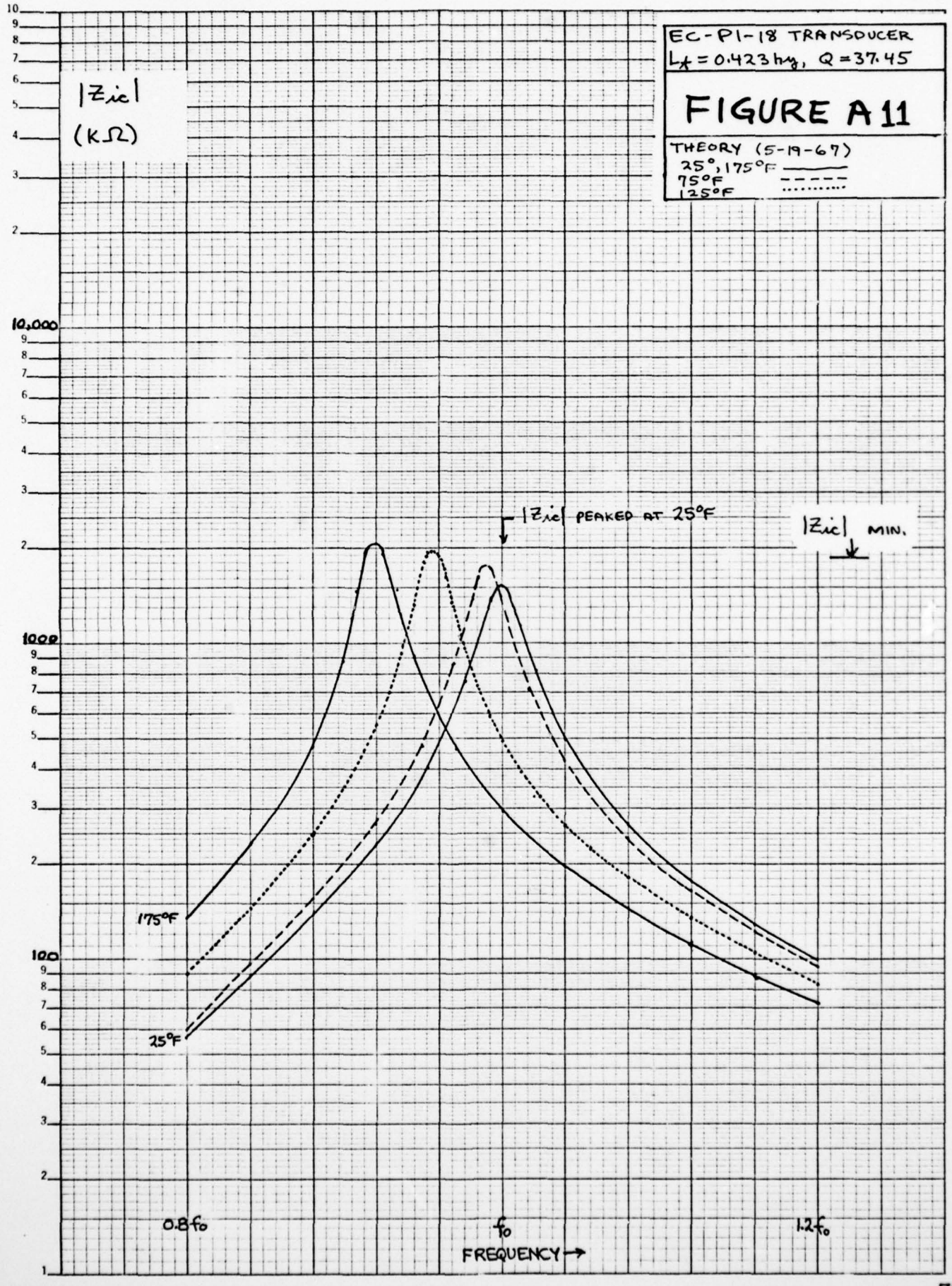

KE SEMI-LOGARITHMIC 46 6010
4 CYCLES X 70 DIVISIONS MADE IN U.S.A.
KEUFFEL & ESSER CO.

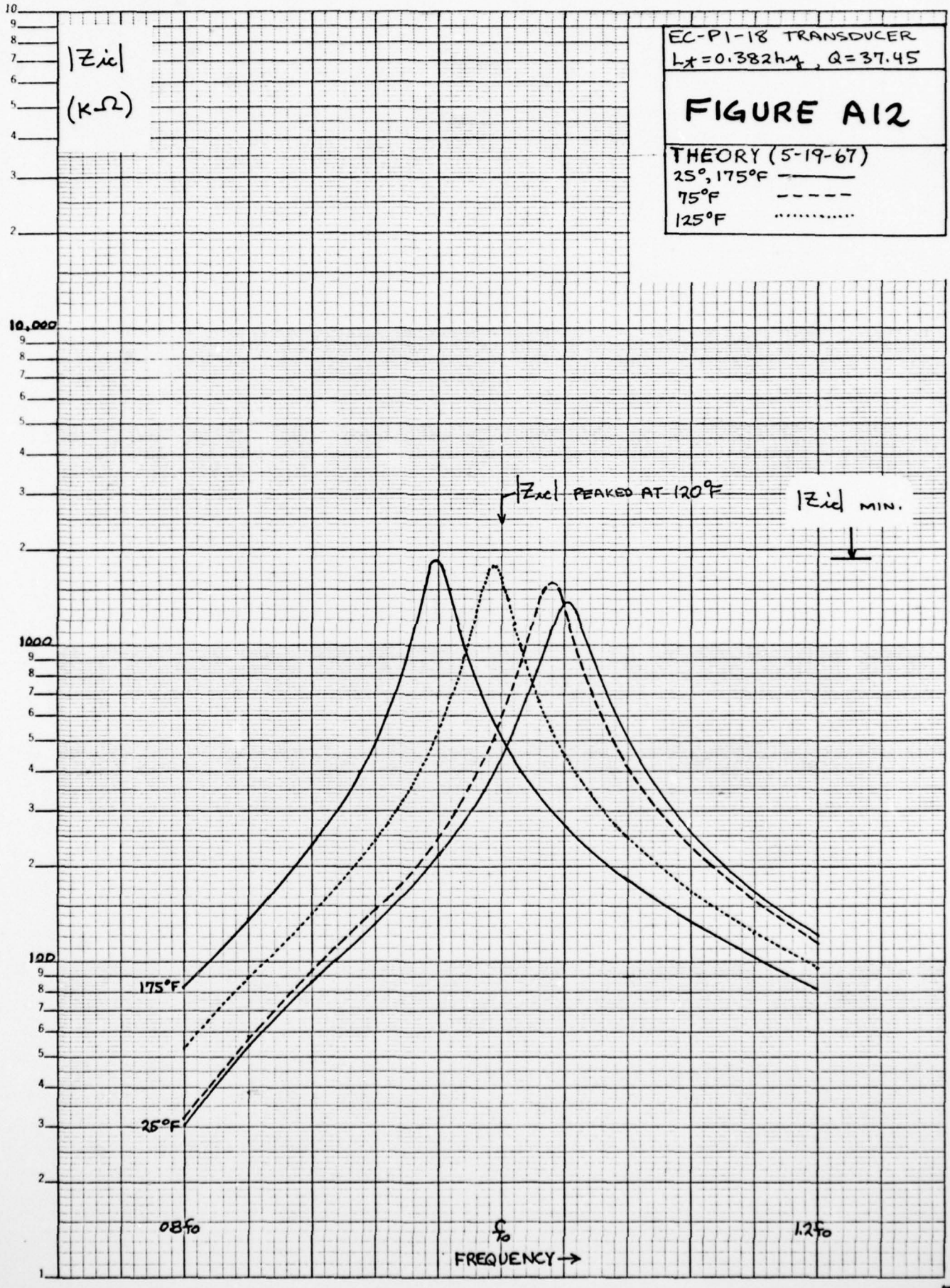

SEMI-LOGARITHMIC 46 6010
4 CYCLES X 70 DIVISIONS MADE IN U.S.A.
KEUFFEL & ESSER CO.

APPENDIX B: TEMPERATURE PARAMETER GENERATION

Prior to the dismantling of the ECP1-18 DUMILOAD composite for temperature parameter measurement and before the C1CM-1 transducer was DUMILOADED for laboratory measurement, we desired some sort of comparison of experimental and theoretical results. The temperature parameters measured for the C1CM-1 on 19 August 1966 (Step Four) were available as were the laboratory measurements of the ECP1-18 transducer. These C1CM-1 temperature parameters were used to "generate" a set of temperature parameters for the ECP1-18 based on stable ECP1-18 ceramic parameters measured in late 1965 (room temperature held fixed at 73°F for two weeks). The resulting predictions computed using these generated parameters are compared to experimental data in Figures #B-1 through #B-7.

Procedure

The method used to generate temperature parameters assumes that the parameters of one transducer vary with temperature by a percentage which is the same for all transducers using the same ceramic configuration. This means that the only differences between the temperature parameters of the C1CM-1 transducer and the ECP1-18 transducer are due to such things as metal to ceramic ratio and frequency of resonance and that the ratio of these two parameters is independent of temperature. The fact that the 1965 ceramic parameters of the ECP1-18 were not measured during the first two hours following a temperature change was ignored as was the aging which occurred in the period prior to DUMILOAD measurements. These limitations should be considered when viewing the results in this Appendix. Also, the goal of this work was limited to obtaining rough comparisons between theory and experiment using only readily available information.

Perhaps the following tables will provide a clear illustration of the process used to generate ECP1-18 temperature parameters by varying the 73°F stable ECP1-18 ceramic parameters by the percentages computed from C1CM-1 temperature parameters dated 19 August 1966. Table B-1 shows

several sets of ceramic parameters measured for the C1CM-1 transducer in RMKS units along with the percentage variation vs temperature.

Name and Exponent		50°F	(50-75)/75	75°F	(100-75)/75	100°F
E33T	$X10^{4}$	.14685	0.239%	.14650	1.365%	.14850
E33TM	$X10^{-2}$	.35967	44.05%	.24963	-17.0%	.20713
G33	$X10^{-1}$	.21381	2.02%	.20958	-1.612%	.20620
G33M	$X10^{-3}$	.20413	0.03359	.17054	-0.01366	.15688
S33D	$X10^{-11}$	.97566	1.103%	.96502	-0.691%	.95842
S33DM	$X10^{-2}$	.26747	29.6%	.20635	-15.44%	.17442

TABLE B-1: C1CM-1 Temperature Parameters (Measured)

The absolute magnitude of the change in G33M vs temperature is used instead of the percentage change because the sign of G33M changes in some instances and the nature of this multiplier is such that the magnitude of change probably has more meaning here. Actually, this process is so crude that the difference is almost academic.

The percentages computed in Table B-1 are now inserted in Table B-2 along with the set of ceramic parameters measured at 73°F in 1965. The resulting 50°F and 100°F parameters are "generated" in a very straightforward manner and tabulated.

Name and Exponent		73°F	Mult (50°)	50°F	Mult (100°)	100°F
E33T	$X10^{4}$	.12765	X1.00239	.12772	X1.01365	.12941
E33TM	$X10^{-2}$	.2076	X1.4405	.2991	X0.8300	.1726
G33	$X10^{-1}$	.23329	X1.0202	.23800	X0.98388	.22953
G33M	$X10^{-3}$	-.5735	+0.0336	-.5399	-0.0137	-.5872
S33D	$X10^{-11}$	1.09113	X1.01103	1.10316	X0.99309	1.08367
S33DM	$X10^{-2}$	.34130	X1.296	.44239	X0.8456	.28849

TABLE B-2: ECP1-18 Temperature Parameters (Generated)

The complete set of these generated temperature parameters was used with our model to predict the behavior of the ECP1-18 transducer. The experimental DUMILOAD data used in the comparison here are identical to those used in Step Two and Appendix A.

Results

The resulting comparisons are shown in Figures #B-1 through #B-7. There is no significant difference in trends of behavior with temperature changes and the overall comparison is favorable. The procedure used to obtain these temperature parameters has forced the predicted value of L_t necessary to peak $|Z_{ic}|$ at f_o at 75°F to be 382 mh. This L_t was used in the DUMILOAD work in June 1966 after eight months of aging and the peak in $|Z_{ic}|$ occurred at f_o at about 25°F. No attempt was made to move these peaks together for the purposes of comparison, however, since the comparison of trends in behavior would not be materially affected.

The results were found to be favorable enough to motivate further work with the ECP1-18 transducer (Appendix A). The procedure for generating temperature parameters has not yet been sufficiently explored to allow understanding of the limitations and exceptions relative to the

use of this process in place of actual measurement. The evidence available supports only the conclusions that generated temperature parameters may be used with our model as a quick and dirty way to successfully predict trends in behavior with temperature if the ceramic behavior is nearly independent of drive level and if the ceramic configuration of the two transducers involved is identical. Perhaps, for very crude work, direct substitution of parameters may be valid under these restrictions although this would necessitate ignoring the effects of differences in metal-ceramic ratio, frequency of measurement, etc.

The trends in behavior shown in Figures #B-1 through #B-7 are identical to those in Appendix A and are therein adequately discussed. The hysteresis loop shown here is a function of the C1CM-1 transducer and no particular justification exists for assuming that these loops represent the hysteresis existent in the ECP1-18 transducer.

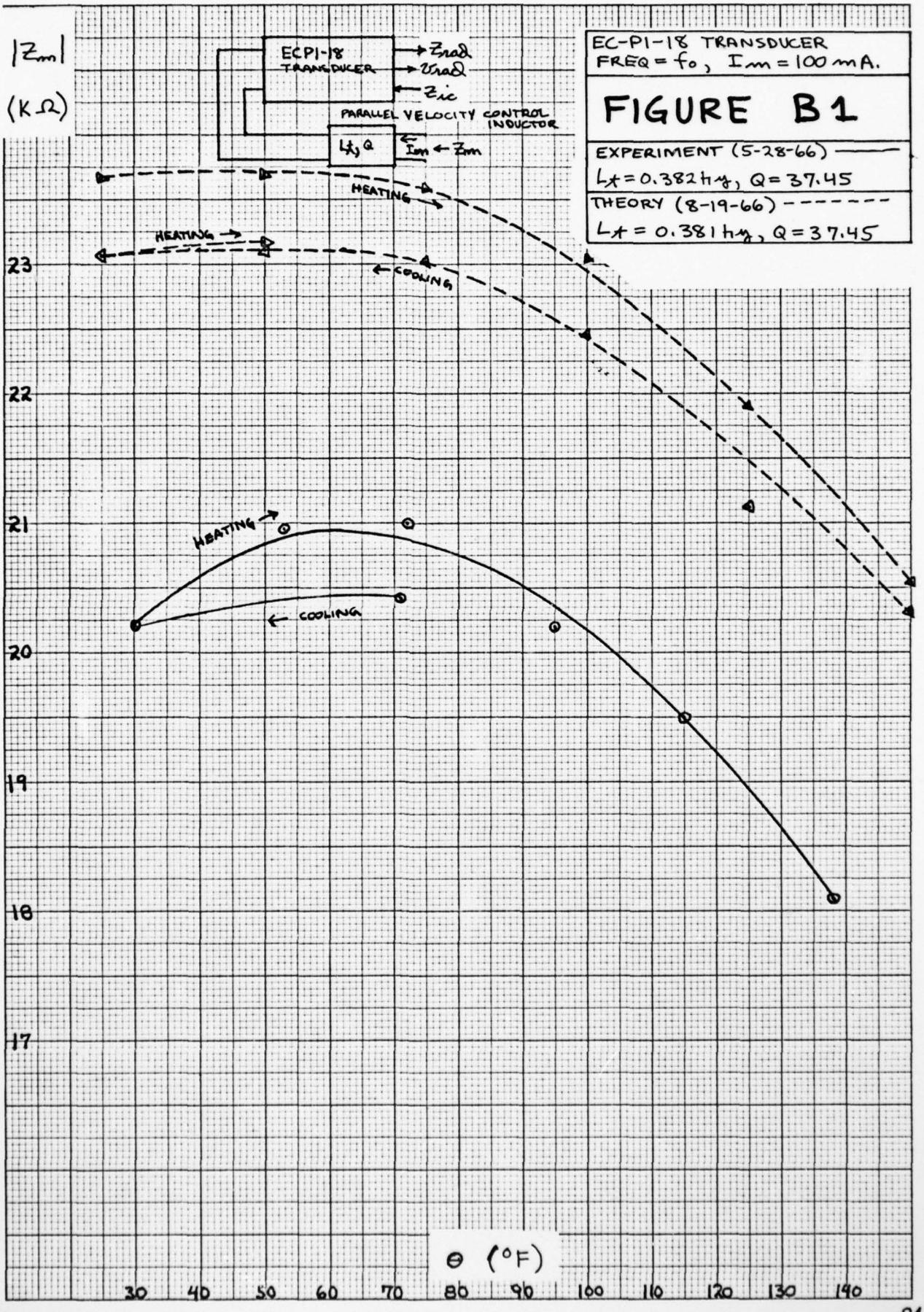

K&E 10 X 10 TO ½ INCH 46 1320
7 X 10 INCHES MADE IN U.S.A.
KEUFFEL & ESSER CO.

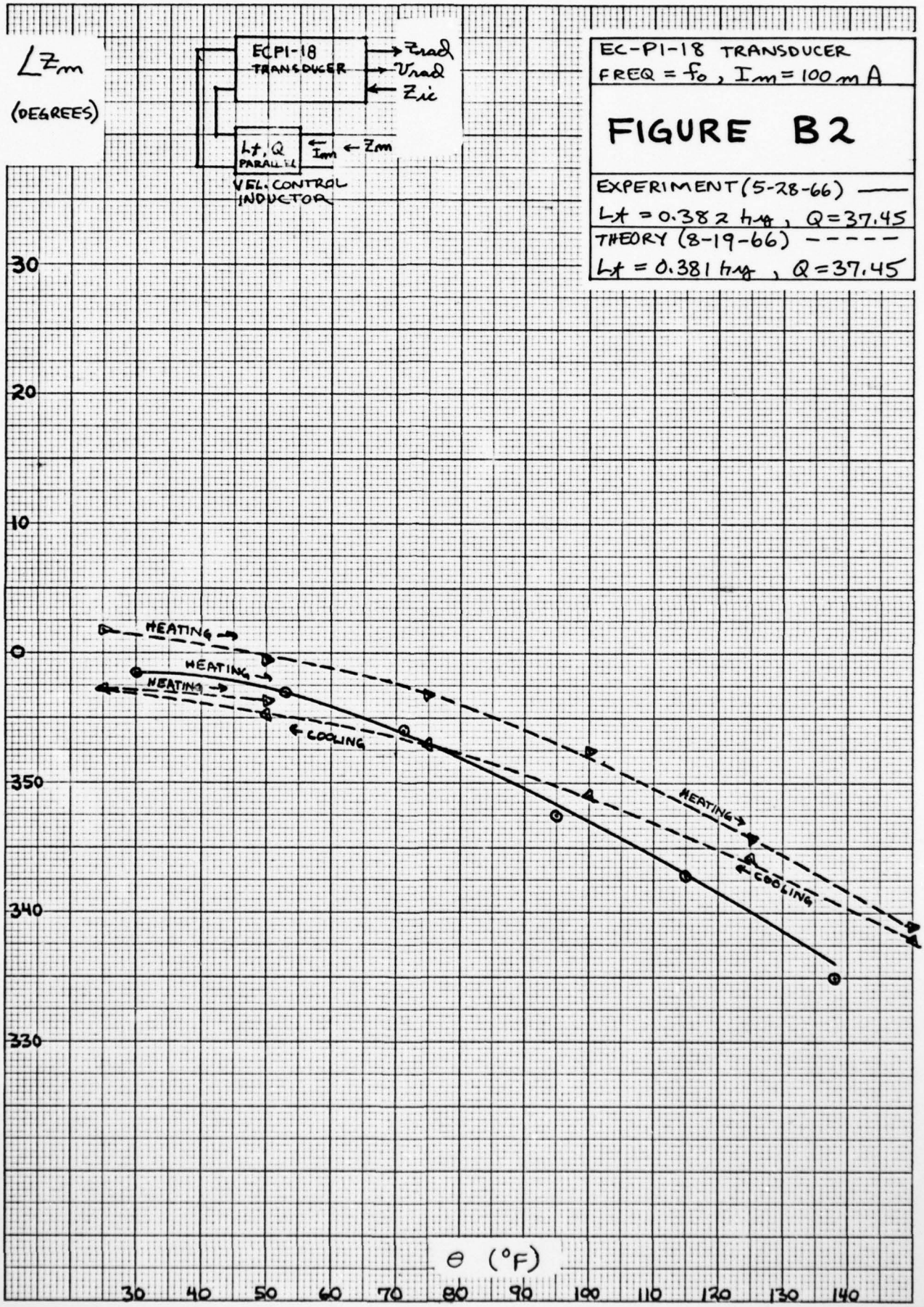

KE 10 X 10 TO ½ INCH 46 1320
7 X 10 INCHES MADE IN U.S.A.
KEUFFEL & ESSER CO.

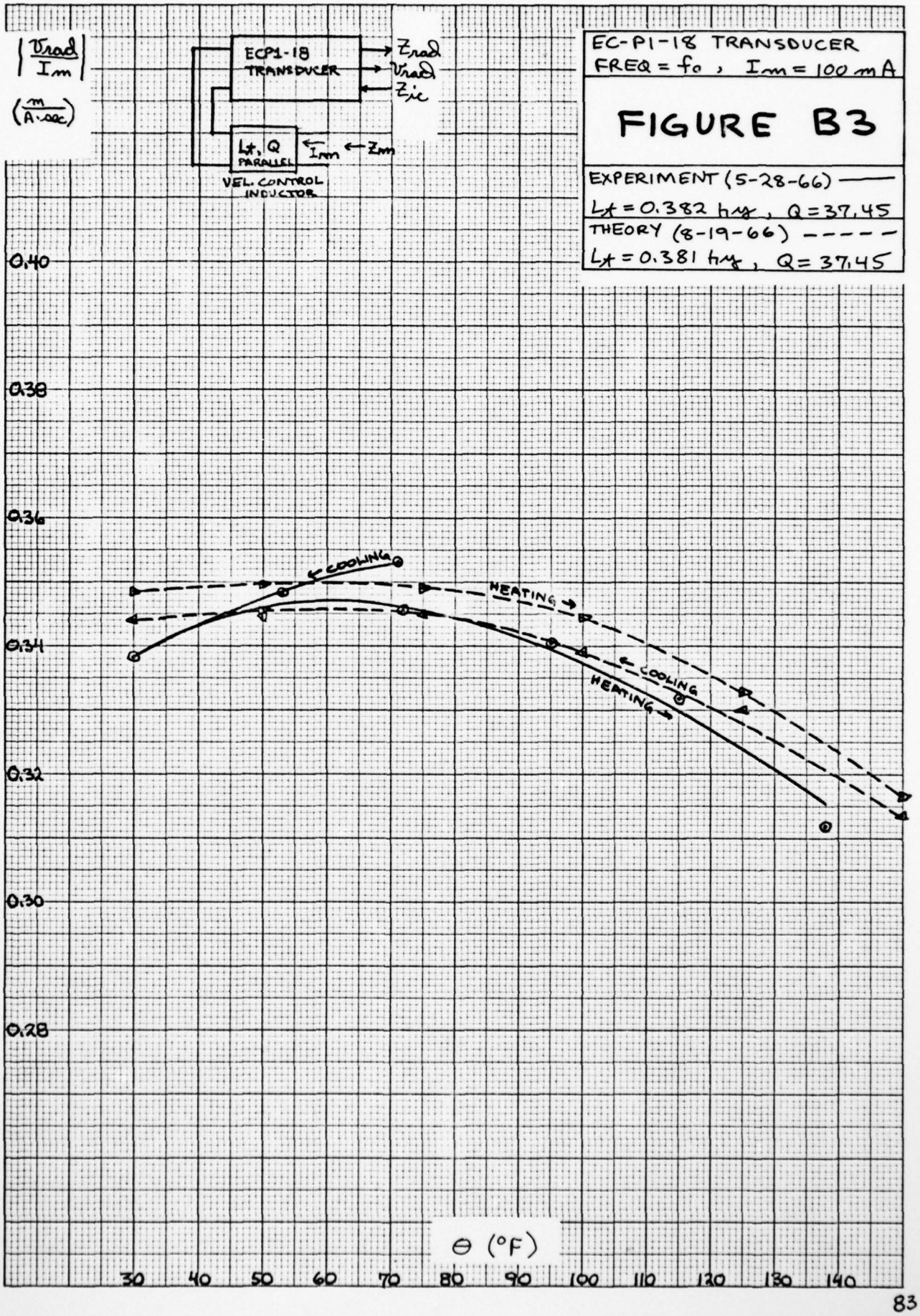

K+E 10 X 10 TO ½ INCH 46 1320
7 X 10 INCHES MADE IN U.S.A.
KEUFFEL & ESSER CO.

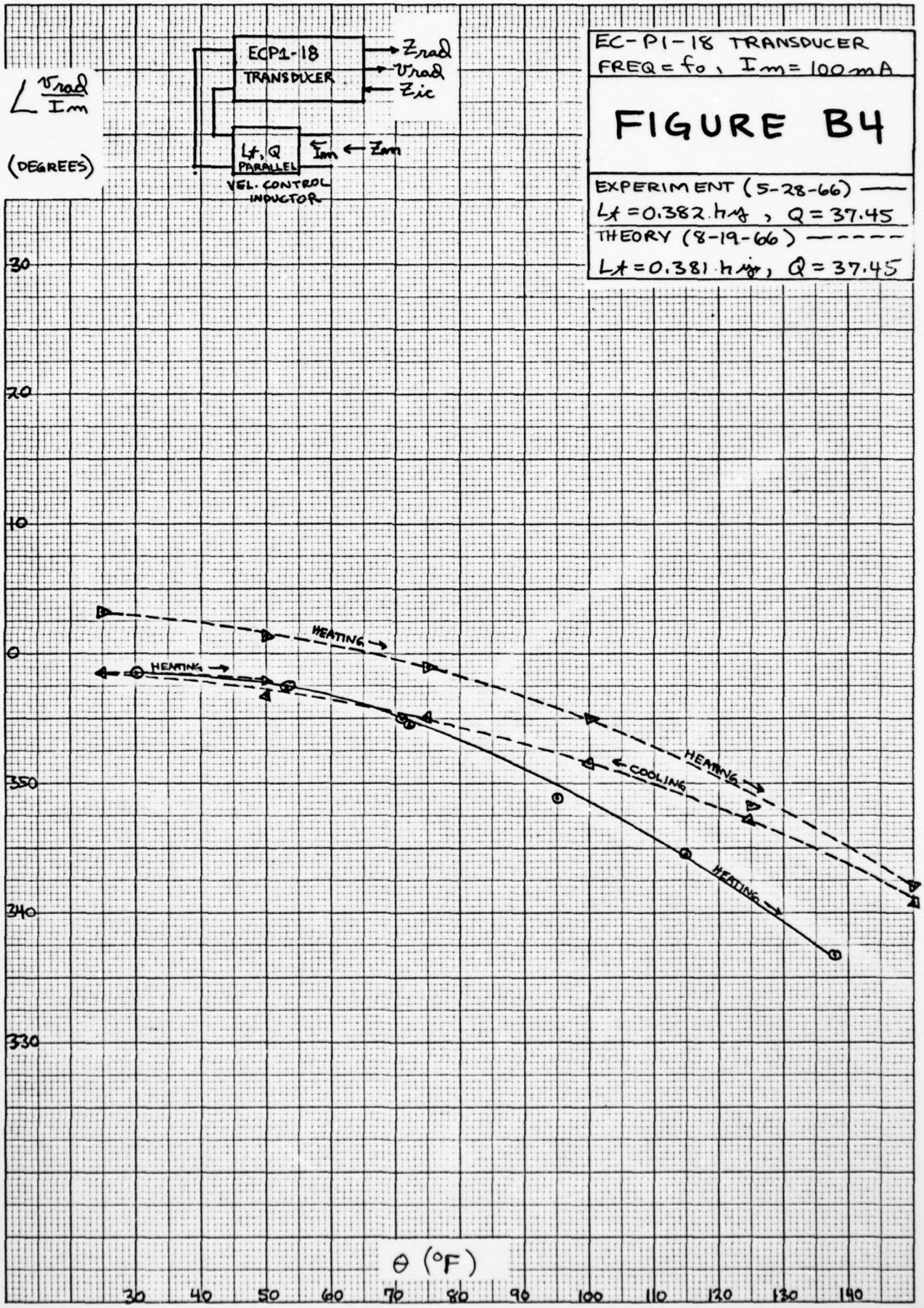

K&E 10 X 10 TO ½ INCH 46 1320
7 X 10 INCHES MADE IN U.S.A.
KEUFFEL & ESSER CO.

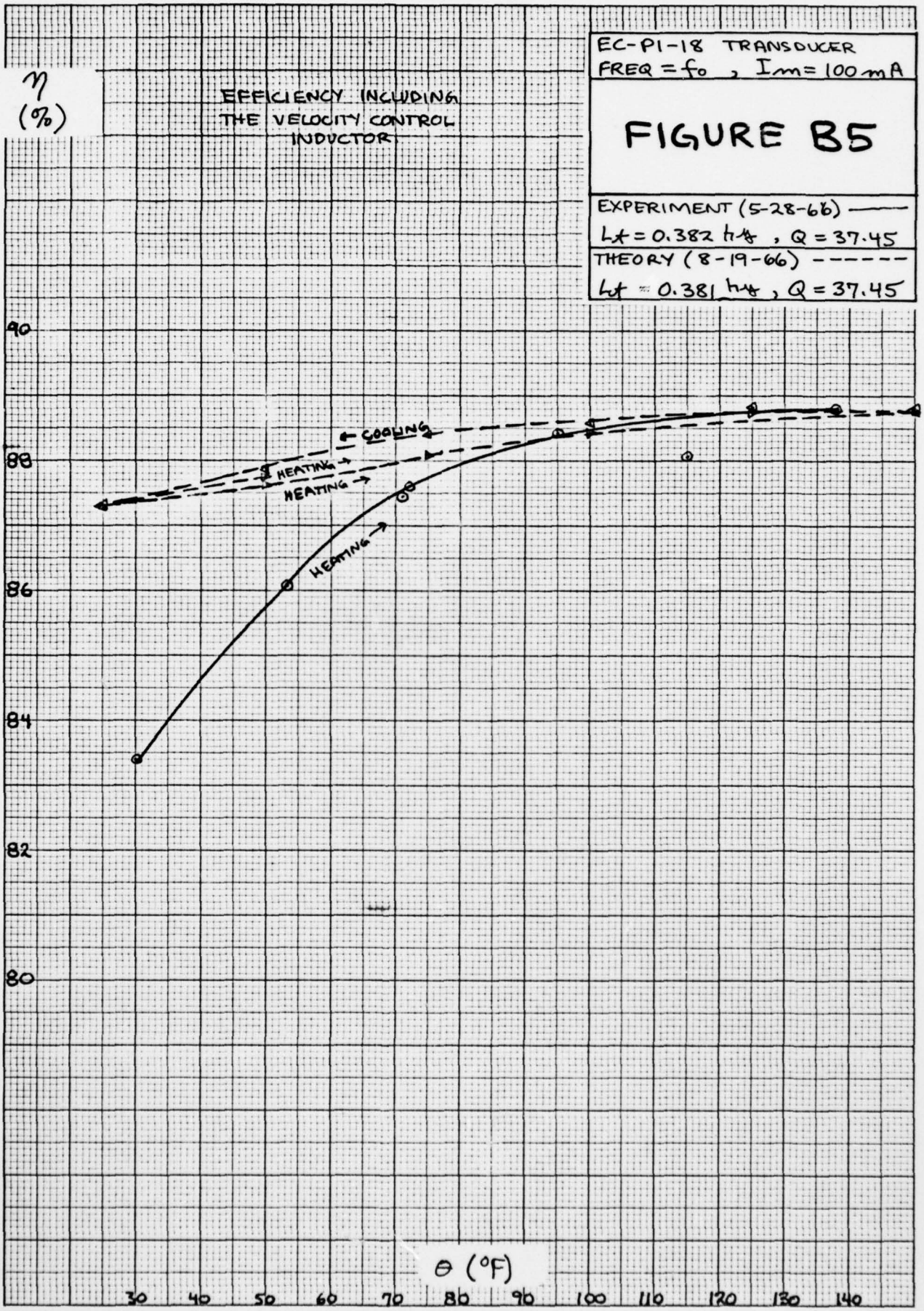

K&E 10 X 10 TO ½ INCH 46 1320
7 X 10 INCHES MADE IN U.S.A.
KEUFFEL & ESSER CO.

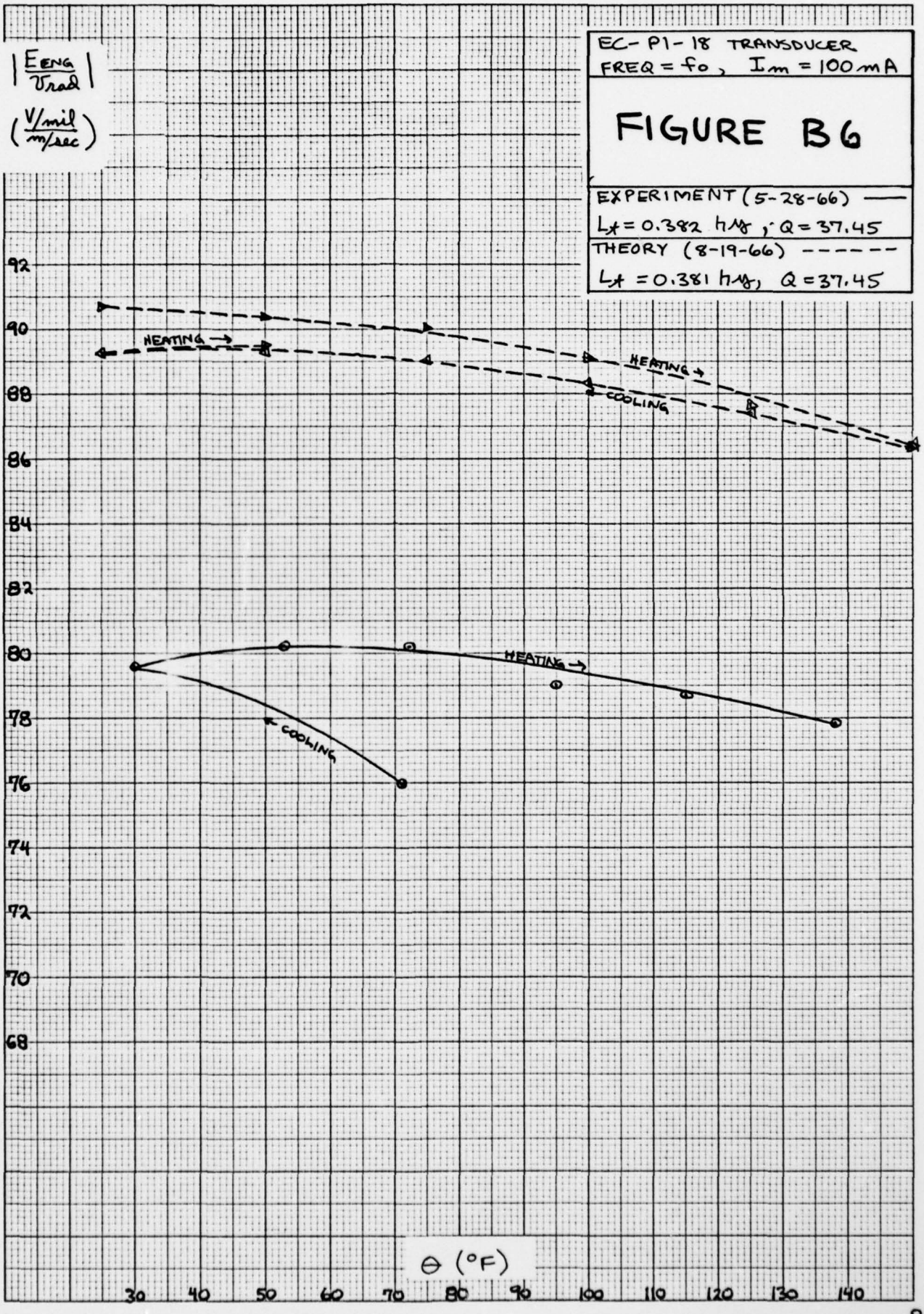

K&E 10 X 10 TO ½ INCH 46 1320
7 X 10 INCHES MADE IN U.S.A.
KEUFFEL & ESSER CO.

EC-P1-18 TRANSDUCER
FREQ = f_o ; Q = 37.45

FIGURE B7

THEORY (8-19-66) ------
USING C1-CM-1 DATA

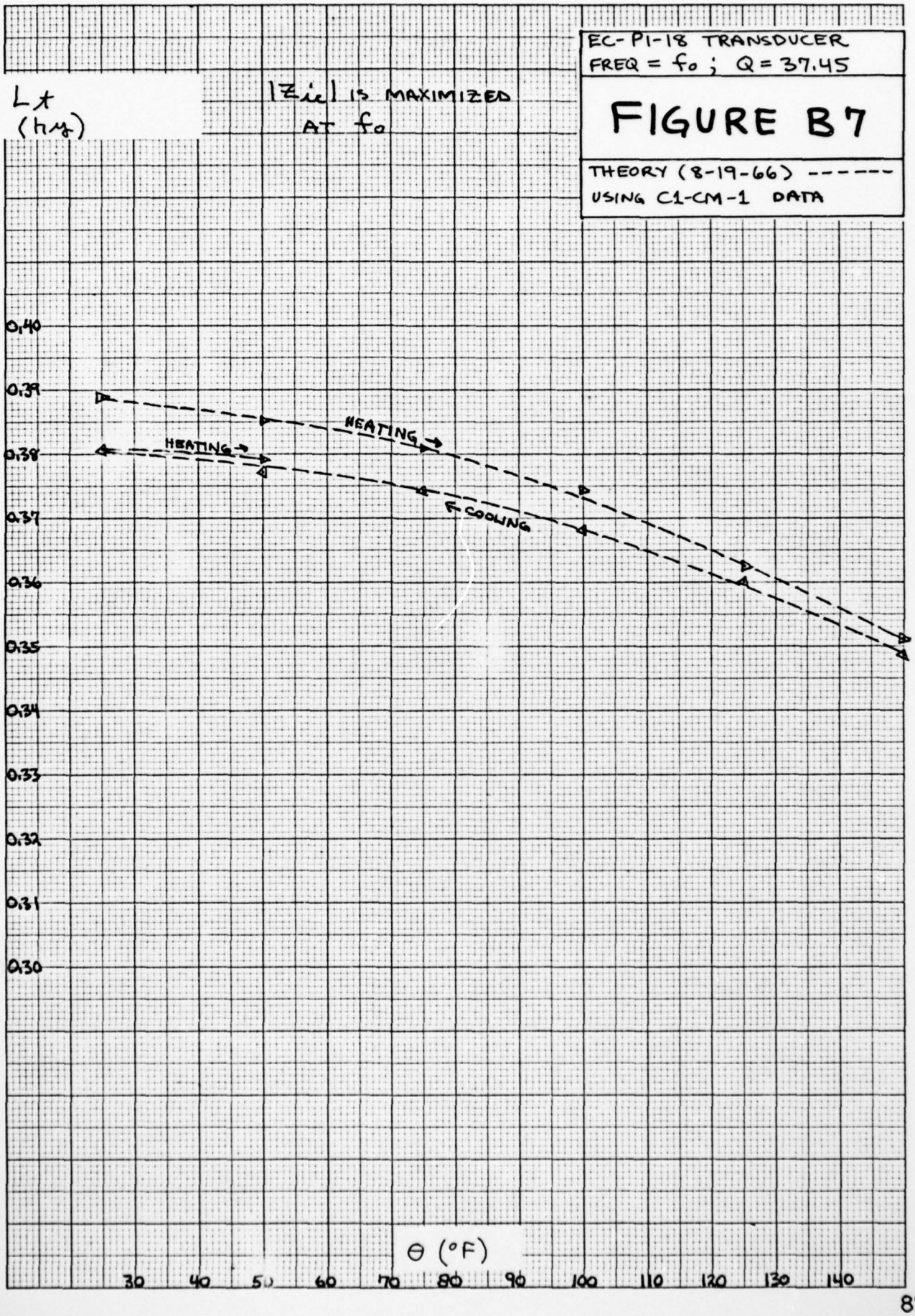

KE 10 X 10 TO ½ INCH 46 1320
7 X 10 INCHES MADE IN U.S.A.
KEUFFEL & ESSER CO.